STRUCTURAL ANALYSIS

Matthew L. Camilleri
Editor

Mathematics Research Developments

NOVA

MATHEMATICS RESEARCH DEVELOPMENTS

STRUCTURAL ANALYSIS

MATHEMATICS RESEARCH DEVELOPMENTS

Additional books in this series can be found on Nova's website under the Series tab.

Additional E-books in this series can be found on Nova's website under the E-book tab.

MATHEMATICS RESEARCH DEVELOPMENTS

STRUCTURAL ANALYSIS

MATTHEW L. CAMILLERI
EDITOR

Nova Science Publishers, Inc.
New York

LIBRARY OF CONGRESS CATALOGING-IN-PUBLICATION DATA

Structural analysis / editor, Matthew L. Camilleri.
p. cm.
Includes bibliographical references and index.
ISBN 978-1-61728-481-6 (eBook)
1. Structural analysis (Engineering) I. Camilleri, Matthew L.
TA645.S743 2010
624.1'7--dc22

2010015605

Published by Nova Science Publishers, Inc. ✣ New York

CONTENTS

PREFACE

Structural analysis comprises the set of physical laws and mathematics required to study and predict the behavior of structures. This new book gathers and presents current research in the field of structural analysis across a broad spectrum of topics. Discussions in this compilation include: evaluating seismic safety using non-linear structural analysis; a structural analysis of how art is made; the structure and function of vegetal ecosystems in semiarid regions of Northeastern Mexico; using a covariance structural analysis as a method for supporting efforts to improve employee motivation; and a method for solving linear algebraic equation sets in FE analysis software.

The focus of Chapter 1 is " How is it that artists know how to make their work and yet do not know how to explain it?" In other words, how do they both simultaneously know and not know?

True solutions to the problems of arid and semiarid zones throughout the world require a mandatory previous evaluation of the natural resources from the study areas. In Chapter 2, the main approach is driven to the structure and functioning of the vegetal ecosystems which intimately involves various interrelated elements such as flora, cattle, and other fauna, taking also into account management and commercialization of wooden and non wooden products.

A great part of the Mexican republic is located in the world desert belt with approximately 20 million hectares, 18 million located in the northeast of the country, mainly covered by xerophytic shrub vegetation (Rzedowski, 1978, Palacios, 2000). There is no evidence to date about the origin of the different types of shrub populations growing as natural climax vegetation.

Structural analysis plays the key role in understanding the relation between the preparation and morphology and intrinsic properties of metal oxide

nanostructures. In Chapter 3 structural analysis of metal oxide nanostructures by variety of fundamental techniques like X-ray diffraction pattern (XRD), Grazing incident X-ray diffraction (GIXRD), Scanning electron microscopy (SEM), field emission scanning electron microscopy (FESEM), transmission electron microscopy (TEM), atomic force microscopy (AFM), energy dispersive X-ray spectroscopy (EDX), and X-ray photoelectron spectroscopy (XPES) etc will be presented. The detailed crystal structure of In_2O_3 pyramids will be presented by XRD analysis. For in-situ examination, grazing incidence small angle scattering and diffraction of X-rays (GIXRD) results of ZnO nanostructures will be presented. The morphological description and the examination of the surface of the structure, which includes the analysis of their eventual structure and their size, shape distribution, cross-section from their surface to the substrate, the analysis of the surface and its inhomogenities will be attained by SEM and FESEM analysis. Detailed structural analysis with single crystalline nature of ZnO nanostructures will be presented by TEM equipped with selected area electron diffraction pattern (SAED) and high resolution transmission electron microscope (HRTEM). The surface roughness of vertically aligned ZnO nanorod arrays will be studied by atomic force microscopy (AFM). In order to know the exact chemical composition, stiochiometry and chemical bonding nature of metal-oxide nanostructures, the energy dispersive X-ray spectroscopy (EDX), and X-ray electron spectroscopy (XPES) techniques will be included.

Chapter 4 elucidates a method for showing the priority of factors used to generate motivation in companies, in order to support efforts to improve employee motivation. The authors verify the effectiveness of the method by a questionnaire survey. This study proceeds towards the above-described objectives in the following three steps. Step 1: Discussing the factors which constitute employee motivation in the literature. Step 2: Contriving a method to set the priority of improvement-forming factors by using covariance structure analysis and graphical modeling. Step 3: Verifying the method proposed in this study based on results obtained. The authors had the employees at a restaurant fill out a questionnaire by the method proposed in this study. They confirmed that the improvement priority was effective as a support for improvement.

In Chapter 5, a block substructure multifrontal method for solution of large symmetrical sparse equation sets that appear in finite element problems of structural and solid mechanics is proposed for desktop multicore computers. The analysis of a structure's topology reduces the fill-ins and allows the coupling of equations into blocks. A symmetrical storage scheme for dense matrices and performance optimizations provide a combination of an efficient usage of random-access memory and a high rate of factorization.

Performance-Based Design is currently accepted commonly as the most advanced design and evaluation approach. However, successful application of this procedure depends largely on the ability to accurately estimate the parameters of structural response.

Determination of these parameters requires application of analysis procedures where the main non-linear behavior features (constitutive and geometrical) of structures are included. Chapter 6 presents and discusses these features of non-linear behavior and how they are incorporated in the process of static or dynamic structural analyses. Non-linear analysis leads to determination of significant structural response parameters whenever estimating seismic responses such as ductility, overstrength, response reduction factor and damage thresholds; being these the main response parameters for evaluating the seismic safety of structures. In order to illustrate application of the non-linear procedure being described, a set of concrete-reinforced moment-resisting framed buildings with various numbers of levels was selected. These buildings were designed according to ACI-318 [1] for high and very high level of seismic hazard.

In: Structural Analysis
Editor: M.L. Camilleri, pp. 1-20
ISBN: 978-1-61668-987-2

Chapter 1

THOSE DUMB ARTISTS: AMNESIACS, ARTISTS, AND OTHER IDIOTS

Dena Shottenkirk and Anjan Chatterjee
Brooklyn College, Brooklyn, New York

Amnesiacs, Artists, and Other Idiots

Henry Molaison, aged eighty-two, died at the end of 2008, and just after noon on exactly the first anniversary of his death, December 2, 2009, scientists began slicing his brain into 2,500 tissue samples. Known primarily in his lifetime as only H.M., he left his brain to science so that it could be dissected and digitally mapped – a gift much beloved by many scientists. An amnesiac in life, H.M. first rose to prominence in 1962 when Dr. Brenda Milner, a pioneer in the field of neuropsychology, demonstrated that though H.M. was severely amnesic and could not remember past activities, he could nevertheless learn certain habits. The experiment involved the now famous mirror drawing, which tests hand-eye coordination, and can be learned over a number of days. Though H.M. had no conscious memory of having had done it before, his performance improved: he learned how to trace the image in the mirror reflection. Amnesiacs do well on mirror drawing, which is a kind of perceptual skill that in turn is a kind of motor skill – a type of skill dependent on brain structures distinct from declarative memory e.g., that memory system that allows us to consciously recall an event or fact. As an amnesiac, his declarative memory system – the part of his brain that could consciously remember – had been damaged. But as the 1962 study of H.M.

showed that he could increase his hand-eye coordination on the mirror drawing, even though he was unable to have any memory of having practiced this task, it also showed that there was another memory system in the brain. In other words, he could remember to do something but not recall his doing of it. He didn't know that he knew.

Artists are often stereotyped as inarticulate – connected to their muse but not to their grammar. The image of the inarticulate artist, caught in the bowels of emotionalism and compulsions, finds a home not only in the shorthand of Hollywood thinking and the therefore easily portrayed van Gogh, Pollock, or Picasso, but also in the more nuanced experiences of art writers, curators, and museum directors who have had the often repeated experience of listening to an artist's inarticulate and overly vague description of his or her work or the compensating opposite of a neatly packaged and overly slick byline-type explanation gleaned from memorizing what others have said about the work. These experiences buttress the opinion often heard that artists simply don't know what they are doing; that is best left up to others to articulate. Hence, curators and critics still have jobs.

There is though a continuing belief that artists *ought* to be able to discuss their own work and artists' training often involves a requirement for the art student to write about his or her work, especially in professional graduate programs. The difficulty of this is the cause of many art department meetings as well as the source of many jokes, though art educators tend to not dismiss art students' inabilities with the same wave of the hand often seen in the professional artworld. Instead, art educators believe the inability is remedial, and to a certain extent that belief is carried over into the professional world that demands such things as interviews and artists' statements. While this is clearly inconsistent (this demand to articulate while simultaneously dismissing artists for being inarticulate), that is not the focus of the current investigation.

Rather, the interest is in the differing abilities relative to an artist being able to discuss others' work and being relatively unable to discuss his or her own work. Returning to the case of academic training, it is routinely noted that the very same art students who have difficulty writing about their own art are quite often very articulate about other art students' work. The contrast between the ability to discuss one's own art and discuss the work of others is sometimes noted by academics and teachers, as students participate in group critiques of other students' work on a regular and successful basis without the stammering, obfuscation, or packaged byline approach that often infuses discussions of their own work. It is often just passed off as a difference resulting from a lack of practice, and hence art students are encouraged to write more about their own

work. But why would art students have less practice in discussing their own work than in discussing others' work? An art student has surely spent more time involved in his or her own work and has had more thoughts directed to that process than thoughts expressed in group critiques of other students' work. The explanation must be elsewhere.

The challenge involved in artists discussing their own work travels beyond the ivory tower, as well. In similar fashion, professional artists routinely discuss work they've seen in galleries and can do so with great fluency often in contradistinction to the explanation they might give of their own work, except that differently from students, they often have gravitated to the overly-practiced byline explanation. Given that there is a bifurcation between the way an artist speaks of his or her own work and the way an artist is able to speak of others' work – in that way functioning more like a critic – the question is why. The fact that there is a difference is a point upon which practitioners in the field readily agree, but the disjunct between the inability of an artist to discuss his or her own work and that same artist's ability to discuss the work of others is rarely highlighted or analyzed.

That is the focus of this investigation. How is it that artists know how to make their work and yet do not know how to explain it? In other words, how do they both simultaneously know and not know?

It is important to note that some psychological explanations are implausible. If one is tempted to adopt a traditional psychoanalytic explanation to the differing semantic abilities, there are in turn two potential candidates: artists might be unwilling to brag or they might be "too close" to the phenomenon. The first hypothesis seems fairly easy to dismiss in most cases as the idea that artists are lacking in strong egos and self-confidence is a hypothesis probably not worth testing. "As meek as an artist" isn't a common truism; that's reserved for a mouse. Art is an activity that often requires not only the offering of one's own impoverishment, at least temporarily but often long-term, but the sacrifice of a stable family life as well – all in the name of expressing one's inner self. Clearly valuing one's "inner self" higher than one's own physical well-being or often the well being of those around one does not speak of humility or self-abnegation. The premises are weak in this argument.

A related notion though could be put forth that artists are "too close" to their own work and therefore unable to get the distance needed to discuss it. While it is true that "closeness" to something can prevent needed objectivity – the oft repeated metaphor of not seeing the forest for the trees – an analysis of what it means to be "too close" is worth a digression. For example, a conflict at work with a fellow colleague can have this flavor as can a conflict with a family member or a loved one. In these kinds of circumstances it is difficult if not

impossible to get the bigger picture and to explicate the situation fairly. One's own version – or one's own vulnerabilities – is often all one sees.

It can be easily argued that this experience tends to happen in an arena where one's own needs are in competition with others' needs and heeding a call to objectivity would potentially endanger one's own position. The protective part of the brain – that old part that institutes a flight or fight response – can shut down the processes that allow for a more reflective and more nuanced objectivity. In this instance the person is "too close" but it is too close to one's own survival that is at issue for the brain. Objectivity in this immediate instance is hardly in one's best interests, or at least short-term best interests. It is thus a self- preservation that prevents objectivity.[1]

But is art in this kind of category? This idea would have some credence if the artist viewed his or her work as an external threat and articulating that work would result in some sort of personal demise. Again, confirmation or disconfirmation of this would be an empirical matter for psychology researchers, but the notion that one's own art could be a source of threat similar to an external threat lacks immediate plausibility.

A Structural Analysis of Knowing

An alternative explanation and one embraced here would be a neurological one: to be "too close" to the information can be explained through a structural analysis of the heterogeneous functions of the brain's memory systems. This is therefore a structural analysis of how art is made, or more precisely, how art is thought.

It is the "thought" part that is essential. An explication of the process of making art – the phenomenon of the creative act, as it were – has elided many writers and philosophers who have been summoned to the challenge of articulating exactly what it is that the artist is doing and how the creative act comes to be. The process at first glance though seems relatively simple. An artist begins to work. Brushes and paints are set up (limiting the example to a visual artist – a conventional painter), the size of canvas has been decided upon, constructed, and primed; the process begins.

But the process had already begun long before that. This physical act is not the beginning. The artist has already engaged in a long period of training, as well as having some existing notion of what is to be created in the present case. It is

[1] Thanks to Dr. Deborah Munczek, clinical psychologist, for her discussion regarding this.

normally only the second of these facts that are focused on when discussing the so-called mystery of the creative act. But the first part is perhaps more important because that embeds the roles of memory and habit formation, essential components for creative activity. Together, these two antecedent facts are at the heart of this paper – an articulation of the mental processes behind an artist's creation.

Two Memory Systems

The beginning then is fairly straight-forward: it is not the singular fact that artists are odd, but the more general fact that the human brain is extraordinarily complex. This is especially true when it comes to learning and memory systems. Neuroscience and neuropsychology have developed over the course of the last few decades a systematic view of the brain's memory systems, in which there are cleaved two basic systems: the declarative and the nondeclarative. These correspond to certain physical regions of the brain, with each of these regions further subdivided both in terms of the physiological structures and in terms of functional roles. The declarative memory system is located in an interaction between the large physiological regions identified as the medial-temporal/diencephalic region and parts of the neocortical region – that part of the human brain other mammals would be jealous of if only they knew. The nondeclarative memory system resides in the basal ganglia, which is located deep within the hemispheres of the brain and the cerebellum, which itself is directly above the brain stem. Declarative memory encompasses both semantic memory, which is the ability to name and identify third-person objects and events, and episodic memory, which is those memories each of us have contextualized in time and therefore more first-person e.g., what I ate for dinner last night, what I was wearing when I got married, etc. Episodic memory involves participation of brain systems in addition to those that support the semantic, particularly the amygdala, which registers emotional events – obviously important in first-person memories; the episodic memory system is also that part of the brain that encodes previous experiences of third-person objects (which is why those childhood hills seemed so very huge). Nondeclarative memory, on the other hand, encompasses skill learning (also thought of a procedural memory e.g., swinging a golf club, playing a piano, etc.), repetition priming (the larger category also including perceptual learning, of which mirror writing is an instance), and classical conditioning (often thought of as stimulus-response kind of pavlovian learning and also sometimes involving the amygdala). These two memory systems also divide along the

explicit/implicit line, with declarative obviously being explicit memory and nondeclarative memory, which is very often implicit. The relationship to language is critical, as anything implicit usually does not have access to language (or the other way around) since only some explicit i.e., declarative, things do have such access.

The argument we are presenting is that making art and thinking about one's own art involves the use of memory systems not activated in the alternate circumstance of critically discussing another artist's work. In the latter, the object is accessed similarly (though not quite identically) to other third-person objects, such as a table, a fork, or a mountain. Making art and therefore retrieving those memories of making one's own art involves other parts of the brain that might not be as accessible to semantic and declarative memory and hence to language.

Amnesiacs and Medial Temporal Lobe Damage

The analogy brought to bear by amnesiacs is to be considered initially. Amnesiacs suffer damage to the medial temporal lobe or midline diencephalon, which is the locale for episodic declarative memory, but they do have access to nondeclarative memory. Working from analogy, if we begin with the established fact that amnesiacs do not have access to declarative episodic memory but can access nondeclarative memory, it is then possible to conceptually frame the issue in a way that divides the ability to remember nondeclarative things from the ability to know – declaratively – that one is remembering something, either a first person or a third person fact. This might then parallel the disjunct between the artist's ability to make something and the ability to know and articulate what one has made, if it can be shown that functions operating in the nondeclarative systems need not fully translate themselves into the declarative mode.

Amnesiacs also show other kinds of nondeclarative memory functions, such as the ability to prime. Priming is when they have been shown a word or image and then at a later date tested on that knowledge, for example, when they are directed to use a particular word to form the first word that comes to mind, and though they have been given that association in the past and are therefore biased by previous exposures, they do not declaratively remember though they implicitly remember. In this, the point is that "memory" in the ordinary usage of the term is absent: the patients cannot remember the word recently given to them. But when asked for quick associations they perform more adequately, indicating that they are drawing on other kinds of memory storage systems.

This establishes the following things. As amnesiacs with lesions in the medial temporal lobe cannot remember that they have increased their learning of mirror drawing, this indicates that others can in theory also draw from nondeclarative memory, establishing in turn that this knowledge is stored in a part of the brain other than the medial temporal lobe e.g., in a part other than the episodic declarative memory system. In theory then it is possible to know (using the word in the way that means implicitly knowing) some kind of perceptual or motor processes but not have linguistic access to it. So while the medial temporal lobe does in the usual case store accessible memories of this kind of visual learning that can then be reformulated as semantic thought in a normal person, the medial temporal lobe obviously doesn't control all learning per se. Perceptual and motor learning is done somewhere else, - (or at least it can in some instances be done somewhere else, as it is possible that only in the instance where the medial temporal lobe is damaged does the nondeclarative memory compensate) – and the mind is able to retrieve that learning and act on it, but it cannot easily share it with others; it cannot be translated into language as it is no longer accessible to the declarative part of the brain.

Like perceptual memory, procedural memory too can continue to function in patients who have undergone surgical removal of the medial temporal lobes (Budson, 696). Procedural memory survives independent of episodic memory and semantic memory as demonstrated not only by amnesiacs who suffer from damage to the medial temporal lobes (which includes both the hippocampus and parahippocampus), but it is also the case that procedural memory functions survive in patients with alcoholic Korsakoff's syndrome that are amnesiac because of damage to the diencephalon. These procedural skills, exemplified in such activities as playing music or swinging a golf club, are dependent upon both the cerebellum region and the supplementary motor area along with the striatum (a part of the basal ganglia), thus like mirror-writing and priming. These areas are active as a new task is learned and thus it governs learning behavioral, cognitive skills and algorithms at an unconscious level. Hence, both perceptual memory and the procedural memory, each part of the nondeclarative memory systems, can continue to function in people without access to declarative memories.

This establishes the fact that at least these nondeclarative memory systems are able to function in the absence of declarative memory function. But it is important to remember that nondeclarative memory systems do not serve the same purposes that declarative systems serve. As Larry Squire, a pioneer in memory research, stated regarding the nondeclarative memory system, "It is dispositional and is expressed through performance rather than recollection. Nondeclarative forms of memory occur as modifications within specialized performance systems. The

memories are revealed through reactivation of the systems within which the learning originally occurred"(Squire, 173-4).

If it is true that the memories are revealed through reactivation of the systems and it is clear that in amnesiacs there is no functioning memory in the episodic declarative area, then it seems to be the case that in healthy persons, who are able to both do the assigned tasks and know that they have done the assigned tasks, must be storing two different sets of related memories; it indicates that the healthy person has both the nondeclarative and the declarative memory systems operating for this particular task. In other words, for a healthy person the memory is stored in two places – one for their own private use, so to speak, that can be called upon to actually do the task and is therefore is activated when they need to put the knowledge to use (on analogy with the amnesia patient) and one that is in use when the knowledge of the task is shared, literally with others. The latter instance would be needed for those times when the activity is codified in language and articulated to others. But it wouldn't be needed otherwise.

Damage to the Basal Ganglia

Where patients with damage to the medial temporal lobe reveal the workings of implicit memory, the obverse situation is revealed in studies done with subjects suffering from Parkinson's and Huntington's. These patients suffer from damage to the organic parts of the brain that affect the nondeclarative memory system, i.e., the basal ganglia. The separate input areas of the basal ganglia most relevant for habit learning are the caudate nucleus and the putamen, along with the globus pallidus and the claustrum. By the late 1970s neurologists had refined the terminology and the basal ganglia was divided into the ventral striatum and the dorsal striatum. Of course this part of the brain like all parts of the brain does not operate in isolation and the basal ganglia receives inputs from all regions of the cerebral cortex. Spines on neurons conduct, via neurotransmitters, information to other neurons and hence other regions of the brain. Along with the striatum, the cerebellum, sitting next to the brain stem, is involved in procedural memory formation. The neural networks that connect these sites to each other and to the cognitive apparatus found in the neocortex are critical for the planning and monitoring of behavior.

The basal ganglia was long associated with motor control, and diseases of the basal ganglia such as Parkinson's and Huntington's highlight these functions. But the basal ganglia is now thought to be associated with certain kinds of learning as well. As nerve cells die as a result of each of these diseases, it is possible to

monitor what corresponding functions are likewise diminished, thus establishing the functional roles of specific parts of the brain. While motor deficits are most obvious in both of these diseases, nonmotor functions including cognitive deficits also exist, indicating a larger role for the basal ganglia in memory functions. (Packard, 2002, 575) Thus recent research has also shown that a part of the basal ganglia, specifically the dorsal striatum, is involved in learning and memory, in particular the kind of learning associated with stimulus-response.

A fascinating function of basal ganglia in habit formation is the role of probabilistic learning. Various tasks have tried to gauge the role of the basal ganglia in probability reasoning, the most famous of which is the weather prediction game (established in the mid 1990s at Rutgers University). In this game, four tarot type cards each with a unique geometric pattern (e.g., squares, diamonds, circles, or triangles) are presented to the subjects. A random selection of the cards would then be given to the participants, sometimes for example, consisting only of one card – a square – or another card – a diamond – or both cards, etc. On each trial, subjects are asked to see the pattern and then predict the weather. They of course believed (cognitively) that they are randomly guessing at the weather, but in truth there was a probability correlation between some of the cards and rain/shine predictions. After 50 trials, healthy subjects improved their prediction capability without consciously knowing that they had done so. Amnesiac patients, who have damage in the medial temporal lobe that are critical for declarative memory, also learn the task normally within 50 trials, whereas neither Parkinson nor Huntington patients do. The results of this test again establish that the basal ganglia is the seat of the nondeclarative memory, whereas episodic declarative memory is found in the medial temporal lobes.

Basal ganglia mnemonic processing also involves skills associated with learning a visuomotor sequence. Tests developed for this have often been variations on a timed finger tapping reaction, such as when the subjects view a series of asterisks on the computer and then are asked to press the key directly below each asterisk as it appears. Though the asterisks are in an ordered sequence, the subjects are not told this and yet their reaction time will improve; again, demonstrating that we know things we don't know we know. The brain can inductively decipher the pattern, and react appropriately to that pattern, and yet the conscious, declarative part of the brain is unaware of it. Again, amnesiac patients, who suffer from damage to the medial temporal lobe/hippocampal system, show no diminished ability to perform this task, also thereby demonstrating that the part of the brain that memorizes inductive patterns and uses those inductive patterns in habit formation is in tact.

Animal studies have been valuable in extracting data relevant for deciphering the different memory systems. Rats were used in various studies beginning in the 1960s to test the mnemonic functions of the dorsal striatum section of the basal ganglia in habit learning, wherein two eight-arm radial maze tasks were used in what was called a "win-stay" version. This test was derived from an older test called the "win-shift" task, which required rats to remember what arms they'd previously visited and to not revisit them; in other words, rats received food when they visited only an arm of the maze that had not been visited before. This tested for spatial memory and/or a kind of cognitive mapping strategy. The newer test, e.g., the "win-stay", was developed in the late 1980s, and also used an eight-arm maze but in this instance some of the arms were illuminated and some were not, with the rats rewarded only when they chose an illuminated arm. This tests for visual discrimination and the acquisition of an stimulus-response (S-R) habit. Brain lesions in the dorsal striatal part of the brain (i.e., the basal ganglia region that controls habit formation) allowed the rats success at the win-shift task (i.e., the task that tested for spatial memory and/or a cognitive mapping strategy), but impaired their ability to succeed in the win-stay task, which tested for the acquisition of an S-R habit. The inverse held for rats with lesions in the hippocampal system (i.e., the system that controls for cognitive memory functions): they were able to succeed at the win-stay task but not the task that tested cognitive mapping strategy, e.g., the win-stay task. In other words, lesions in the hippocampal region impair cognitive functions whereas lesions in the dorsal striatal region of the basal ganglia impair habit formation. The rats with lesions in the hippocampal system would, like H.M., know but not know they knew (if indeed rats can be said to know at all…). The question of course is whether or not artists also find themselves in that position.

The Two Memory Systems: War and Peace

Of course the two parts of the brain – the medial temporal lobe and the basal ganglia – are not wholly cordoned off from one another. The relationship between the various memory systems has also been a source of recent research and again is pertinent to present purposes. Several different neural pathways have been found travelling between the basal ganglia and the medial temporal lobe, such as output projections to frontal cortical regions, which then in turn project to the medial temporal lobe (Packard 2002, 583).

The details of the relationship between the various parts of the brain are of course revealed in knowledge of the molecular level. The basal ganglia receives

input in the spiny neurons found in the striatum and these spiny neurons receive convergent signals from various areas of the cerebral cortex. Using dopamine as a neurotransmitter, these spiny neurons are thought to recognize patterns of activity. Upon registering this context, the spiny neurons discharge their dopamine which is thought to disinhibit thalamocortical loops to initiate sustained activity in clusters of frontal cortical neurons (Houk, Davis, Beiser, 1995). In this way the originally detected contexts would be recognized as working memories. Repeated activation gives an increase in the efficiency of the synaptic transmission and is called long-term potentiation (LTP). This is thought to construct memory formation, and recent research has been done on exactly what kinds of transmitters are necessary for this process. While the cellular-level research will ultimately answer many questions as to the precise mechanisms that underlie memory formation, the important fact for present concerns is that the existence of separate memory systems is now widely accepted. Questions currently under investigation are how these memory systems interact with one another in the functional construction and retrieval of memories.

Neuorimaging studies have corroborated the notion that memory is not a singular entity nor accomplished through a single organ, and current focus for study is the cellular mechanisms of the system as well as the relationship between the larger parts. Research involving patients with brain lesions, and in particular H.M., began the field of study, but it is neuroimaging – both positron emission tomography (PET) and functional magnetic resonance imaging (fMRI) – that is more reliable as the behavior of memory-impaired patients with brain lesions would demonstrate not the function of the damaged brain isolated from the rest of the brain but also a brain that has compensated for that damage (Gabrieli, 1998). Some of these neuorimaging studies are particularly important for present purposes. In the mid and late 1990s, studies revealed that the caudate nucleus part of the basal ganglia was activated during a serial reaction-time task, but this part of the brain was not activated when the subjects were told beforehand and could therefore explicitly anticipate the stimulus (Packard & Knowlton, 2002, 578 – referring to Doyon et al. 1996): need to find this original source to double check) This is important as it points to the fact that explicitly knowing something is in inverse relationship to implicit knowledge and habit formation.

The relationship between the two main systems of memory – the basal ganglia and the medial temporal lobe system (sometimes also referred to as the hippocampal system) seem to both exhibit competition and cooperation. In some tests, there is evidence that the beginning of learning shows a simultaneous activation in both regions, with the hippocampal system activating the learning that initially controls behavior, but that that activity then shifts to the basal ganglia

region, particularly the caudate memory system, which then controls for a slower process of S-P habit formation (Packard & Knowlton, 2002, 579).

But scientists have inferred from other studies that there are instances where the memory systems compete. D.F. Sherry and D.L. Schacter, in "The Evolution of Multiple Memory Systems", written in 1987, have given an evolutionary story hypothesizing that the inability of one memory system to successful solve problems and adapt to situations led to the development of multiple and heterogeneous systems. The fact that a brain suffering from a lesion in one part can experience enhanced and compensatory learning in another part of the brain is sometimes evidenced as proof for this theory. Experiments using artificially induced neurotransmitters (in the form of pharmacologically enhanced thinking) have proven that the different memory systems can be both enhanced and diminished, biasing animals toward one or the other. But as some researchers have noted, "…in some cases of caudate-dependent sequence learning, explicit knowledge of the sequence can impair acquisition as measured by reaction time, which suggests that effortful retrieval of explicit knowledge can interfere with the performance of the implicitly learned sequence" (Packard & Knowlton, 2002, 582). Poldrack (2003) has noted that activation in the caudate nucleus and medial temporal lobe is negatively correlated within subjects, a point crucial for present purposes.

It is conceivable that the making of art does not have to be data that is stored in both memory systems. But as declarative memory is both semantic and episodic, (the latter relies on some of the same structures as does the semantic memory system plus the frontal lobe) then the claim that speaking about one's work is inaccessible to declarative memory must then also entail a claim that memory about (or conscious knowledge of) an artist's own work is not stored in *either* the semantic nor the episodic memory system. This would be the logical conclusion but it is counter-intuitive. We intuitively think of making artwork as just that kind of activity that one locates as those "personal experiences framed in our own context" i.e. episodic. If that is true and if making one's art is just like remembering other first person events, then it would not make sense to claim that the experience of making one's own work would be less accessible to verbalizing than would be others' artwork. In other words, my art seems like my art, which can't be that different from my birthday. Or is it?

It makes sense to conceptualize this as a system of interdependent signals. It is known that memory systems operate in parallel and independently, sometimes working parallel to support one another. In these instances they seem to replicate each other and reinforce a memory as when a fear of heights (in the

nondeclarative memory system) is coupled with the specific memory of falling off the porch as a small child (in the declarative memory system).

But there are also competing situations where multiple systems are operating such as when, to again quote Squire, "…humans acquire a difficult habit learning task, structures important for habit learning and structure important for memorizing (i.e., declarative memory) can appear to compete for control of performance" (Squire 174). Recent research by Poldrack and Packard points to some instance of competition among systems, but in the example provided earlier, in the early phase of learning the difficult task, fMRI showed the activity in the medial temporal lobe, a pattern found if subjects were attempting to memorize the task, but as their performance improved, the fMRI activity decreased in the medial temporal lobe but the activity in the neostriatum increased. In other words, the activity increased in the area of the brain that controls habit formation. Thus, these two brain functions related inversely in the activity of learning a difficult new task. This could indicate, as Squire would want to argue, that the two parts of the brain are competing with one another. But it could also indicate a kind of evolutionarily devised cooperation among mutually symbiotic systems, as it could though also be the case that both functions are necessary in order to satisfactorily learn the new task – both memorizing the data in the immediate short-run and committing that data to a habit formed system, for purposes of easier retention. In this interpretation the system would be set up to optimize the different kinds of memory dependent on the task at hand. In that scenario, the memories are not primarily stored in the declarative system, however episodic the origins of those memories might be. In other words, it would not be just like one's birthday.

Whether the system is one of competition or cooperation, it is still the case that the different memory systems process different activities and store the data differently. It also needs to be noted, somewhat parenthetically, that it seems to be the case that these memory systems are not completely physiologically mutually exclusive. Rather, these systems are interconnected and overlap in places. So when we speak of different memory systems our language is provisional at least in part. These should not be taken as isolated systems necessarily blind to each others' workings.

It is also worth noting that research comparing the ways humans learn pattern discrimination differently from monkeys shows that the same thing can be learned differently: the monkeys seem to learn it by depending on the temporal lobe – neostraital pathway i.e., the procedural memory system, whereas humans learn it as a kind of memorization using the medial temporal lobe i.e., the semantic memory system. But, Squire notes, "To achieve a two-choice discrimination task for humans that is an acquired skill, and in the way that monkeys learn the pattern

discrimination task, one might ask humans to learn to discriminate between the paintings of a master and the paintings of a talented forger" (Squire 174). Procedural memory is important in the kind of feedback and gradual learning system that seems reflective of the process of learning how to distinguish the subtleties that differentiate the original painting from the fake. It seems clear that procedural memory would also be involved in functioning as a critic (in addition to the obvious main role of semantic memory), in that critics might learn pattern discrimination in the experience of learning to see the difference between the fake and the real, but it might very well also be true that that critic would be unable to explain to someone else exactly why – in every detail – the fake was distinguishable from the real.

The Amygdala's Role in Emotional Memories: The Gist

None of this discussion though has touched upon a very important aspect of the brain: the amygdala. Nominally a part of the declarative memory system, the amygdala is near the hippocampal formation, and stores highly emotional memories, such as instances of fear, and matures in small children sooner than the hippocampal memory system (LeDoux, 1996, 202), which explains why children cannot retain explicit memories and yet will have phobias that result from early childhood events. A stimulus that reminds the brain of the earlier experience will thus be experienced both in the hippocampal memory system - in declarative memory – and in the implicit memory system controlled by the amygdale. In this instance the two memory systems meet and the product is the profound and emotionally intense re-experience.

Recent studies have demonstrated that amygdala damage impairs the brain's ability to retain the emotional gist of an event (Adolphs, Tranel & Buchanan, 2005, 512). Patients with damage to their amygdala showed no enhanced memory when experiencing something under an emotionally encoding experience (e.g., a picture of parents in a car travelling down the road versus the same picture with the explanation that they are on the way to retrieve the remains of their children who died in a plane crash). In subjects without brain damage, their memory of the traumatic photograph would be enhanced as that memory would have stored itself in the amygdala. In other words, in healthy subjects, the experience of viewing a photograph of parents on the way to retrieve the remains of their dead children would be startling and horrifying enough to "register" on their brains: their memories would be seared into them. It is probably what Plato was trying to articulate when he gave the metaphor of a wax imprint for memory; certain things

leave their mark. But this is not the case with in people with damage to their amygdala.

Furthermore, these memories when stored in the amygdala are encoded primarily for their "gist" – their overall feel, the generalized emotional response that they elicit, rather than for the details of the event. This is a crucial point. Subjects with amygdala damage showed worse gist memory under emotionally encoding experiences rather than under neutral encoding experiences. This result was not exemplified with patients who had medial temporal lobe damage, including to the hippocampus, but excluding the amygdala. This again confirmed that the amygdala is the locus of the generalized gist of an emotional experience. In addition, the amygdala can affect both medial temporal lobe structures during the encoding of a memory as well as participating in fear conditioning independently of the hippocampus. There is also evidence that it has a limited role in declarative memory (Gabrieli, 1998, 92), and in its relationship to the hippocampus it is bidirectional as it both influences and is influenced by the hippocampus, thus making the amygdala crucial in its role in various memory systems (Adolphs, Tranel & Buchanan, 2005, 516).

Memory is in a labile state when it is first acquired. Neurotransmitters, such as acetylcholine, dopamine and glutamate, conduct the synaptic and cellular mechanisms, insuring either a continuation of the signals (long-term potentiation - LTP) or long-term depression – LTD. These "up" or "down" signals convey not only discrete bits of information that determine whether the stimulus is continued or not, they create patterns as well. Thus the amygdala participates in both implicit memory formation via fear conditioning and explicit memory formation via aversive reaction to remembered negative stimuli.

To Know Yet Not Know

Two things are worth noting. The already obvious point that emotions can embed experience in a way a neutral context cannot, and that a memory must transition from its initially coded state to a more permanent one. The latter can be accomplished in two distinct ways: either through time or through sleep. "It came to me in a dream…" is perhaps more true than we used to think.

"I dream of painting and then I paint my dream", Van Gogh was quoted as saying. He was also quoted as saying, "Poetry surrounds us everywhere, but putting it on paper is, alas, not so easy as looking at it." It is easy, when viewing an artwork, to describe the lines, the colors, the shapes, the objects depicted. Van Gogh for example did quite a bit of that. It is much harder to encapsulate and

translate the meaning – to put down the poetry. This is the function of a critic, and the task is quite difficult. When we look at a van Gogh what are we taking away from that experience? What does a van Gogh mean?

People are always quite moved when they stand in from of a van Gogh. It is not a cooling experience. It is about a naked, unadorned reality – the tempestuousness of everyday perceptual fact that in turn seems mildly generous and decorative but is, with a mere slight of one's head – like those hologram cards that switch between Elvis sequined and Elvis naked – immediately destabilized, and somewhat threatening in its psychedelic unfolding of the deeper reality. Emotions broiling, thoughts unhealed. Life blazed for van Gogh, heeded by the call to its immanent decay. For him, it was always a hot fire and reality was always bare.

It is the job of philosophy to tell us what's meaningful and how exactly it is that it becomes meaningful. Philosophy breaks up into its segregated disciplines as it "cleaves the animal at the joints" (to paraphrase Aristotle): logic tells us about the syntax of our reasoning, epistemology about how we absorb knowledge, metaphysics tells us about the reality that is absorbed before it is absorbed. And aesthetics is supposed to tell us something about art.

But our recent understanding of the brain tells us that we don't always tell ourselves everything. Language constructs only those things the declarative brain has access to. And the declarative brain is not the know-it-all it pretends to be. Our reality is concatenated (to steal a word from Kant) – it is pieced together from bits of data that are formed in the process of absorption. As the data enters us we process it in ways that fundamentally constructs the form the data now takes for us – unprocessed material is unformed material. In a fundamental way, it is non-existent. At least, again to steal from Kant, phenomenologically. Both Kant and Nelson Goodman were correct about this. The important fact now available for us is that much of what we concatenate – much of what our brain has processed and is now using – is unavailable for the declarative, language part of our brains. And yet we can be said to still "know" it. Trauma victims, for example, are not able to necessarily linguistically access the source of their trauma or even to recall it consciously, yet they "know" it. Our knowledge of how to ride a bike, or swing a golf club, is procedural knowledge held in the nondeclarative memory system and while we can be said to "know" it we cannot access that information linguistically. We need to show it to someone, not tell someone. And if quizzed on this knowledge and pressured into explaining it, we will seem to not know. We will seem stupid.

A related point was much of Wittgenstein's thesis in *The Philosophical Investigations*: inductive knowledge is powerful yet often without explicit,

linguistic guiding posts. Different parts of the brain absorb data differently, use it differently, and recall it differently. The nondeclarative memory system is dispositional, and we use it when we are embedded in that particular task, often a physical task.

Art is an activity, in part a mental one and in part a physical activity, one that is repeated over and over, until the artist develops a practice. In fact, that word "practice" is often used by artists in referring to their own art. "My practice" embeds within it one's habitual use of not only images and materials, but one's basic intent: the meaning behind one's work. "This is what I do; this is my practice." This notion includes the meaning behind the art – the content of the art – of which one is almost peripherally aware, a tangential force that though motivates the production of art. Like the "gist" of an emotion known only by the amygdala, an artist's practice is that intentional and dispositional force that is not amenable to detailed description, at least by the artist. It is a "gist"; a deeply felt perspective of the world, a profoundly remembered attitude of what it means to be this distinct, physically embedded individual.

And if it is the case, as noted earlier (cf. Packard & Knowlton, 2002, 582), that explicit knowledge of an instance of caudate-dependent sequence learning can impair the acquisition of that caudate-dependent (i.e., implicit) knowledge, then there is very good reason for artists *not* articulating the detailed explanation of their work. If in fact it is true that there's an inverse relationship between certain kinds of explicit knowledge and implicit knowledge such that "…effortful retrieval of explicit knowledge can interfere with the performance of the implicitly learned…" task, then the demand for the dominance of declarative retrieval needs to be rethought. The argument would be that an artist articulating the meaning behind his or her own work would be similar to the experiments with subjects and the weather prediction task, e.g., there seems to be competition between the caudate section of the basal ganglia and the medial temporal lobe memory system. The recent fMRI study (cf. Poldrack et al. 1999) that shows a negative correlation between the activation in the declarative memory system (e.g, medial temporal lobe) and the nondeclarative memory system (e.g., the basal ganglia) points not only to the problem artists have in articulating their own work but quite exactly to a claim for *not* demanding that.

Artists know but don't always know that they know and furthermore know that if they know they will no longer be able to have that fluid access to knowing without knowing. That can be parsed as follows. Artists often implicitly know things without explicitly knowing them, and furthermore implicitly know that if they explicitly know they will no longer be able to have access to that fluid part of the brain that implicitly knows. The medial temporal lobe will crush the basal

ganglia in triumphant evolutionary zeal. The creative role of the basal ganglia – the role of procedural memory – would be undermined if it were fully translated into the declarative part of the brain. In other words, to gain explicit knowledge of something is, to some extent and in some situations, to loose it.

This though would be viewed differently from the point of view of the critic, as there is no artistic procedural practice and no originating amygdala "gist". Obviously the declarative memory system is primarily involved in the critic's process, and would involve not only the semantic but the other declarative memory system, e.g., episodic, as the critic would also bring in some of his or her own personal associations. But the semantic part of declarative memory would be the main source upon which the critic would rely as it encodes third person objects with designated definitions; art only differs from other human artifacts in that a symbol system has been embedded such that understanding the artwork involves negotiating the relationship between the sign and the thing signified. But this language – again, as Wittgenstein was correct to point out – is socially arrived at, and precludes a private language. We can look at a Pollock and agree on what it "is saying" because we agree on the use of symbols. In that it is different from the recognition of a cup, a mountain, or any other noun. Artworks encode meaning. And because they do, they have value. But for our current purposes it is important to note that the act of looking at an artwork is similar to looking at any other object in that we have not only jointly defined that object, but because the neurological process of viewing an external, empirical object is identical in each of us and involves well known processes.

But the same thing would not be true from the point of view of the artist. If the hippocampus controls memory acquisition for cognitive functions while the basal ganglia controls memory acquisition for habit formation and procedural memory, it is reasonable to postulate that creative thinking and production involve at least both of those regions of the brain, though again, that relationship may sometimes be competitive while at other times being cooperative. Memories are stored in the brain through the cellular processes involved in the changes of synaptic strength, and the hippocampus is the source for processing memory about events and ideas. While the ability to discuss others' work (i.e., to function as a critic) would involve the articulation of facts in the world that are similar to discussing other third-person objects, the ability to make objects would stem from other sources especially the habit formation region. It takes a lot of repeated actions to form a habit; it takes a lot of making art to find one's practice – to find one's own voice. This would make those regions of the brain much more significant for the artist than for the critic.

Thus the inability of an artist to discuss his or her own work would mean that the process of making the work is stored in memories not accessible to the declarative memory system, such that it would instead be stored in the various kinds of nondeclarative memory systems including procedural, perceptual learning, and classical conditioning. We can know but we can not know that we know, or perhaps more exactly, we cannot access language to tell either ourselves or others what it is that we know. And that's ok. It is perhaps exactly the notion of which van Gogh was aware: "…putting it on paper is, alas, not so easy as looking at it."

And it is the looking at it that counts. Viewers recreate and re-experience the artist's viewpoint. I look at a van Gogh and experience the tumultuousness, the intense emotionality in the instability of the world as it transitions from ultra-saturated and ultra-ripe to almost ebullient decay. Aesthetic theories have often weakly accomplished their goal of explaining what art is doing and how it is doing it. It is perhaps partially due to the reliance on language as philosophy is of course corseted by that milieu, but it is also because aesthetics has seen art as either a material artifact easily translatable into language; an experience similar to other physical pleasures; or a platonic transformation of beauty into fact. It is none of those things. It is the recreation in the viewer of the various parts of the artist's brain that is constituent of experience qua experience: the intense "gist" recorded in the amygdala, the procedural learning in the caudate, the habit formation along with the perceptual learning and conditioning in the larger basal ganglia, combined again with the episodic memories stored in the hippocampus and that region's role in the declarative memory system. It is experience, experienced both explicitly and implicitly. The experience of an individual, embedded in a physical body, the caretaker of memories, processer of thoughts; experience profoundly felt and deeply cared about. Whether they will find that in one of the 2,500 slices of H.M.'s brain is to only be hoped…

Works Cited

Adolphs, R., Tranel, D. & Buchanan, T. W. (2005). Amygdala damage impairs emotional memory for gist but not details of complex stimuli. *Nature Neuroscience,* **8,** 512-518.

Budson, A. E., Price, B. H. (2005). Memory dysfunction. *N Engl J Med.,* **352**, 7.

Diekelmann, S. & Born, J. (2007). One memory, two ways to consolidate? *Nature Neuroscience,* **10**, 1085-1086.

Gabrieli, J. D. E. (1998). Cognitive neuroscience of human memory. *Annu. Rev. Psychol.,* **49**, 87-115.

Goda, Y. (2008). Along memory lane. *Nature,* **456**, 590-591.

Houk, J. C., Davis, J. L. & Beiser, D. G. (1995). Models of Information of Processing in the Basal Ganglia. Cambridge, Mass: MIT.

LeDoux, J. (1996). *The Emotional Brain*. NY: Simon & Schuster.

Ofen, N., Kao, Y. C., Sokol-Hessner, P., Kim, H., Whitfield-Gabrieli, S. & Gabrieli, J. (2007). Development of the declarative memory system in the human brain. *Nature Neuroscience,* **10**, 1198-1205.

Packard, M. G. & Knowlton, B. J. (2002). Learning and memory functions of the basal ganglia. *Annu. Rev. Neurosci.,* **25**, 563-93.

Poldrack, R. A. & Packard, M. G. (2003). Competition among multiple memory systems: converging evidence from animal and human brain studies. *Neuropsychologia,* **1497**, 1-7.

Poldrack, R. A., Prabhakaran, V., Seger, C. & Gabrieli, J. D. E. (1999). Striatal activation during cognitive skill leanrning. *Neuropsychologia,* **13**, 564-74.

Sherry, D. F. & Schacter, D. L. (1987). The evolution of multiple memory systems. *Psychol. Rev.,* **94**, 439-54.

Squire, L. R. (2004). Memory systems of the brain: a brief history and current perspective. *Neurobiology of Learning and Memory,* **82**, 171-177.

In: Structural Analysis
Editor: M.L. Camilleri, pp. 21-50
ISBN: 978-1-61668-987-2

Chapter 2

THE STRUCTURE AND FUNCTION OF VEGETAL ECOSYSTEMS OF SEMIARID AREAS IN NORTHEASTERN MEXICO

P. Rahim Foroughbakhch*, Glafiro J. Alanis Flores, Jorge L. Hernández Piñero and Artemio Carrillo Parra
Facultad de Ciencias Biológicas, UANL, A.P. F-2, 66451 San Nicolás de los Garza, N.L., México

Introduction

True solutions to the problems of arid and semiarid zones throughout the world require a mandatory previous evaluation of the natural resources from the study areas. Our main approach is driven to the structure and functioning of the vegetal ecosystems which intimately involves various interrelated elements such as flora, cattle, and other fauna, taking also into account management and commercialization of wooden and non wooden products.

A great part of the Mexican republic is located in the world desert belt with approximately 20 million hectares, 18 million located in the northeast of the country, mainly covered by xerophytic shrub vegetation (Rzedowski, 1978, Palacios, 2000). There is no evidence to date about the origin of the different types of shrub populations growing as natural climax vegetation.

* E-mail address: rahim.f@gmail.com rahimforo @hotmail.com. Tel/Fax (+52) 8181143465

Structurally, a great part of the semiarid ecosystems is composed of wooden shrubs somehow called "matorral" or thornscrub growing under diverse climatic conditions all over from stony or rocky soils, saline and non saline areas with accelerated erosion to areas located at the base of the mountains (SAG, 1975). This type of vegetation is characterized by the occurrence of diverse structures (Follet, 2001), biological forms and floristic diversity (WWF, 2001). The practice of under-controlled overgrazing in this area ranks in the third place in importance within the forest destruction causes after agricultural clearing and irrational forest exploitation. This is done because of the need of the farmer to survive who incurs to cattle ranch activities but without considering a sustained use of the vegetation neither the implementation of management techniques which unavoidably affect the vegetation at the end (French, 1979).

It is important to remark that despite anthropogenic activities have been severe in some localities they have not yet replaced or totally eliminated the ecosystems in semiarid zones (Crains et al., 2000). However, current scrubs could be occurring as secondary or disclimax vegetation as a consequence of the overgrazing of savanna scrubs, *i.e.* open scrubs mixed with natural pasture or great extensions of natural pasture disseminated even before colonial times. Similar circumstances have occurred in the invasion process of shrubs and woody vegetation over great extensions of pasture and open savanna throughout the southwest of the United States of America (Hastings, 1965; Jacoby, 1985) which is believed that extended up to the borders of the Tamaulipan Biotic Province (Johnston, 1963; Archer *et a*l., 1988).

Johnston (1963) made a synopsis of the natural vegetation of southern Texas and northeastern Mexico based in documents from chronicler of the XIX century. He mentions that the dominant vegetation was the matorral or scrub, as it is still now, with the exception of two sandy and coastal plains, the White Horse Desert at the south of Texas and the sandy-calcite plains at the northeast of Soto de la Marina, Tamaulipas, which originally were pasture extensions of edafic climax type that were later invaded by scrub vegetation (Peñaloza and Reid, 1989).

Rojas Mendoza (1965) confirmed that the vegetation of the coastal plains has the typical scrub physiognomy with more or less abundant grass in the clear open spaces of the matorral. The climax pasture occurs in southeastern Mexico only in limited portions of the Sierra Madre Oriental Mountains or in other certain areas of the North. Regarding to those changes caused to the original vegetation by cattle it is mentioned that certain groups of plants have remarkably decreased, such as herbs and grasses, while others have increased in density: shrubs, dwarf trees and some succulents such as "nopal" cactus, although the general

physiognomy has been maintained (Maldonado, 1992; Návar, 2004, Foroughbakhch *et al.*, 2006).

Study Area and Environmental Factors

The study area is located in northeastern Mexico between 22°13' and 25° 10' North latitude and 97°45' and 103°50' West longitude. It limits to the North with the United States of America, Durango and Chihuahua States to the West, and Zacatecas and San Luis Potosi States to the South.

The Northeast of Mexico is constituted by three States with distinct physiognomy each: a) Coahuila with a surface of 149,511 km2 (7.68%), b) Nuevo Leon with 64,210 km2 (3.29%) and c) Tamaulipas with a surface of 78,932 km2 (4.05% of Mexico's surface).

According to the Köppen climatic classification this region is located under the influence of a climate ranging from hot semidry, semiarid, subhumid, and temperate to a very dry and desert climate with an average annual temperature of 22-26°C and a mean precipitation of 600-800 mm. Thus the climate is extreme.

Precipitation intensity (amount per unit time period), soil characteristics (e.g., texture and antecedent moisture conditions), and soil-surface features together determine whether precipitation events result in infiltration or runoff (Whitford 2002, Breshears et al., 2003). If precipitation intensity exceeds the soil infiltration rate, runoff will be generated – increasing the potential for soil erosion.

Soils in northeastern Mexico vary according to the FAO/UNESCO/ISRIC classification from vertisol, chesnut towards the south, good for agriculture, and leptosol in mountain forests, to regosol, calcisol and greyzem in the North area. In the Mountain chain areas litosol and xerosol with superficial hard rock occurs. Soil resources, including mineral nutrients, organic matter (including litter), water, and soil biota, are fundamental determinants of ecosystem structure and function (Jenny 1980, Vitousek 1994, Reynolds et al. 2003). Due to low rates of weathering and pedogenic processes in dryland environments, the relative importance of parent material as a determining factor of soil properties generally increases with aridity (Jenny 1941).

In general, water has been described as the soil resource that most commonly limits the productivity of dryland ecosystems (Noy-Meir 1973, Ehleringer et al. 2000). Water resources in northeastern Mexico have been considered as low or scarce. It is important to remark that there are interconnections between the surface and subterranean water bodies and that the former integrate hydrologic basins which represent ecological systems where main streams are interconnected.

The retention of limiting water and nutrient resources is essential for sustaining the structure and functioning of dryland ecosystems (Ludwig and Tongway 1997, 2000). Dynamic soil properties important for water and nutrient retention include soil structure, infiltration capacity, soil-surface roughness, organic matter content, soil aggregate stability, and soil biotic activity (Herrick et al., 2002).

Vegetative Types of Desert (BW), Semidesert (BS) and Temperate Subhumid (C(W)) Ecosystems in Northeastern Mexico

At a broad level, vegetation is generally recognized as the dominant functional type in terrestrial ecosystems. In addition to conducting photosynthesis, aboveground structures of vascular plants protect soil from erosive raindrops, obstruct erosive wind and overland water flow, and enhance the capture and retention of soil resources (Miller & Thomas, 2004). Vegetation provides fuel for fire, as well as resources and habitat structure for belowground and aboveground organisms ranging from fungi and bacteria to birds and large mammals (Wardle 2002). Finally, carbon storage and the mediation of earth-atmosphere energy/water balances are additional plant functions that are increasingly emphasized by researchers investigating global-change processes (Breshears and Allen 2002, Asner et al. 2003). Small trees, shrubs, dwarf shrubs, and perennial grasses are the vegetative life forms with the greatest effects on the structure and functioning of dryland ecosystems.

Vegetation is considered as the most immediate manifestation of the environmental factors. Due to these factors major parts of the coastal plain is covered by matorral. The vegetation types occurring in northeastern Mexico have been classified by COTECOCA (1973) and Rzedowski (1978) according to their botanical and ecological characteristics in the following groups:

Semiarid Ecosystems with Tall Shrubs

Structurally the following types of vegetation dominate in these ecosystems:

High Thornscrub

This type of vegetation is located at the piedmont of the Sierra Madre Oriental adjacent to the subinermis high matorral and the subinerm medium matorral; it is characterized by the predominance of tall shrubs or small trees 3 to 5 meter high. The dominant species in the area are *Helietta parvifolia, Diospyros palmeri, Acacia berlandieri, Celtis pallida, Zanthoxylum fagara, Acacia rigidula, Cordia boissieri, Leucophyllum texanum, Pithecellobium pallens,* and *Schaefferia cuneifolia.*The most abundant graminae are: *Bouteloua filiformis, Leptochloa dubia, Bouteloua trífida, Setaria marcostachya* and *Cenchrus pauciflorus*.

Tamaulipan Thornscrub

This community is located in the North of Nuevo León State, extending into Coahuila to the North and Tamaulipas to the Northeast. From the historical point of view the description of the biotic unit of the Tamaulipan thornscrub is owed to Muller (1974) defining it as an ecological system of a great floristic diversity with tall thorny arboreal species including abundant herbaceous and grass species. This author located its distribution to the east of Sierra del Carmen and Sierra Madre Oriental in Coahuila, in the southeast of Texas, in the north of Nuevo León and Tamaulipas and in the coastal plain of the Gulf of Mexico, listing the characteristic species *Acacia rigidula*, *Cercidium texanum*, *Acacia berlandieri*, *Lippia ligustriana*, *Guaiacum angustifolum*, *Acacia farnesiana*, *Castela teaxana*, *Prosopis glandulosa*, *Colubrina texensis*, *Cordia boissieri*, *Shaefferia cuneifolia*, *Lantana camara*, *Parkinsonia aculeata*, *Diospyros texana*, *Lycium berlandieri*, *Lysium pallidum*, *Viguiera stenoloba*, *Bumelia lanuginosa*, *Yucca rostrata*, *Opuntia lindheimeri*, *Eysenhardtia texana*, *Sophora secundiflora*, *Leucophyllum minus*, *Salvia balloteaflora*, *Celtis pallida*, *Opuntia leptocaulis*, *Condalia lyciodes*, *Jatropha dioca*, *Koeberlinia spinosa*, *Opuntia imbricada*, *Agave lechuguilla*, *Condalia hookeri*, *Leucophyllum frutescens*, *Bernardia myricaefolia*, *Forestiera angustifolia, Citharexylum berlandieri*, *Karwinskia humboldtiana* and *Microrhammus ericoides*. He also reports that the genera *Larrea* and *Flourensia* are also present in the North part in the borders of Nuevo León and Coahuila.

It is important to notice that in the Tamaulipan thornscrub is possible to find small patches of Quercus (*Quercus virginiana, Q. fusiformis*) in alluvial soils and humid habitats at the mid north of the State living together with some other species such as *Sapindus saponaria*.

Caducifolious Prosopis Forest

This vegetal community broadly distributed in Mexico, sometimes as apparent secondary vegetation. It is frequently found growing within the communities of the Tamaulipan thornscrub in deep clay soils over river terraces or stream banks where mezquitales are located with both high capacity to adapt to clay soils and high salinity tolerance. This type of vegetation is dominated by mesquite species with arboreal components 4 to 10 meter high with well defined trunks wider than 60 cm in diameter. This type of vegetation is surrounded by the high thorny matorral which is characterized by the predominance of leguminosae species. The most important representatives are *Prosopis glandulosa, Acacia berlandieri, Acacia wrigthii, Acacia rigidula, Celtis pallida; Ebenopsis ebano, Opuntia engelmannii, Randia rhagocarpa, Yucca filifera,* and *Zanthoxylum fagara.* The most abundant graminae are *Bouteloua trífida, Aristida spp.* and *Setaria macrostachya.*

It is common in northeastern Mexico to find mixtures of mesquite with *Olneya tesota* and *Cercidium spp* being the latter the dominant species. Due to technical and methodological characteristics these two species and part of the thorny forest or lower thorny forest are joined in this group.

Submountain Matorral

This community is mainly composed of inermis (without prickles or thorns) and caducifolious elements of short duration. It grows between the borders of the arid matorral, oak forest and lower caducifolious forest, especially both lower sides of the Sierra Madre Oriental in their northern portion.

It is a shrubby and arboreal formation rich in a variety of life forms. Vigor, size and distribution of the dominant and co-dominant species are subjected to the type of soil and its available moisture content. The occurring dominant biological forms are shrubs or trees 4 to 6 meter high with short leaves, caducifolious and subthorny. It is located in the lower slopes of the Sierra Madre Oriental mountain chain. In fact this type of vegetation forms an extended barrier that separates the elements of the tamaulipan arid and thorny matorral in the plains from the subhumid or dry forest occurring in the mountain slopes.

Despite the existence of some morphological and ecological variations the most representative species in general are: *Helietta parvifolia, Cordia boissieri, Gochnatia hypoleuca, Neopringlea integrifolia, Decatropis bicolor, Fraxinus greggii, Havardia pallens, Leucophylum frutescens, Acacia amentacea, Acacia*

berlandieri, Acacia farnesiana, Caesalpinia mexicana, Prosopis spp Dyospiros palmeri, D. texana, Zanthoxylum fagara, Flourencia laurifolia, Karwinskia humboldtiana, Leucophyllum sp and *Pithecellobium pallens*. In some protected habitats with plenty of moisture and deep soil some small clusters of *Quercus* can be found.

In this type of vegetation the Chinese palm presence is remarkable due to its aspect. Other species occurring in this matorral are S*olanum erianthum, Mascagnia macroptera, Jacobinia spicigera, Hibiscus cardiophyllus* and *Rubus afftriviales*.

Herbaceous Vegetation – Grazing Lands

Grazing lands are vegetal communities characterized by the dominance of herbaceous species with long and narrow leaves specially graminae although some other families may also be present such as Compositae, Leguminosae and Chenopodiaceae. The natural climax grazing lands occupy reduced extensions and common associations of graminoids are found in open spaces within some other community types such as the matorral. In special sites with specific edaphic conditions, soil with insufficient drainage, prone to floods and with abundant salts and gypsum some grazing species, called gypsophiles, may also be found.

In the northeast of Mexico there is a partial open grazing land which is characterized by the presence of such species as *Bouteloua gracilis*, *Boutelova curtipendula*, *Boutelova irsuta* and *Tridens muticus*. In gypsum calcareous soil *Bouteloua chasei* is also found. This gypsophilous grazing land can be found mixed with the desert microphyllous scrubland.

In saline soils and closed basins it is found an open halophyte graze land with the following typical species: *Hilaria mutica*, *Hilaria jamesii*, *Sporobolus tiroides* and *S. pyramidatus*. Besides, there may be mixtures of halophyte shrubby scrub species such as *Atriplex canescens, A. confertifolia* and succulent species such as *Sauceda spp*. A variant of this type of graze land is located in small sites in open areas of the thorny tamaulipan like scrubland.

The open bunch grazing land located in shallow soils of colluvial origin occurs in the transition zone between the halophyte grazing land and the mountainous zone. This graminae community is characterized by the presence of plants with thin, narrow and long leaves; botanically these leaves are fasciculate which confer a bunchy aspect to the grazing land. The species belonging to this community are *Bouteloua gracilis*, *Boutelova curtipendula*, *B.*

uniflora, *Tridens muticus*, *Eragrostis hagens*, *Heteropogon contortus* and *Muhlenbergia mundula*.

Semiarid Ecosystems with Median Size Shrubs

Intermediate Subinerm Matorral

It is found adjacent to the high subinerm matorral and the high thorny matorral and it is characterized by the predominance of middle size shrubs 1 to 2 meters high. The most important components are *Acacia rigidula, Cercidium floridium, Celtis pallida, Prosopis glandulosa, Condalia obovata, Acacia farnesiana*; while the most important graminae species are: *Bouteloua trifida, Cenchrus pauciflorus* and *Leptoloma cognatum*.

Subtropical and Temperate Ecosystems with Medium and Tall Trees

Sclerophyll Oak Forest

It is located in the mountainsides; east to the Sierra Madre Oriental chain and adjacent to the pine-oak forest and to the high subinerm matorral. It is characterized by the presence of mid size trees 8 to15 meters high. It is a forest inhabited by individuals of the genus *Quercus* in highly diverse ecological conditions at altitudes from 600 to nearby 2000 masl. The main species in this type of vegetation are the following: *Quercus fusiformis, Q. laceyi, Quercus canbyi, Quercus glaucoides, Juglans spp., Hicoria pecan, Ungnadia speciosa, Arbutus arizonica.* The most abundant graminae are: *Setaria texana, Bouteloua curtipendula, B. hirsuta,* and diverse species of *Bromus spp.*

Pine And Oak Forest

It is located in the upper parts of the Sierra Madre Oriental Mountains adjacent to the oak forest. It is composed of trees 10 to 18 meters high dominated by the species of the genus *Pinus* and *Quercus*. It develops under different

ecological conditions, being frequent in forest areas highly exploited or in disturbed conditions of the pine or pine-oak forest.

The dominating species in this vegetation type are the following: Quercus rysophylla, Quercus polymorpha, Quercus canbyi, Quercus mexicana, Quercus cupreata and different species of pines such as Pinus pseudostrobus, P. montezumae, P. teocote, Arbutus xalapensis and Ugnadia speciosa. The most important graminae species are: Bouteloua curtipendula, Setaria texana, and Poa mulleri.

Lower Caducifolious Jungle

It is a jungle which may reach 10 to 15 m (in tropical and subtropical ecosystems of Tamaulipas State) growing in warm subhumid, semidry or dry climate where most of the individuals (75-100%) throw their leaves during the dry season which is long lasting. Dominant trees are commonly inermis. It is broadly distributed over the sides of hills with well drained soils in the coast of the Tamaulipas State and may be in contact with the intermediate jungle, forest and matorral of semiarid zones. It is frequent to find communities of *Bursera spp*, *Lysilomia spp*, *Jacaratia mexicana*, *Ipomoea spp*, *Pseudoborbax palmeri*, *Erithryna sp.*, *Ceiba sp*. and *Cordia sp*.

Arid Ecosystems with Short Shrubs

Desert Vegetation

This community is the most representative of the arid zones of northeastern Mexico where numerous endemic species grow. These species are identified in the official list of the Mexican government for species at risk NOM-059-SEMARNAT-2001 in any of the existing risk categories (Table 1). This type of matorral is described as follows.

Table 1. List of the occurring flora in the matorral and grazing lands of Nuevo León State as for the norm NOM-059-SEMARNAT-2001.

Family	Genus	Species	Common name in the studied area (Spanish)	Category	Distribution
Agavaceae	*Agave*	*Bracteosa*	Maguey huasteco	T	Not endemic
	Agave	*Victoria-reginae*		E	Endemic
Cactaceae	*Ariocarpus*	*Kotschoubeyanus*	Biznaga-maguey pata de venado	Pr	Not endemic
	Ariocarpus	*Retusus*	Biznaga-maguey, peyote común	Pr	Not endemic
	Ariocarpus	*Scapharostrus*		E	Endemic
	Ariocarpus	*Trigonus*	Biznaga-maguey chautle	T	Endemic
	Astrophytum	*Asterias*	Biznaga-algodoncillo de estrella, cacto estrella	E	Endemic
	Astrophytum	*Capricorne*	Biznaga-algodoncillo de estropajo	T	Endemic
	Astrophytum	*Myriostigma*	Biznaga-algodoncillo de mitra	T	Endemic
	Astrophytum	*Ornatum*	Biznaga-algodoncillo liendrilla	T	Endemic
	Aztekium	*Hintonii*	Biznaga-piedra del yeso	Pr	Endemic
	Aztekium	*Ritteri*	Biznaga-piedra viva	T	Endemic
	Coryphantha	*Poselgeriana*	Biznaga-partida de Poselger	T	Endemic
	Coryphantha	*Pseudoechinus*	Biznaga-partida de falsas espinas	Pr	Endemic
	Echinocactus	*Platyacanthus*	Biznaga-tonel grande	Pr	Not endemic
	Echinocereus	*Knippelianus*	Órgano-pequeño	T	Endemic
	Echinocereus	*Longisetus*	Órgano-pequeño de cerdas largas	Pr	Endemic
	Echinocereus	*Poselgeri*	Sacasil	Pr	Not endemic
	Echinomastus	*Mariposensis*		T	Endemic
	Epithelantha	*Micromeris*	Biznaga-blanca chilona	Pr	Not endemic
	Ferocactus	*Pilosus*	Biznaga-barril de lima	Pr	Not endemic
	Geohintonia	*Mexicana*	Biznaga-del yeso	Pr	Endemic
	Leuchtembergia	*Principis*	Biznaga-palmilla de San Pedro	T	Endemic
	Mammillaria	*Carretii*	Biznaga de Icamole	Pr	Endemic
	Mammillaria	*Klissingiana*	Biznaga de Calabazas	T	Endemic
	Mammillaria	*Lenta*	Biznaga de Biseca	T	Endemic
	Mammillaria	*Plumosa*	Biznaga plumosa	T	Endemic
	Mammillaria	*Sanchez-mejoradae*		E	Endemic

Table 1. Continued

Family	Genus	Species	Common name in the studied area (Spanish)	Category	Distribution
	Pelecyphora	*Strobiliformis*	Cacto piña de pino	T	Not endemic
	Peniocereus	*Greggii*	---	Pr	Not endemic
	Thelocactus	*Macdowellii*	Biznaga-pezón de Macdowell	T	Endemic
	Thelocactus	*Tulensis*	Biznaga-pezón de Tula	T	Endemic
	Turbinicarpus	*Beguinii*	---	Pr	Not endemic
	Turbinicarpus	*Hoferi*	Biznaga-cono invertido de Hofer	T	Endemic
	Turbinicarpus	*Mandrágora*	Mandrágora	T	Endemic
	Turbinicarpus	*Pseudopectinatus*	Peyotillo pectinado	Pr	Not endemic
	Turbinicarpus	*Schmiedickeanus*	Uñita	T	Endemic
	Turbinicarpus	*Subterraneus*	Biznaga-cono invertido subterránea	T	Endemic
	Turbinicarpus	*Swobodae*	Biznaga-cono invertido	T	Endemic
	Turbinicarpus	*Valdezianus*	Biznaga-cono invertido de Valdez	Pr	Not endemic
Frankeniaceae	*Frankenia*	*Johnstonii*	---	E	Not endemic
Nolinaceae	*Calibanus*	*Hookeri*	---		
	Dasylirion	Longissimum	Sotol vara cohete, junquillo, sotol manso	T	Not endemic
Palmae	Brahea	Berlandieri	Palma Berlandier	Pr	Endemic
Zamiaceae	Dioon	Edule	Chamal o palma de Dolores	T	Endemic

T= threatened, Pr= protected, E= endangered

Desert Rosetophyllous Vegetation

This is a vegetal community characterized by the dominance of species with rosette like leaves with or without thorns, generally acaulescent (stemless) although rosette species with well developed trunks are typical. This community grows in the slope of the hills over rock outcrops or skeletal soils or lithosols, over shallow soils in lower hills, in the higher parts of alluvial fans or over conglomerates. Its distribution is wide over arid and semiarid zones. In these areas the matorral lose vigor and covering, decreasing its floristic richness and the size of the individuals of the main species. The components that dominate this matorral are conspicuous elements characterized by presenting succulent leaves grouped in rosettes, some with terminal thorns each called a mucron.

The most common species are Dasylirion berlandieri y D. texanum, Hechtia glomerata, Agave striata, Agave bracteosa, Agave lechuguilla, Euphorbia antisyphilitica, Opuntia leptocaulis, Opuntia microdasys, Echinocactus platyacanthus, Ferocactus pilosus and Oputia spp. In some places Yucca treculeana, Dasylirion longissimum and Fouqueria splendens are found.

Desert Microphyllous Vegetation

This type of vegetation is characterized by the dominance of shrub species with short aromatic leaves or leaflets growing mainly over alluvial terrains in arid and semiarid zones in the north of Mexico. Numerous cacti of round or plain stems are found and other plants such as the desert plant (*Yucca filifera*) as the most noticeable elements. It is located abundantly in plain terrains or in lower alluvial fans of the Mexican Altiplano hills.

The typical species of this type of vegetation are: gobernadora (*Larrea tridentata*), hojasén (*Flourensia cernua*), Mariola (*Parthenium incanum*), candelilla, albarda, afinador (*Mortonia greggii*), guayule (*Parthenium argentatum*), quebradora (*Lippia ligustrina*), popotillo (*Ephedra aspera*), biznaga de dulce, chaparro prieto, chaparro amargoso, huajillo, granjeno, mezquite, palma pita, palma samandoca (*Yucca carnerosana*), órgano (*Marginatocereus marginatus*), nopal cegador (*Opuntia microdasys*), coyonostle, nopal rastrero (*Opuntia rastrera*) and tasajillo. In some places in the south of the State succulent, rosette scrubs or crassulaceae are found i.e. branched cacti with succulent stems where garambullo (*Myrtillocactus geometrizana*) is the most noticeable species.

Desert Microphyllous Vegetation with Palms or Izote Plants

This is a variant of the desert microphyllous vegetation with abundant compact groups of desert palms or pita palms with remarkable elements or eminences making some small forest patches of palms associated to this type of scrub. They are located in flat places or alluvial fans of the hills on the Mexican Altiplano. The main species that make this type of vegetation are Palma loca (*Yucca filifera*) and Palma samandoca. Typical species are: gobernadora, hojasén, panalero, cruceto (*Condalia lycioides*), chaparro prieto, agrito (*Berberis trifoliata*), popotillo (*Ephedra aspera*), tasajillo, coyonostle, nopal rastrero and nopal cegador.

Sand Desert Vegetation

These are vegetation patches invading dunes or arid zones getting established progressively, generally coming from neighboring areas which are frequently composed of *Prosopis spp* (mesquite tress), *Larrea tridentata* (gobernadora), *Opuntia spp* (nopal), *Atriplex spp* (saladillo), *Ambrosia dumosa* (hierba del burro), *Ephedra trifurca*, Dalea *emoryi, Eriogonum desertícola, Petalonyx thurberi, Coldenia palmeri, Hilaria rigida, Hymenoclea monogyra,* etc.

The presence of the above mentioned species in the different ecosystems indicates that they are capable to adapt to the different ecological conditions showing their high competitive advantage in so extremely different ecosystems.

Biological and Utility Value of Plants from Arid and Semiarid Ecosystems

With the established methodology all the taken data allowed to make a structural analysis on the arid and semiarid ecosystems in northeastern Mexico based in the existing vegetal resources, their use and management of each one of them. This analysis has contributed with useful information about the floristic composition of vegetal ecosystems, the number of species and their ecological behavior.

Vegetal communities in interrelation with the climatic, topographic, and soil elements favor the survival and *habitat* of the wild and domestic fauna in addition to the basic and sub-basic products they provide to mankind. Tropical and temperate forests as biological units of dense covering offer ecological stability in

their function as carbon capture, hydrologic cycle, soil protection and biodiversity. In a comparative way the arid and semiarid zones, where vegetal communities with scrub and grazing lands of low covering are present represent the typical characteristics of the ecological conditions of these areas hence rational management of the existing resources might be applied without any transgression to the rules that govern their functioning since these are fragile ecosystems of difficult recovering.

Typical scrub and grazing lands of northeastern Mexico are the masterpiece consequence of evolution and time with a legacy that has resulted in an important ecological biodiversity for hundreds of years which is today admired and used. This plant community extends over plains, hills, crests, slopes and canyons. The plant species composing scrubs and grazing lands and their associations make a vegetal coverage poorly dense although providing a series of products and multiple services from the ecological perspective.

The great floristic diversity existing in the different arid and semiarid ecosystems in northeastern Mexico offers the availability of a comprehensive "material bank" useful to provide:

Table 2. Some species of the useful flora of arid and semiarid ecosystems of northeastern Mexico.

Usage	Common name in the area(Spanish)	Scientific name	Part used and/or method
Construction	Mesquite	*Prosopis glandulosa*	Full stem or sawn lumber
	Ebano	*Ebenopsis ebano*	Full stem
	Encino molino, E. bravo o E. siempreverde	*Quercus fusiformis Quercus virginiana*	Full stem or sawn lumber
	Palma pita	*Yucca filifera*	Stems in house walls and fences
	Palma samandoca	*Yucca carnerosana*	Stems in house walls and fences
	Sotol	*Dasylirion texanum*	Leaves for roof and sheds
Shelves and cattle fences	Mezquite	*Prosopis glandulosa*	Stems for poles
	Ebano	*Pithecellobium ebano*	Stems for poles
	Barreta	*Helietta parvifolia*	Stems for shelves
	Anacahuita	*Cordia boissieri*	Stems for shelves
	Huizache	*Acacia farnesiana*	Stems for shelves
	Brasil	*Condalia hookeri*	Stems for shelves

Table 2. Continued

Usage	Common name in the area(Spanish)	Scientific name	Part used and/or method
Living fences	Albarda	*Fouqueria splenden*	The whole plant
	Nopales	*Opuntia ssp*	The whole plant
	Plama pita o china	*Yucca filifera*	The whole plant
	Palma samandoca	*Yucca carnerosana*	The whole plant
Making of tillage instruments	Tenaza	*Havardia pallens*	Stem for shovel shafts
	Barreta	*Helietta parvifolia*	Stem for axe handles
	Anacachuita	*Cordia boissieri*	Stems for plows
	Guayacán	*Guaiacum angustifolium*	Stem for machete handles
	Coma	*Burnelia lanuginosa*	Stems for yoke beams
Furniture and utensils manufacture	Tenaza	*Havardia pallens*	Stem for chairs and rockers
	Tenaza	*Havardia pallens*	Stems for baskets and moorings
	Mezquite	*Prosopis glandulosa*	Stems for chairs and banks
	Ébano	*Pithecellobium ebano*	Stems for chairs and banks
Construction of rural transportation devices	Mezquite	*Prosopis glandulosa*	For wagon axles
	Ébano	*Ebenopsis ebano*	Hard stems for tables and wagon wheels
Firewood and vegetal charcoal	Mezquite	*Prosopis glandulosa*	Stems and branches
	Ébano	*Ebenopsis ebano*	Stems and branches
	Brasil	*Condalia hookeri*	Stems and branches
Fiber production	Lechuguilla	*Agave lecheguilla*	Ixtle fibers
	Cortadillo	*Nolina sp*	Fibers from the leaves
	Palma pita	*Yucca filifera*	Palm ixtje fibers from the leaves
	Palma samandoca	*Yucca carnerosana*	Palm ixtje fibers from the leaves
Production of wax and raw material for rubber manufacture	Candelilla	*Euphorbia antisyphilitica*	Wax from the stems
	Guayule	*Parthenium argentatum*	Raw materials from the whole plant

Table 2. Continued

Usage	Common name in the area(Spanish)	Scientific name	Part used and/or method
Native flora used as ornamentals.	Mezquite	*Prosopis glandulosa*	The whole plant
	Cenizo	*Leucophyllum texanum*	The whole plant
	Ébano	*Ebenopsis ebano*	The whole plant
	Hierba del potro	*Caesalpinia mexicana*	The whole plant
	Anacahuita	*Cordia boissier*	The whole plant
	Laurel de montaña, colorín	*Sophora secundiflora*	The whole plant
	San Pedro o tronadora	*Tecota stans*	The whole plant
	Lantana	*Lantana cámara*	The whole plant
	Palma pita	*Yucca filifera*	The whole plant
	Encino molino, encinobravo	*Quercus fusiformis Quercus virginiana*	The whole plant
Condiments	Orégano de la sierra	*Monarda citriodora*	Leaves for condiments
	Oreganillo	*Lippia graveolens*	Leaves for condiments
Soap and detergent substitute	Calabacilla loca	*Cucurbita foetidissima*	Raw fruit
	Amole de castilla	*Agave bracteosa*	Stems and roots
	Jaboncillo	*Sapindus saponaria*	Ripe fruit
Food	Nopales	*Opuntia ssp*	Ripe fruit, young stem
	Chile de monte o chile piquín	*Capsicum annum var. aviculare*	Fresh and dry fruits
	Pitaya	*Selenicereus spinulosos*	Ripe fruits
	Maguey	*Agave americana*	Cooked flower stem (quiote)
	Palma pita	*Yucca filifera*	Flowers for prepared foods and salads
	Palma samandoca	*Yucca carnerosana*	Flowers for prepared foods and salads
	Ébanos	*Ebenopsis ebano*	Seeds as coffee substitute
	Granjeno	*Celtis pallida*	The ripe fruit is consumed
	Brasil	*Condalia hookeri*	The ripe fruit is consumed
	Coma	*Bumelia lanuginosa*	The ripe fruit is consumed
	Mezquites	*Prosopis glandulosa*	Fresh and dry fruits

Table 2. Continued

Usage	Common name in the area(Spanish)	Scientific name	Part used and/or method
Alcoholic beverages	Maguey	*Agave americana*	Beverages and "mezcal" from stems
	Sotol	*Dasylirion texanum*	A "sotol" called beverage obtained from stems
Forage	Mezquite	*Prosopis glandulosa*	Leaves, young branches and fruits
	Cuajillo	*Acacia berlandieri*	Leaves and young branches
	Vara dulce	*Eysenhardtia polystachya*	Leaves and young branches
	Guayacán	*Porliera angustifolia*	Leaves
	Nopales	*Opuntia ssp*	Young and mature stems
	Chamizo	*Atrilpex canescens*	Leaves and young stems
	Navajita roja	*Bouteloua trifida*	Leaves and young stems
	Navajita azul	*Bouteloua gracilis,*	Leaves and young stems
	Zacate toboso	*Hilaria mutica*	Leaves and young stems
	Pajita tempranera	*Setaria spp.*	Leaves and young stems
	Zacate piramidal	*Sporobulus pyramidatus*	Leaves and young stems

a). Food, fuel, fiber, forage, raw material for industries (wax, tannins, pigments) and constructions materials (Table 2).
b). Medicines, taking into account that Mexico counts with about 3,000 species recognized by their curative properties, many of them growing in arid and semiarid ecosystems of northeastern Mexico (Table 3).
c). Toxic plants with their toxic compounds useful in many cases for healing tumor diseases (Table 4).

Overview of the Sustainability and Conservation of Dryland Ecosystems

According to Miller & Thomas (2004) sustainable ecosystems, as defined by Chapin et al. (1996), are persistent. Through the typical pattern of dynamics driven by disturbance events and climatic fluctuations such ecosystems maintain their characteristic diversity of their major functional groups, productivity, and rates of biogeochemical cycling. Inherent in the notions of ecosystem sustainability and persistence is the hypothesis that ecosystems can be driven to transition from one state to an alternative state. Though capable of existing in the

same physical location, these alternative ecosystem states are distinguished by relatively large differences in their structure and their rates of ecological processes such as erosion, nutrient cycling and disturbance. Such differences in structure and processes typically are matched by great differences in ecosystem dynamics. A transition from one state to an alternative state may occur gradually or relatively rapidly as the result of natural processes (e.g., climatic disturbances) or human actions (e.g., land-use activities).

Table 3. Medicinal species, their abundance-dominance and uses of the flora in Villa Santiago, Nuevo León, Mexico. (Source: Valdez Tamez, 2002).

Scientific name	Common name in the area (Spanish)	A.L.	Illness or disease	Part of the plant used	Way of use
Acacia amentácea D.C.	Chaparro Prieto	3	Antibiotic	Bark	H (O)
Acalypha hederácea Torr.	H. del cáncer	1	Wounds, acne	Plant	H (L)
Achillea millefolium L.	Plumajillo		Insomnia, headaches	Leaves	C,I (O)
Ageratum corymbosum Zucc.	H. dulce		N.A.	Leaves	I (O)
Antigonon leptopus Hook & Am.	San Diego	1	Swelling, mumps	Leaves	I (O)
Arbutus xalapensis H.B.K.	Medroño	2	Kidney ache	Leaves	H (O)
Arctostaphylos pungens Kunth	Pinguica	3	Kidney ache	Leaves/flowers	H (O)
Asclepias linaria Cav	Plumita	1	Earache	Leaves	M (L)
Berberis gracilis Benth.	Cuasia	1	Colic, appetite supressant	Stems	H (O)
Bidens pilosa L.	Acahual	1	Kidney ache	Branches	I (O)
Bouvardia termifolia Cav.	Candellio	1	Stitches, scratches	Leaves	I (O)
Budleja scordioides Kunth	Glondrina	1	Blood enhancer	Roots	C (O)
Bumelia lanuginosa Michx	Coma	2	Indigestion	Bark	I (O)
Castela texana	Chaparro amargo	2	Diabetes	Leaves and sprouts	I
Celtis pallida Torr.	Granjeno	2	Headache	Leaves	M (L)
Chilopsis linearis Cav. (Sweet)	Lantrisco		Expectorant	Leaves, flowers	C (L)

Table 3. Continued

Scientific name	Common name in the area (Spanish)	A.L.	Illness or disease	Part of the plant used	Way of use
Chimaphila maculata L.	Jikjoñio		Heartbeat	Plant	C (O)
Chimaphila umbellata L.	Ontejol	1	Stomachache	Leaves/stems	I (O)
Chrysactinia mexicana Gray.	Talatencho	1	Stomachache	Plant	I (O)
Clematis drumondii Torr. & Gray	Barba chivo	1	Acne, constipation	Leaves	M (L)
Cordia boissieri DC.	Anacahuita	2	Cough, flu	Fruits	S (O)
Corwania plicata DC.	Rosa castilla	3	Diarrhea, stomachache	Leaves	H (O)
Croton torreyanus	Salvia	1	Cholesterol control	Leaves	H(I)
Cuphea cyanea Wald.	N.A.	1	Love potion	Branches	G (L)
Decatropis bicolor Zucc. Radlk.	N.A.	2	Antibacterial activity	Leaves, branches	I (O)
Desmodium psilo-phyllum Schtdl.	Pega pega	1	Dysentery	Roots	Lo (O)
Dondonea viscosa Jacq.	Cajuele		Postpartum bath	Fresh leaves	I (E)
Dyssodia setifolia (Lag.)Rob.	Paraveña	1	Digestive, emotional	Leaves/stems	C (O)
Equisetum leave - gatum Bartelett	Tull		Diuretic, kidney ache	Branches	I (O)
Eryngium serratum Cav.	H. de sapo		Aphrodisiac	Leaves and roots	I (O)
Eysenhardtia texana scheel	Palo dulce	2	Antibiotic, urinary	Roots, stems	H (O)
Flourensia cernua	Leavesén	2	Diarrhea	Leaves, flowers	H(I)
Geranium seemanni Peyr.	Ranxh	3	Wounds	Plant	P (L)
Gymnosperma nítida Rothr.	Sempiterna		Heart	Flowers	C(O)
Gymnosperma glutinosum Spreg.	Talalencho	1	Rheumatism	Leaves, branches	I (L)
Hedeoma drummondii	Poleo	2	Asthma, bronchitis	Leaves, fruits	I(H M)
Heimia salicifilia (H.B.K.) Link.	Jarila	1	Stomachache, ankle ache	Leaves, branches	T (L/O)

Table 3. Continued

Scientific name	Common name in the area (Spanish)	A.L.	Illness or disease	Part of the plant used	Way of use
Helietta parvifolia (Gray.) Benth.	Barreta	3	Teeth strength	Stem and leaves	I (O)
Juniperus deppeana Steud.	Sabino		Chronic fatigue	Stem and leaves	I (O)
Karwinskia humboldtiana Zucc	Coyotillo	2	Antitumor	Leaf and fruits	I (O)
Lantana cámara L.	Crozuz	2	Cough, scare, kidney, acne	Leaves, stem	H,C (O)
Lepidium virginicum L.	Letejilla	2	Wounds	Leaves, stem	H (L)
Litsea novoleontis Bartlett.	Laurel	1	Cough, asthma, heart	Leaf	I (L9)
Litsea priglei Bartlett.	Laurel	1	Dizziness, asthma, nerves	Leaf	I (O)
Parthenium hysterophorus L.	Cunario	2	Fever, body pain, malaria	Leaf, branches	M (L)
Parthenium incanum	Mariola	1	Arthritis	Leaves, flowers	I
Pinus montezumae Lamb.	Ocote	2	Hoarseness	Stem	H (O)
Pinus pseudo--strobus Lindl.	Ocote	1	Hoarseness	Stem	H (O)
Plantgo major L.	Lantén	1	Tonsils, diarrha,	Leaf	I,C (O)
Polypodium guttatum Maxon.	Calaguale		Pain in bonds	branches	I (O)
Polypodium polypoides L. watt	siempreviva	1	Asthma	branches	I (O) I
Populus tremuloides Michx	Alamillo		Fever, pains	Leaf	I (O)
Pteridium aquilinum L.	Pesma	1	Stomachache	Roots	H (O)
Quercus affinis Scheld.	Encino bco.	3	desinflamatory	Bark	C (O,L)
Quercus laeta Liebm.	Encino laurel	3	desinflamatory	Bark	I (L)
Rhus toxicodendron L.	Hiedra	1	Skin, leprosy, scabies	Leaf, stem	C (L)
Rhus virens Gray. Lindh.	Lantrisco	2	Medicinal	N.A.	N.A.
Stevia saliciforma Cav.	Chacal	1	Tonsils, diarrhea, asthma	branches	M (L)
Tagetes lucida Cav.	Pericón	1	Postpartum bath	Plant	C (L)

Table 3. Continued

Scientific name	Common name in the area (Spanish)	A.L.	Illness or disease	Part of the plant used	Way of use
Teucrium cúbense Jacq.	Gallina ciega	1	Indigestion	Leaf, roots	H (E)
Salvia spp	*Salvia*	2	Parkinson, hemorrhage	Leaf	I (L)
Selaginella lepidophylla Gray	Flor de peña		Kidney, bronchitis	Plant	I (L)

C= cooking, E= external, H = boiled, I= Infusion, s = syrup, L= local, Lo= Lotion, M= macerated., Mo= ground, P= powder, N.A.= not available. A.D.= adaptation level: 1for low, 2 for medium, 3 for high.

Recent studies on the earth's climate change show an increase in temperature concomitant with a decrease in humidity believed to be caused by the concentration raise of atmospheric CO2 from 265 to 350 ppm in the last 25 years. This increase represents a physiological advantage for C3 plants, mainly woody species which are more adapted to these conditions than C4 plants, including grasses (Mayeux et al., 1991). This process supports the hypothesis that the raise in woody shrub species in the natural scrub and graze land communities of the south of the United States and northeastern of Mexico is related to these atmospheric climate changes and not only attributed to human activities in terms of management (Archer 1994).

Frequently, human activities and natural processes interact each other to cause persistent transitions among states (Westoby et al. 1989, Bestelmeyer et al. 2003, 2004, Stringham et al. 2003). Of greatest concern from a conservation perspective are alternative ecosystem states that reflect a degraded capacity to perform desired ecosystem functions. Ecosystems that have been driven across the thresholds of degradation cannot be restored to previous conditions simply by removing the stressor.

In the extensive areas of the arid and semiarid ecosystems of northeastern Mexico the primary use of the vegetation is based on extensive grazing. However, if livestock activities using herbaceous graminoid species were considered, the increase in thorny woody shrub plants density would limit this activity due to a lower density of graminae and other forage species and to the difficult transportation of cattle. This situation makes it imperative the creation of strategic programs for integral management that yield a more efficient use of the scrub phytoresources.

Table 4. Main toxic plants from northeastern Mexico.

Scientific name	Common name in the area (Spanish)	Family	Toxicity
Acacia berlandieri	Huajillo	Leguminosae	Leaves and fruits. The N-methyl-beta-phenylethylamine is responsible for the ataxia and prostration, sometimes death in cattle. Mechanism similar to ephedrine.
Acacia gregii	Uña de gato	Leguminosae	Leaves. Mydriasis, tachypnea, convulsions and death may occur In intoxicated animals. Symptoms are similar to those present in hydrocyanic acid poisoning.
Agave lechuguilla	Lechuguilla	Agavacea	Leaves. A saponin (Hepato-nephro-toxine) and a skin photosensibilizator.
Allium canadense	Cebollín	Liliaceae	The whole plant. An undetermined alkaloid causes anemia, hematuria, gastro-enteritis and death.
Anagallis arvensis	Coralillo	Primulaceae	The whole plant. Toxic compounds such as glycosides triterpenes, antifungal, flavonoids and cucurbitacins. Lethal toxic effects on sheep and symptoms such as diarrhea, anorexia and depression, injuries including bleeding in the kidney and heart, congestion of lungs and liver damage.
Argemone mexicana	Cardo Santo	Papaveraceae	All the plant. Alkaloids berberine. Lung congestion and damage to kidneys in laboratory rabbits and protopine (narcotic action). These alkaloids are removed by animals through the milk. The seed contains isoquinoline alkaloids: sanguinarine and dihydrosanguinarine which show irritant effect on skin and mucosal areas.
Asclepias latifolia	Hierba lechosa	Asclepiadaceae	Leaves and young stems. The galitoxin is the dominant toxicant in the latex. In lesser quantity cardiac glycosides and poisonous alkaloids. Animals show motor and respiratory problems resulting in death.
Astragalus wootoni	Hierba loca	Leguminosae	The whole plant. Presence of hydrogen cyanide and other toxic substances. Alkaloids and saponins contained act as emulsifying agents for fats and haemolysis of red blood cells due to its affinity with colestrin and lecithin.
Brassiica nigra	Mostaza	Cruciferae	Seed. Glycoside: sinigrin. Irritating to skin and mucous membranes. Abortion.

Table 4. Continued

Scientific name	Common name in the area (Spanish)	Family	Toxicity
Centaurium calycosum	Centauro	Gentianaceae	The whole plant. Concentrated bitter glycosides (gentiopicrin) during flowering. In large amounts causes abundant watery diarrhea, polyurea, general weakness and sometimes coma and death.
Cephalanthus occidentalis	Mimbre	Rubiaceae	The whole plant. Poorly studied. Cephalotin, a substance that destroys red blood cells, causes vomiting, convulsions and paralysis of the limbs.
Citrus aurantium	Naranjo Agrio	Rutaceae	Fruits and flowers. Three glycosides contained: Hesperidin, Isohesperidin and aurantiamarin which are sedative of the central nervous system.
Clematis dioica	Barbas de chivato	Ranunculaceae	Leaves. Protoanemonin, Hederagenin saponins, oleanolic acid derivatives, anemonol. Used in small doses against varicose ulcers and rheumatic pains.
Convolvulus arvensis	Correhuela	Convolvulaceae	Tender leaves and shoots. Poisonous to livestock. There is a lack of reliable information.
Croton ciliato	Canelillo	Euphorbiaceae	Ripe fruits and nuts. Glycosides and resins. Just half to one drop causes burns to the digestive system.
Cuscuta sp.	Tripa de Judas	Convolvulaceae	The whole plant. Cuscutina glucoside, resin, tannins, uncharacterized flavonoids (stems and flowers).
Chenopodium album	Hedionda	Quenopodiaceae	The whole plant. Cyanogenic glycosides. Ascaridol (high concentrations cause severe liver and kidney lacerations).
Chenopodium ambrosioides	Epazote	Quenopodiaceae	The whole plant. Ascaridol.
Drymaria arenarioides	Alfombrilla	Cariofilaceae	Leaves and Stems. Saponins, oxalic acid, alkaloids (thebaine, narcotine, narcein solanine and ergotoxin).
Euphorbia maculata	Hierba de la Golondrina	Euphorbiaceae	The whole plant. Rubber-resin (Euforbona).
Fluorenscia cernua	Hoja Sen	Compositae	Dry fruits. Glycosides and a not characterized resin.

Table 4. Continued

Scientific name	Common name in the area (Spanish)	Family	Toxicity
Gutierrezia sarothrae	Hierba de San Nicolás	Compositae	Leaves. Saponins
Hordeum vulgare	Cebada	Graminaceae	The whole plant. Barley embryos develope an alkaloid (hordenine).
Karwinskia humboldtiana	Coyotilo Tullidora	Rhamnaceae	Leaves. Antracen. Hindquarter paralysis and death with seeds and fruits. Weak decay with nausea.
Ligostrum japonicum	Trueno	Oleaceae	Leaves and fruits. Glucoside (privet), tannins.
Lobelia berlandieri	Diente de víbora	Lobeliaceae	The whole plant. Alkaloid: lobelia of sympathetic-mimetic action, antispasmodic and dilator of the bronchial tissue. Intoxication causes decreased respiratory rate, muscle atrophy, prolonged coma and death.
Lophophora williamsii	Peyote	Cactaceae	The whole plant. Strychnine alkaloids that increase reflex irritability to the point of spasms. Morphine-type alkaloids have sedative and sleeping action.
Medicago sativa	Alfalfa	Leguminosae	The whole plant. Large ingestion causes trifoliosis with mouth inflammation and skin irritation.
Melia azedarach	Canelo	Meliaceae	The whole plant. Azedarine alkaloid (central nervous system) and paraisin (insect repellent), Hemolyzing saponins and tannins, essential oils and resins.
Melilotis officinalis	Trébol oloroso	Leguminosae	The whole plant. Warfarin or dicumarol, anticoagulant. Coumaric and melitotic acid.
Melochia piramidata	Chichibe	Esterculiaceae	Alkaloids. Chloroform extract in mice resulted in hind incoordination, prostration and death.
Nerium oleander	Laurel	Apocinaceae	Glycoside. Cardiac arrhythmia, diarrhea, death.

Table 4. Continued

Scientific name	Common name in the area (Spanish)	Family	Toxicity
Nicotiana glauca	Tabaco	Solanaceae	Alkaloids: narcotine, colchicine, lobeline, nicotine, anabasine, and so on. The anabasine are presented in greater proportion and apparently is responsible for poisoning.
Nicotina Tabacum	Tabaco	Solanaceae	Leaves. Nicotine.
Nolina texana	Sacahuiste	Liliaceae	Buds, flowers and fruits. Filoeritrina and a hepato-nephro-toxin, toxicity similar to that of A. lettuce.
Phoradendron tometosum	Injerto del Mesquite	Lorantaceae	Berries. Highly toxic phenols.
Prunus serotina	Capuli	Rosaceae	The whole plant. Cyanogenic glycoside (amygdalin). Breathing difficulty, spasms, coma and sudden death.
Quercus spp.	Encino	Fagaceae	Leaves and acorns. Tannic acid and other undetermined toxic precursors.
Rhus radicans	Hiedra	Anacardiaceae	Latex of stems, branches and leaves. 3-n-pentadecyl-catechol reacts rapidly with proteins in the skin and mucous membranes.
Solanum nigrum	Hierba mora	Solanaceae	Glycoside: solanine. Loss of sensation, bloating, diarrhea, dilated pupils.
Tribulus terrestris	Torito	Zygophyllaceae	Seeds. Nitrates. Photosensitization.

Source: Valdez Tamez, 2002

It is urgent to considerate that the management programs of the distinct scrub and grazing lands should be based on integral projects and multidisciplinary actions, i.e. the conservation and multipurpose use of the involved resources (Sánchez and Aguirre 2004). This requires considering a complex of strategies, including:

1. Diverse livestock with management of domestic livestock and wildlife systems.
2. Multiple uses of shrub and arboreal species employed for both forage and goods supply (wood, firewood, fibers, wax, among others) and environmental services (soil protection, microclimate, landscape, urban arboriculture, etc.).

To perform a better and proper resource management of communities of the scrub/grassland located phytogeographically in arid and semiarid zones certain disturbance thresholds or onset indicators of disturbances should be established although they should not go beyond compromising the ability of self-restoration and autoregulation of ecosystems. The observation of these thresholds would result in conservation criteria and sustainable use of the existing communities and their related resources such as water, soil and biotic resources.

Costly, manipulative restoration efforts are frequently required (Hobbs and Norton 1996, Whisenant 1999, Suding et al. 2004) but success of such restoration efforts is usually uncertain, and in some cases restoration may be impractical due to financial and technical constraints. Dryland ecosystems and aquatic ecosystems are the most-frequently cited examples of systems characterized by multiple alternative states (Rapport and Whitford 1999, Scheffer and Carpenter 2003).

References

Archer, S., Scifres, C., Bassham, C. R. & Maggio, R. (1988). Autogenic succession in a subtropical savanna: Conversion of grassland to thorn woodland. *Ecological Monographe*, **58**, 111-127.

Archer, S. (1994). Woody Plant Encroachment into Southwestern Grasslandas and Savannas: Rates, Patterns and Proximate Causes, en *Ecological Implications of Livestock Herbivory in the West* (M. Vavra, W. Laycock, y R. Pieper (Eds.) Denver, Colorado: Society of Range Management, 13-68.

Asner, G. P., Seastedt, T. R. & Townsend, A. R. (1997). The decoupling of terrestrial carbon and nitrogen cycles. *BioScience,* **47**, 226-234.

Bestelmeyer, B. T., Brown, J. R., Havstad, K. M., Alexander, R., Chavez, G. & Herrick, J. E. (2003). Development and use of state-and-transition models for rangelands. *Journal of Range Management,* **56**, 114-126.

Bestelmeyer, B. T., Herrick, J. E., Brown, J. R., Trujillo, D. A. & Havstad, K. M. (2004). Land management in the American Southwest: A state-and-transition approach to ecosystem complexity. *Environmental Management,* **34**, 38-51.

Betancourt, J. L. & Van Devender, T. R. (1981). *Holocene vegetation in Chaco Canyon*, New Mexico.

Breshears, D. D. & Allen, C. D. (2002). The importance of rapid, disturbance-induced losses in carbon management and sequestration. *Global Ecology & Biogeography,* **11**, 1-5.

Breshears, D. D., Whicker, J. J., Johansen, M. P. & Pinder, J. E. (2003). Wind and water erosion and transport in semi-arid shrubland, grassland and forest ecosystems: Quantifying dominance of horizontal wind-driven transport. *Earth Surface Processes and Landforms,* **28**, 1189-1209.

Cairns M. A., Haggerty, P. K., Alvarez, R., De Jong, B. H. J. & Olmsted, I. (2000). Tropical Mexico's recent land-use change: a region's contribution to global carbon cycle. *Ecological Applications, 10*, 1426-1441. doi: 10.1890/1051-761(2000)0102.0.CO;2.

Chapin, F. S., Torn, M. S. & Tateno, M. (1996). Principles of ecosystem sustainability. *The American Naturalist,* **148**, 1016-1037.

Cotecoca. (1973). *Coeficientes de agostadero de la República Mexicana, estado de Nuevo León,* México: Secretaría de Agricultura y Ganadería, Comisión Técnica Consultiva para la Detección de Coeficientes de Agostaderos, 174-179.

Ehleringer, J. R., Schwinning, S. & Gebauer, R. (2000). Water use in arid land ecosystems. Pages 347-365 in M. C., Press, J. D. Scholes, & M. G. Barker, eds. *Physiological Plant Ecology.* Proceedings of the 39th Symposium of the British Ecological Society, 7-9 September 1998, University of York. Blackwell Science, Boston.

Follett, R. F. (2001). Soil management concepts and carbon sequestration zin cropland soils. *Soil & Tillage Research.,* **61**, 77-92. doi: 10.1016/S0167-1987(01)00180-5.

Foroughbakhch, R, Alvarado, M. A., Hernández-Piñero, J. L. & Guzman, M. A. (2006). Establishment, growth and biomass production of 10 tree woody species introduced for reforestation and ecological restoration in northeastern Mexico. *Forest Ecology & Management,* **235**, 194-201.

Hastings, J. R. R. M. (1965). *The Changing Mile*, Tucson: University of Arizona Press.

Herrick, J. E., Brown, J. R., Tugel, A. J., Shaver, P. L. & Havstad, K. M. (2002). Application of soil quality to monitoring and management: paradigms from rangeland ecology. *Agronomy Journal,* **94**, 3-11.

Hobbs, R. J. & Norton, D. A. (1996). Towards a conceptual framework for restoration ecology. *Restoration Ecology,* **4,** 93-110.

Jacoby, P. W. (1985). Restoring mesquite savanna in western Texas, USA through brush and cacti management, en: J.C. Tothill, y J.J. Mott (Eds.), Ecology and Management of the World's Savannas, Canberra: *Australian Academy of Science*, 223-228.

Jenny, H. (1941). *Factors of soil formation: a system of quantitative pedology*. McGraw-Hill, New York. 281.

Jenny, H. (1980). *The soil resource: origin and behavior*. Springer-Verlag, New York., 377.

Johnston, M. C. (1963). Past and present grassland of southern Texas and northeastern Mexico, *Ecology*, **44**, 456-466.

Ludwig, J. A. & Tongway, D. J. (1997). A landscape approach to rangeland ecology. Pages 1-12 in J., Ludwig, D., Tongway, D., Freudenberger, J. Noble, & Hodgkinson, K. eds. *Landscape ecology, function and management: principles from Australia's rangelands*. CSIRO Publishing, Collingwood, VIC, Australia.

Ludwig, J. A. & Tongway, D. J. (2000). Viewing rangelands as landscape systems. Pages 39-52 in O., Arnalds, & Archer, S. (eds). *Rangeland desertification*. Kluwer, Dordrecht.

Maldonado, A. (1992). Desertificación en la subcuenca del Rio Limon, Linares, N.L. *Tesis Profesional de Licenciatura.* Facultad de Ciencias Forestales, UANL Linares, NL, Mexico.

Mayeux, H. S., Johnson, H. B. & Polley, H. W. (1991). *Global Change and Vegetation Dynamics,* 62-74, en: Noxious Range L. F., Weeds, J. O., James, M. H. & Evans, B. J. Raphs, y Singler. (Eds.), Boulder, Colorado: Westview Press.

Miller, M. E. & Thomas, L. P. (2004). The Structure and Functioning of Dryland Ecosystems–Conceptual Models to Inform the Vital-Sign Selection Process. USGS: *Science for changing World,* 1-77

Muller, C. H. (1947). *Vegetation and climatic in Coahuila, México,* Madroño **9,** 33-57.

Návar, J., Méndez, E., Graciano, J., Dale, V. & Parresol, B. (2004). Biomass equations for shrub species of Tamaulipan thornscrub of northeastern Mexico. *Journal of Arid Environments.,* **59,** 657-674. doi: 10.1016/j. jaridenv. 2004.02.010.

Noy-Meir, I. (1973). Desert ecosystems: Environment and producers. *Annual Review of Ecology and Systematics,* **4**, 25-51.

Palacios-Prieto, E. (2000). La condición actual de los recursos forestales en Mexico. Resultados del Inventario Nacional Forestal 2000. *Investigaciones Geograficas.,* **43**, 183-203.

Peñaloza, R. & Reid, N. (1989). Pasado, presente y futuro del uso de la tierra en el matorral tamaulipeco del noreste de México, en: Memoria, II, *Simposio Agrofestral en México, Linares,* Nuevo León, México: Facultad de Ciencias Forestales, UANL, Gobierno del Estado de Nuevo León, INIFAP-SARH, 663-684.

Rapport, D. J. & Whitford, W. G. (1999). How ecosystems respond to stress: Common properties of arid and aquatic systems. *BioScience,* **49**, 193-203.

Reynolds, R. C., Belnap, J., Reheis, M., Lamothe, P. & Luiszer, F. (2001). Aeolian dust in Colorado Plateau soils: Nutrient inputs and recent change in source. *Proceeedings of the National Academy of Sciences,* **98**, 7123-7127.

Rojas Mendoza, P. (1965). Generalidades sobre la vegetación del estado de Nuevo León, y datos acerca de su flora. Tesis doctoral, Facultad de Ciencias, UANM, México, D.F. 7-23.

Rzedowski J. (1978). *Vegetacion de Mexico*. Limusa, Mexico., 432.

S. A. G. (1975). Manual de Agostología. SAG., México, D.F.

Sánchez S. & Agguirre, O. (2004). Manejo forestall con base científicas. *Madera y Bosques,* **10**(4), 3-6.

Scheffer, M. & Carpenter, S. R. (2003). Catastrophic regime shifts in ecosystems: Linking theory to observation. *Trends in Ecology & Evolution,* **18**, 648-656.

Semarnat, (2001). *Diario Oficial de la Federación*, NORMA Oficial Mexicana NOM-059-ECOL-2001. Protección ambiental- Especies nativas de México de flora y fauna silvestres-Categorías de riesgo y especificaciones para su inclusión, exclusión o cambio-Lista de especies en riesgo, México, D.F.

Stringham, T. K., Krueger, W. C. & Shaver, P. L. (2003). State and transition modeling: An ecological process approach. *Journal of Range Management,* **56**, 106-113.

Suding, K. N., Gross, K. L. & Houseman, G. R. (2004). Alternative states and positive feedbacks in restoration ecology. *Trends in Ecology & Evolution,* **19**, 46-53.

Tongway, D. J., Sparrow, A. D. & Friedel, M. H. (2003). Degradation and recovery processes in arid grazing lands of central Australia. Part 1: soil and land resources. *Journal of Arid Environments,* **55**, 301-326.

Valdés-Tamez V, Foroughbakhch, R., Treviño-Garza, E. J., García-Alvarado, J. S., Alanis-Flores, G., Alvarado-Vazquez, M. A. & Jurado-Ibarra, E. (2002).

Flora Medicinal del municipio de Santiago, N.L., México: su importancia y distribución en la vegetación. *Phyton,* 173-179.

Vitousek, P. M. (1994). Factors controlling ecosystem structure and function. Pages 87-97 In: R. G., Amundson, J. W. Harden, & M. J. Singer, eds. *Factors of soil formation: a fiftieth anniversary retrospective. SSSA special publication no.* **33**. Soil Science Society of America, Madison, WI.

Wardle, D. A. (2002). *Communities and ecosystems: Linking the aboveground and belowground components*. Princeton University Press, Princeton, NJ. 392.

Westoby, M., Walker, B. & Noy-Meir, I. (1989). Range management on the basis of a model which does not seek to establish equilibrium. *Journal of Arid Environments,* **17**, 235-239.

Whitford, W. G. (2002). *Ecology of desert systems*. Academic Press, San Diego. 343.

Whisenant, S. G. (1999). *Repairing damaged wildlands: A process-oriented, landscape-scale approach*. Cambridge University Press, Cambridge., 312.

WWF. (2001). Ecoregions of the World. Neartic Desert and Shrublands. *Tamaulipan Mezquital (NA1312).*

In: Structural Analysis
Editor: M.L. Camilleri, pp. 51-71
ISBN: 978-1-61668-987-2

Chapter 3

STRUCTURAL ANALYSIS OF METAL-OXIDE NANOSTRUCTURES

Ahsanulhaq Qurashi[1, 2,*], M. Faiz[2] and N. Tabet[3]
[1]School of Engineering, Toyama University, 3190 Gofuku,
Toyama 930-8555, Japan
[2]Chemistry Department, and Center of Research Excellence in
Nanotechnology at, King Fahd University of Petroleum
and Minerals, Dhahran, Saudi Arabia
[3]Physics Department, and Center of Research Excellence in Nanotechnology
at, King Fahd University of Petroleum
and Minerals, Dhahran, Saudi Arabia

Abstract

Structural analysis plays the key role in understanding the relation between the preparation and morphology and intrinsic properties of metal oxide nanostructures. In this chapter structural analysis of metal oxide nanostructures by variety of fundamental techniques like X-ray diffraction pattern (XRD), Grazing incident X-ray diffraction (GIXRD), Scanning electron microscopy (SEM), field emission scanning electron microscopy (FESEM), transmission electron microscopy (TEM), atomic force microscopy (AFM), energy dispersive X-ray spectroscopy (EDX), and X-ray photoelectron spectroscopy (XPES) etc will be presented. The detailed crystal structure of In_2O_3 pyramids will be

* E-mail address: ahsanulhaq06@gmail.com Fax: +81-76-445-6734 (Author to whom correspondence should be addressed: Ahsanulhaq Qurashi).

presented by XRD analysis. For in-situ examination, grazing incidence small angle scattering and diffraction of X-rays (GIXRD) results of ZnO nanostructures will be presented. The morphological description and the examination of the surface of the structure, which includes the analysis of their eventual structure and their size, shape distribution, cross-section from their surface to the substrate, the analysis of the surface and its inhomogenities will be attained by SEM and FESEM analysis. Detailed structural analysis with single crystalline nature of ZnO nanostructures will be presented by TEM equipped with selected area electron diffraction pattern (SAED) and high resolution transmission electron microscope (HRTEM). The surface roughness of vertically aligned ZnO nanorod arrays will be studied by atomic force microscopy (AFM). In order to know the exact chemical composition, stiochiometry and chemical bonding nature of metal-oxide nanostructures, the energy dispersive X-ray spectroscopy (EDX), and X-ray electron spectroscopy (XPES) techniques will be included.

1. Introduction

The development in material science has focused interest on the properties and performance of materials on the scale of nanometers. Recently science has offered the means to maneuver materials on an atom-by-atom basis and established procedures for material characterization on the small size scales. These expansions are having an almost instantaneous impact on technology and severe efforts are been made to develop them in various applications. In last two decades, extensive interest has surfaced in the synthesis of nanoscale materials [1-12]**.** Metal-oxides represent an assorted and appealing class of materials with properties which cover the entire range from metals to semiconductors and insulators and almost all aspects of material science and physics. Metal-oxides have a great potential in various applications due to their interesting physical properties, such as superconducting, semiconducting, ferroelectric, piezoelectric, pyroelectric, ferromagnetic, optical, and sensing [13-23]. Nano-scaled oxide materials have attracted great interest in the last decade because they can exhibit different physical properties than their bulk counterparts. Due to their special shapes, compositions, chemical and physical properties, metal-oxide nanostructures are the focus of current research efforts in nanotechnology since they are the commonest minerals in the earth [24-40]. Metal-oxide nanostructures have now been widely used in many areas, such as ceramics, catalysis, sensors, transparent conductive films, electro-optical and electro-chromic devices [41-45].

Structural analysis of metal-oxide nanostructures comprises the set of physical instruments required to study and predict the behavior, and properties of nanostructures. To perform an accurate analysis and study the complex properties of metal-oxide nanostructures, nanotechnologist usually determines their

morphology, crystal quality, chemical composition, stiochiometry, and other related properties. In this chapter we present different techniques employed to characterize and study the behavior of metal- oxides at nanoscale.

2. Structural Characterization of Metal-Oxide Nanostructures

Structural analysis of metal-oxide nanostructures is carried out by variety of techniques includes XRD, GIXRD, SEM, FESEM, EDX, TEM, AFM, and XPES.

2.1. XRD

The X-ray diffraction is knowledge of determining the arrangements of atoms within crystal from the manner in which a beam of X-ray is scattered from the electrons with in the crystals. The discovery of X-rays in 1895 enabled scientists to probe crystalline structure at the atomic level. X-ray diffraction has been in use in two main areas, for the fingerprint characterization of crystalline materials and the determination of their structure. Each crystalline solid has its unique characteristic X-ray powder pattern, which may be used as a "fingerprint" for its identification. Once the material has been identified, X-ray crystallography may be used to determine its structure, i.e. how the atoms pack together in the crystalline state and what the inter-atomic distance and angle are etc. X-ray diffraction is one of the most important characterization tools used in solid-state chemistry and materials science. We can determine the size and the shape of the unit cell for any compound most easily using the diffraction of X-rays. The distance between similar atomic planes in mineral called d-spacing is measured in angstroms. The angle of diffraction known as theta angle and is measured in degrees. For practical reasons the diffractometer measures an angle twice that of the theta angle. Not surprisingly, we call the measured angle '2-theta'. The wavelength of the incident X-radiation, symbolized by the Greek letter lambda and, in our case, equal to 1.54 angstroms. These factors are combined in Bragg's law, which is explained below.

The path difference between two waves:

$$2\,x = 2d\sin(\theta) \tag{2.1}$$

For constructive interference between these waves, the path difference must be an integral number of wavelengths:

$$n \times \lambda = 2x \tag{2.2}$$

This leads to the Bragg's equation:

$$n \times \lambda = 2d\sin(\theta) \tag{2.3}$$

This equation was proposed by physicists Sir W.H. Bragg and his son Sir W.L. Bragg in 1913 to explain why the cleavage faces of crystals appear to reflect X-ray beams at certain angles of incidence (theta,θ). The variable "*d"* is the distance between atomic layers in a crystal, and the variable lambda is the wavelength of the incident X-ray beam while n is an integer [46]. The X-ray diffraction (XRD) patterns were recorded on a Rigaku, D/max 2500 diffractometer. The X-ray source of this diffractometer emits Cu-Ka radiation with wavelength of 1.5418 Å. The diffractometer is calibrated with reference to standard oriented Si wafer. For usual structural phase analysis, a scan rate between 4- 8 º per min. was used. XRD is first and foremost technique to be used to know the phase, crystal structure and purity of materials. The XRD spectrum of In_2O_3 nanostructures shown in Figure 1. All the XRD peaks are indexed to the pure cubic phase with lattice parameter a = 1.011Å (JCPDS No. 89–4595), indicating that pure phase [47]. However, no any other impurities existed in the sample.

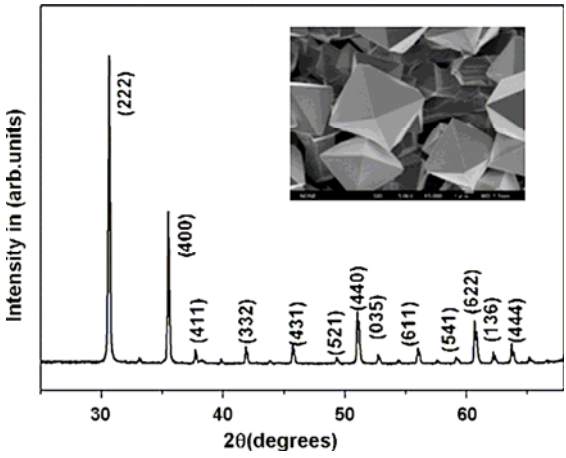

Figure 1. XRD spectra of In2O3 pyramids. Reprinted from Ref. [47], with permission from copyright 2010 Elsevier.

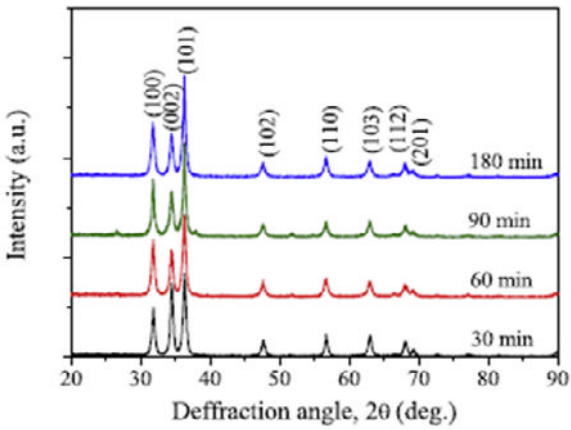

Figure 2. GIXRD of ZnO nanostructures with various deposition times (a = 0.48) Reprinted from Ref. [48], with permission from copyright 2010 Elsevier.

2.2. Gixrd

Grazing incidence X-ray diffraction is an excellent technique to analyze crystal phase of material compared to the XRD. The penetration depth of X-rays is often found in the 10-100 µm range. In most thin film investigations the thickness is substantially lower causing a large fraction of the diffractogram as measured in the symmetric $\theta/2\theta$ configuration to stem from the substrate. Especially for the analysis of thin films X-ray diffraction techniques have been developed for which the primary beam enters the sample under very small angles of incidence. In its simplest variant this configuration is denoted by GIXRD that stands for grazing incidence x-ray diffraction. The small entrance angle causes the path traveled by the x-rays to significantly increase and the structural information contained in the diffractogram to stem primarily from the thin film. The GIXRD spectrum of ZnO nanostructures grown for different deposition time was illustrated in Figure 2 [48]. All the GIXRD peaks indicated wurtzite hexagonal crystal structure of ZnO nanostructures. The sharp peaks particularly (1 0 0) and (1 0 1) peaks of the ZnO nanorods indicate good crystal quality. With the help of GIXRD measurement, it was found that both these peaks increase with the deposition time, which enhanced the crystallinity as well as the quantity of nanorods. Also full width half maximum (FWHM) was calculated by using GIXRD results.

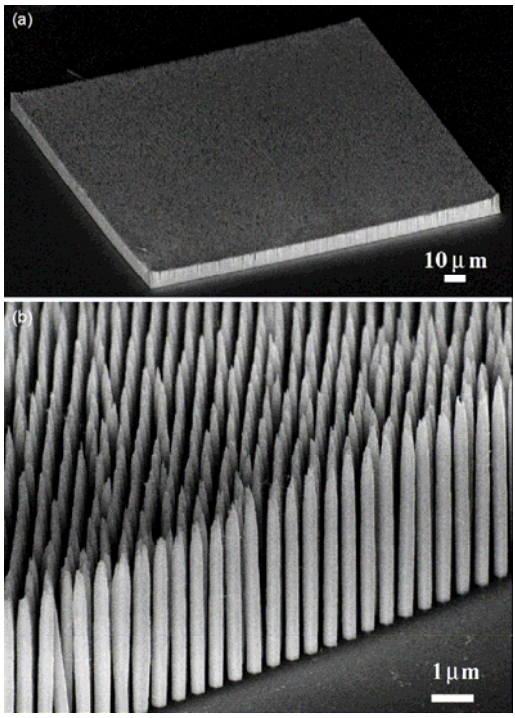

Figure 3. (a) Low magnification and (b) high magnification SEM images of the ZnO NW arrays grown on a GaN substrate using a hydrothermal approach. Reprinted from Ref. [51], with permission from copyright 2010 American Chemical Society.

2.3. SEM and FE-SEM

Scanning electron microscopy and field emission scanning electron microscopy techniques are commonly used to find out morphological details of nanostructures, their surfaces and size respectively. Field-emission cathode in the electron gun of a scanning electron microscope provides narrower probing beams at low as well as high electron energy, resulting in both improved spatial resolution and minimized sample charging and damage. The scanning electron microscopy (SEM) was pioneered by Manfred von Ardenne in the 1930s [49, 50]. SEM can scan the surface of a sample with a finely focused electron beam to produce an image when the electrons hitting the surface are reflected and are detected by a fluorescent screen or computer monitor. The instrument provides resolution of 1 nm at 30 kV and 4 nm at 1.0 kV. SEM images of ZnO nanorod arrays (NRAs) grown on GaN substrate is illustrated in Figure 3 [51]. The

morphology, length and top view surface can be easily observed from the SEM of ZnO NRAs. The field-emission scanning electron microscope (FESEM) uses a Schottky field-emission source for electrons. The Schottky emitter combines with the high brightness and low energy spread of the cold field emitter that have the high stability and low beam noise of thermal emitters. The instrument is equipped with about 100 times the emitting area as a cold emitter, and as a result, has much higher probe currents that give it an advantage for analytical applications. The electron gun is directly linked to a beam booster. This linkage eliminates, among other things, crossover of electrons along the beam path, which aids in operating at very low beam energies. The field-emission scanning electron microscope is equipped with two secondary electron detectors: below-lens for low-resolution work and in-lens for high-resolution imaging. The backscattered electron detector is a solid state detector and is optimized for short working distances. The four diodes of the detector are designed for both low- and high-accelerating voltage operations.

This instrument may be applied to several areas of research, including materials science, nanotechnology, geology, and biology. For FESEM observation, the samples are first made conductive. The samples were coated with an ultrathin layer (1.5-3.0 nm) of gold, gold-palladium or platinum. After that, the objects must be able to sustain the high vacuum and should not alter the vacuum, for example by losing water molecules or gasses. For the structural analysis, a small piece of the substrate, which contains the deposited products, was pasted on the sample holder using the carbon tape. The object is inserted through an exchange chamber into the high vacuum part of the microscope and anchored on a moveable stage. The object can be moved in horizontal and vertical direction, and its position can be changed in the chamber left-right axis, or forward and backward. In addition, the object can be tilted, rotated and moved. FESEM gives us morphological features, size and surface at high-magnification mostly less than 100 nm.

Figure 4 shows plane and 45° tilted view images of hexagonally patterned ZnO NRAs [52]. From the tilted view image one can find out the diameter, length and surface of the sample. This is the most convenient method to know the vertical alignment of 1D nanostructures with the substrate. Figure 5 shows top view low and high magnification FESEM images of In_2O_3 nanopushpins [53]. With the help of high-magnification FESEM images we can see the clear view, smoothness and geometry of In_2O_3 nanopushpins and their pyramidal tips. In order to know precisely the exact thickness, diameter, and length of nansotructures grown on the substrate, traditionally rm cross-section FESEM analysis of nanostructures will be carried out.

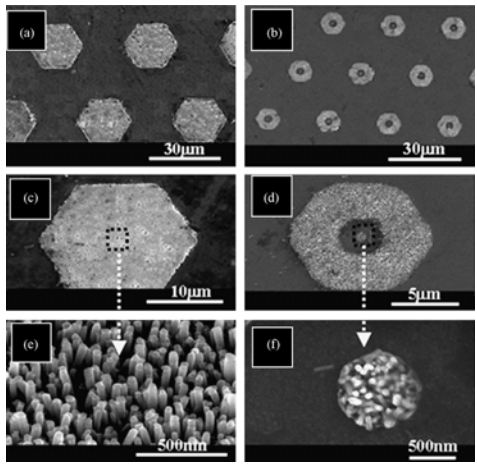

Figure 4. (a) and (b) Low magnification FESEM image of ZnO NRAs grown in hexagonal patterns with the size of 15 and 10m, respectively; (c) and (d) represent their magnified FESEM images; and (e) and (f) high magnification 45◦ tilted FESEM image taken from the center of hexagon and circle patterns, respectively. Reprinted from Ref. [52], with permission from copyright 2010 Elsevier.

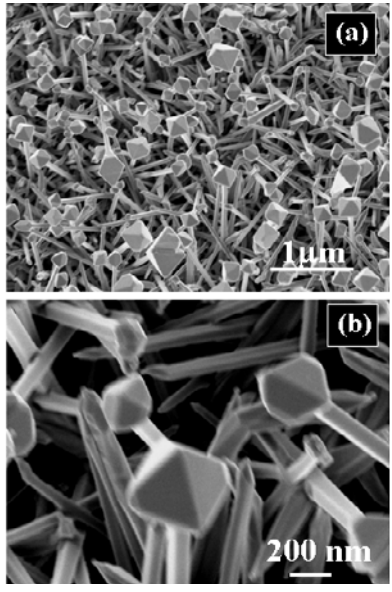

Figure 5**.** (a) and (b) low and high magnification FESEM images of In2O3 nanopushpins Reprinted from Ref. [53], with permission from copyright 2010 American institute of physics.

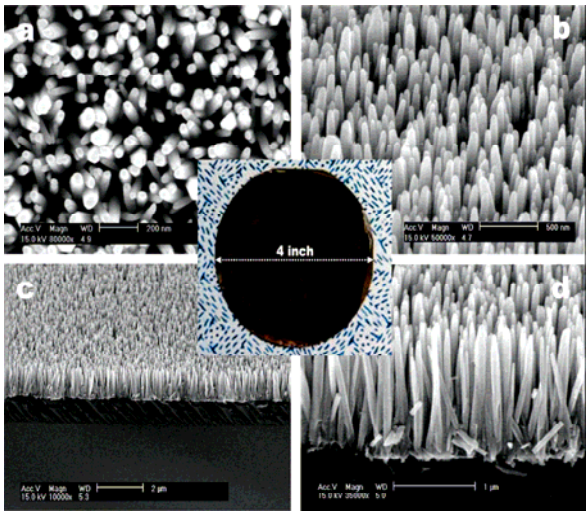

Figure 6. SEM images of ZnO nanorods grown on Zn/Si substrate (a) top view, (b) tilt view, (c,d) edge tilt view. Center photograph (inset) demonstrates uniform ZnO nanorod growth on a 4-in. Si wafer. Reprinted from Ref. [54], with permission from copyright 2010 American Chemical Society.

Figure 6 shows the cross-section FESEM analysis of ZnO NRAs grown on Zn-coated silicon substrate [54]. The alignment of ZnO nanowires with the substrate can be easily seen and their thickness/length can be obtained by this method. However as compared to tilted and surface view sample preparation for cross-section is somewhat difficult.

2.4. TEM

Transmission electron microscopy (TEM), is an imaging technique whereby a beam of electrons is transmitted through a specimen, then an image is formed, magnified, and directed to appear either on a fluorescent screen or layer of or to be detected by a sensor such as a CCD camera The first practical transmission electron microscope was built by Albert Prebus and James Hellier at the University of Toronto in 1938 using concepts developed earlier by Max Knoll and Ernest Ruska [55]. TEM uses electrons as “light source” and their much lower wavelength make it possible to get a resolution a thousand times better than with a light microscope. A schematic diagram of transmission electron microscopy is shown in Figure 7. A "light source" at the top of the microscope emits the electrons that travel through vacuum in the column of the microscope. Instead of

glass lenses focusing the light in the light microscope, the TEM uses electromagnetic lenses to focus the electrons into a very thin beam. The electron beam then travels through the specimen. Depending on the density of the material present, some of the electrons are scattered and disappear from the beam. At the bottom of the microscope the unscattered electrons hit a fluorescent screen, which gives rise to a "shadow image" of the specimen with its different parts displayed in varied darkness according to their density. The image can be studied directly by the operator or photographed with a camera. One can see objects to the order of a few angstrom (10^{-10} m). The possibility for high magnifications has made the TEM a valuable tool in both medical biological and materials research. For TEM analysis, the nanostructures were ultrasonically dispersed from the substrate in acetone and a drop of acetone, which contains the nanostructures, was placed on a carbon coated copper TEM grid and examined.

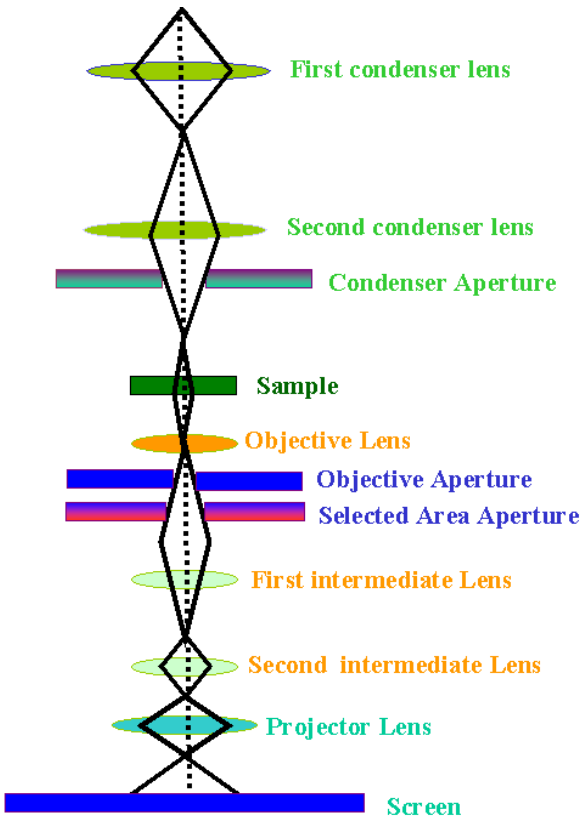

Figure 7. Schematic diagram of transmission electron microscopy.

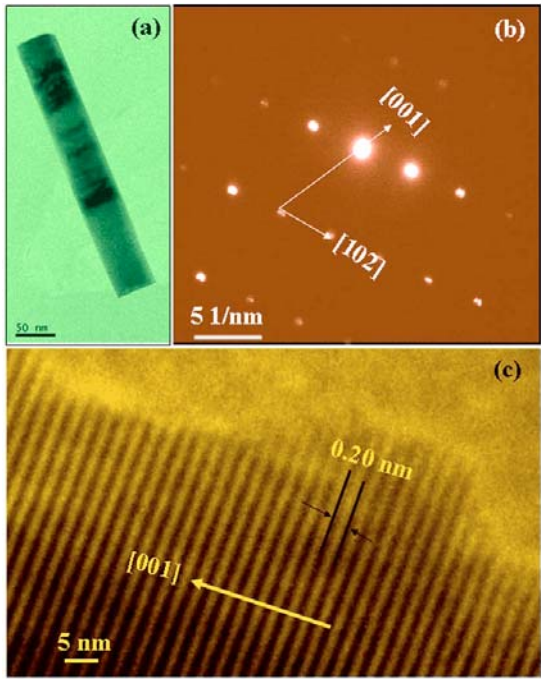

Figure 8. (a) TEM, (b) SAED, and (c) HR-TEM images of ZnO NR gown on ZnO/ Si substrate. Reprinted from Ref. [20], with permission from copyright 2010 American institute of physics.

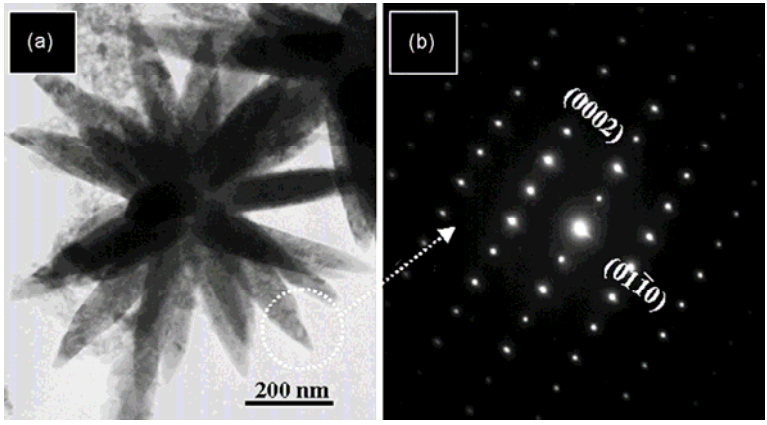

Figure 9. TEM image of the flower-shaped ZnO structure grown for 9 h (a) and its corresponding SAED pattern (b). Reprinted from Ref. [10], with permission from copyright 2010 Elsevier.

By using transmission electron microscopy analysis detailed structural information can be obtained. Figures 8 (a-c) represent a transmission electron microscopy [TEM], selected area electron diffraction (SAED), and high-resolution (HRTEM) images of single ZnO nanorod respectively [20]. These results reveal that the as-grown nanorods are fairly single crystalline and are crystallized hexagonally along the [001] direction with homogeneous geometry. It is possible to know the crystal plane of and their corresponding spots in SAED by using camera constant. Also by HRTEM, we can find out the lattice parameters and growth axis very easily as shown in Figure 8. Figure 9 shows another typical example of TEM analysis of large sized flower shaped structures with corresponding SAED pattern [10]. Each petal of the flower-shaped structures shows a single crystalline nature and grown along the c-axis in [0002] direction

2.5. EDX

Energy dispersive X-ray spectroscopy (EDS or EDX), is an analytical tool predominantly used for chemical characterization. Being a type of spectroscopy, it relies on the investigation of a sample through interactions between light and matter, analyzing X-ray in its particular case. Its characterization capabilities are due in large part to the fundamental principle that each element of the periodic table has a unique electronic structure and, thus, a unique response to electromagnetic waves. This EDX system is either attached with SEM/FESEM or TEM.

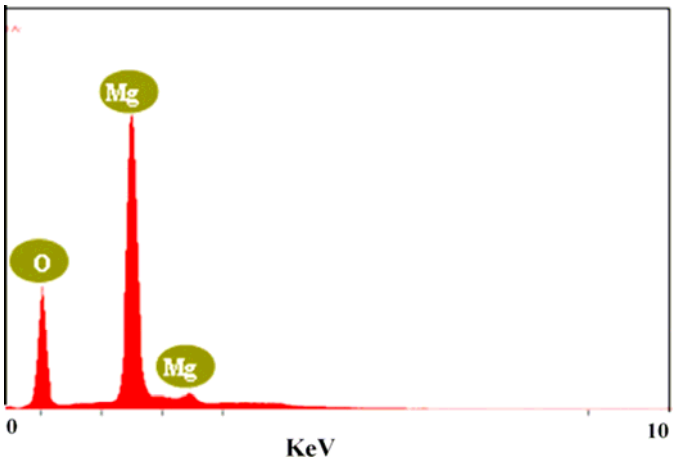

Figure 10. Shows the EDX analysis of MgO nanoflakes. Reprinted from Ref. [56], with permission from copyright 2010 Elsevier.

Figure 10 shows EDX spectrum of MgO nanoflakes [56]. In this case the EDX was attached with SEM. The EDX analysis showed the chemical composition of magnesium and oxygen with an atomic ratio of approximately 1:1, which is in a good agreement with the stoichiometric ratio of MgO. To know the appropriate chemical composition of individual nanostructure, EDX equipped with TEM is usually performed. Figure 11 illustrates the EDX spectrum of single In_2O_3 nanowire taken during the TEM analysis [57]. The EDX spectrum in Figure 10 shows that the single crystalline nanowire composed of only In, O and Au respectively.

2.6. AFM

The atomic force microscope (AFM) is one kind of scanning probe microscopes (SPM). SPM are designed to measure local properties, such as height, friction, and magnetism with a probe. To acquire an image, the SPM raster scans the probe over a small area of the sample, measuring the local property simultaneously. The atomic force microscope (AFM), or scanning force microscope (SFM), is a very high-resolution type of scanning probe microscopy, with demonstrated resolution of fractions of a nanometer, more than 1000 times better than the optical diffraction limit. The AFM was invented by Bining, Quate and Gerber in 1986, and is one of the foremost tools for imaging, measuring, and manipulating matter at the nanoscale [58]. The AFM consists of a microscale cantiliver with a sharp tip (probe) at its end that is used to scan the specimen surface. A shematic diagram of AFM is shown in Figure 12. The cantilever is typically silicon or silicon nitride with a tip radius of curvature on the order of nanometers.

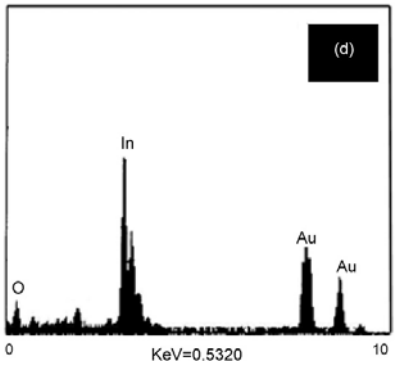

Figure 11. EDX spectrum for In2O3 nanowire, Reprinted from Ref. [57], with permission from copyright 2010 Elsevier.

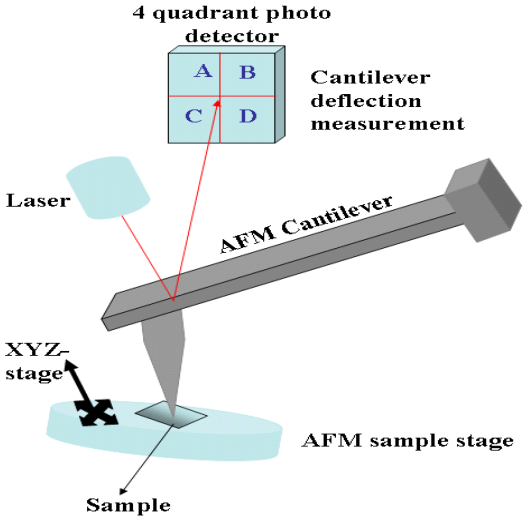

Figure 12. Schematic diagram of atomic force microscopy.

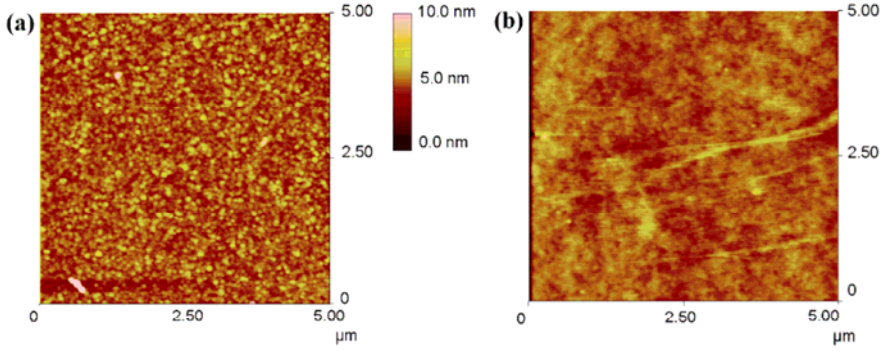

Figure 13. AFM images of Al-doped ZnO film on (a) a Si wafer and (b) a PET substrate. Reprinted from Ref. [59], with permission from copyright 2010 American chemical Society.

When the tip is brought into proximity of a sample surface, force between the tip and the sample lead to a deflection of the cantilever according to Hook's law. Depending on the situation, forces that are measured in AFM include mechanical contact force, van der Wall forces, capillary forces, chemical bonding, electrostatic forces, magnetic forces, casimir forces, and solvation forces etc. Figure 13 (a) shows AFM image of small islands on Si substrate which serve as nuclei for the growth of ZnO nanorods. Two substrates were compared in terms of

uniformity. In Figure 13(b) we see the PET surface does not have uniform island size and distribution compared to that of Si substrate [59].

The AFM 3D images are shown in Figure 14 that represents (a) ZnO nanorods grown in a single strip pattern and (b) the surface of the as-grown nanorods within the strip. An average rms surface of the nanorods is found to be 39 nm [60]. The as-grown ZnO nanostructures with firm adhesion to the substrate of sufficiently minimal topography are easily classified. This adhesion of aligned nanorods to the surface is to guarantee that the probe tip does not push the sample around during imaging.

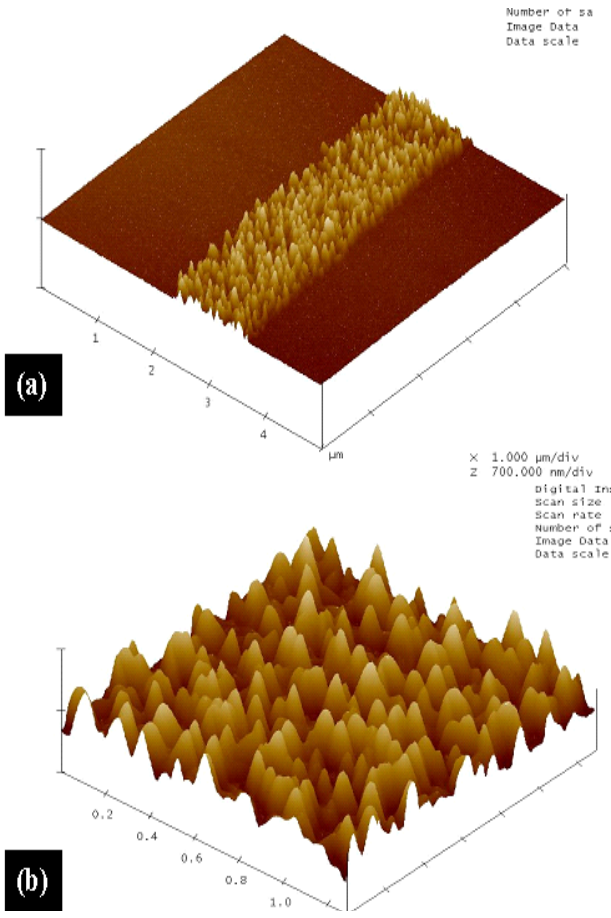

Figure 14. (a and b) AFM images ZnO nanorods grown on strip patterns. Reprinted from Ref. [60].

2.7. XPES

X-ray Photoelectron Spectroscopy (XPES) is a quantitative spectroscopic surface chemical analysis technique used to estimate the empirical formula or elemental composition, chemical state and electronic state of the elements on the surface (upto 10 nm) of a material X-Ray irradiation of a material under ultra high vacuum (UHV) leads to the emission of electrons from the core orbitals of the top 10 nm of the surface elements of the material being analyzed.

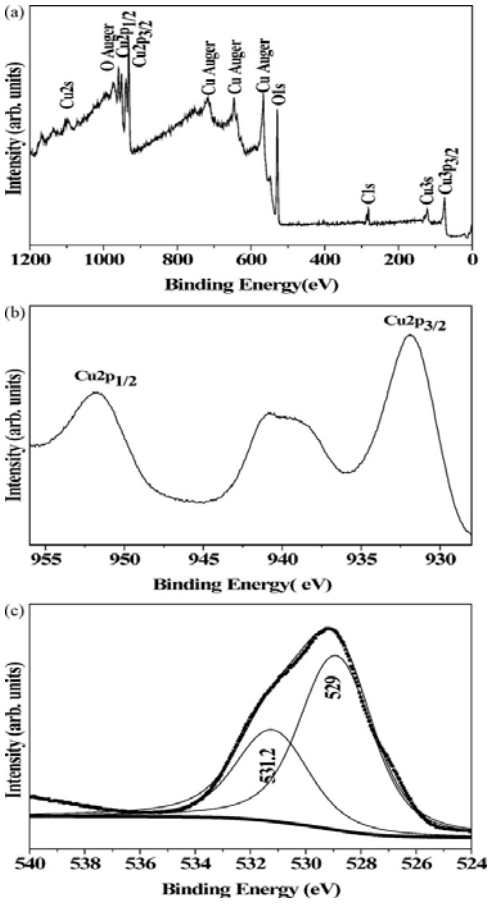

1s core-level spectrum and two O 1s peaks resolved by using curve-fitting procedure.
Reprinted from Ref. [63], with permission from copyright 2010 Elsevier.

Figure 15. (a) Wide XPS survey scan spectra of the as-grown nanobat-like CuO nanostructures; (b) the peaks attributed to the Cu 2p3/2 and Cu 2p1/2; and (c) the O.

Measurement of the kinetic energy (KE) and the number of electrons escaping from the surface of the material gives the XPS spectra. From the kinetic energy, the binding energy of the electrons to the surface atoms can be calculated. The binding energy of the electrons reflects the oxidation state of the specific surface elements. The number of electrons reflects the proportion of the specific elements on the surface. XPS is used to measure elements that contaminate a surface, uniformity of elemental composition across the top surface and uniformity of elemental composition as function of ion beam etching.

XPS can also be used to analyze the change in surface chemistry of a material after chemical or physical treatments such as: leaching, reduction, fracture, cutting or scraping in air or UHV to expose the bulk chemistry, ion beam etching to clean off some of the surface contamination, exposure to heat to study the changes due to heating, exposure to reactive gases or solutions, exposure to ion beam implant, exposure to UV light, etc. XPS is used to determine; 1) what elements and the quantity of those elements that are present within ~10 nm of the sample surface; 2) what contamination, if any, exists in the surface or the bulk of the sample; 3) empirical formula of a material that is free of excessive surface contamination; 4) the chemical state identification of one or more of the elements in the sample; 5) the binding energy (BE) of one or more electronic states; 6) the thickness of one or more thin layers (1–8 nm) of different materials within the top 10 nm of the surface. To count the number of electrons at each KE value, with the minimum of error, XPS must be performed under UHV conditions because electron counting detectors in XPS instruments are typically one meter away from the material irradiated with X-rays. As the energy of a particular X-ray wavelength used to excite the electron from a core orbital is a known quantity, we can determine the electron binding (BE) of each of the emitted electrons by using an equation that is based on the work of Ernest Rutherford (1914):

$$E_{binding} = E_{photon-} E_{kinetic} - \Phi \tag{2.4}$$

where $E_{binding}$ is the energy of the electron emitted from one electron configuration within the atom, E_{photon} is the energy of the X-ray photons being used, $E_{kinetic}$ is the kinetic energy of the emitted electron as measured by the instrument and Φ is work function of the spectrometer (not the material) [61,62].

A typical XPS spectrum is a plot of the number of electrons detected (Y-axis, ordinate) versus the binding of the electrons detected (X-axis). Each element produces a characteristic set of XPS peaks at characteristic binding energy values that directly identify each element that exist in or on the surface of the material being analyzed. These characteristic peaks correspond to the electron

configuration of the electrons within the atoms, e.g., 1s, 2s, 2p, 3s, etc. The number of detected electrons in each of the characteristic peaks is directly related to the amount of element within the area (volume) irradiated. To generate atomic percentage values, each raw XPS signal must be corrected by dividing its signal intensity (number of electrons detected) by a "relative sensitivity factor" (RSF) and normalized over all of the elements detected. The main components of XPS system include; 1) A source of X-rays; 2) An ultra high vacuum (UHV) stainless steel chamber with UHV pumps; 3) An electron collection lens; 4) An electron energy analyzer; 5) Mu-metal magnetic field shielding; 6) An electron detector system. Typically, the diameter (diagonal) of the sample should be <22.0mm, and its thickness should be <3.5 mm. For preparing XPS samples, the samples and the sample holders should be handled with clean tweezers and gloves. Using the optimized procedure, metal-oxide nanostructure samples can be characterized. The phase purity, chemical state and chemical composition of CuO nanobat-like structures was investigated by XPES [63]. Figure 15 (a) illustrates wide survey scan spectra of the CuO nanostructures and only CuO and C peaks could be seen. The peaks related to Cu 2p3/2 and Cu2p1/2 is shown in figure 15 (b). However in figure 15 (c) the O 1s core-level spectrum is broad, and two O 1s peaks can be resolved by using curve-fitting procedure. Using the fitting procedure any suppressed peak can be resolved to know it chemical nature and origin. Also using XPES technique we can easily find out the stiochiometry of nanomaterials.

3. Summary

Structural analysis of metal-oxide nanostructures includes the set of physical instruments required to study and predict the behavior, and properties of nanostructures.

The typical example of In_2O_3 pyramids in terms of XRD mentioned. For in-situ examination, grazing incidence small angle scattering and diffraction of X-rays (GIXRD) of ZnO nanstructures were included. The morphological description and the examination of the surface of the ZnO and In_2O_3 nanostructures, which includes the analysis of their eventual structure and their size, shape distribution, cross-section from their surface to the substrate, the analysis of the surface and its inhomogenities preseneted by SEM and FESEM analysis. Detailed structural analysis with single and polycrystalline nature of ZnO nanorod-like structure and flower-like nanostructures presented by TEM equipped with selected area electron diffraction pattern (SAED) and high resolution transmission electron microscope (HRTEM). The surface roughness of

well-aligned and strip patterned ZnO NRAs, on lattice matching substrates were studied by AFM. The exact chemical composition, surface functionality, stiochiometry and chemical bonding nature of MgO, In_2O_3 and CuO nanostructures, studied by EDX, and XPES techniques .

References

[1] Ijima, S; Ichihashi, T. *Nature*,1993 363, 603-605.

[2] Yousefi, R; Kamaluddin, B; *Appl. Surf. Sci.,* 2009, 255, 9376-9380.

[3] Yousefi, R; Kamaluddin, B; *Appl. Surf. Sci.,* 2009, 256*,* 329-334.

[4] Kim, WH; Shim, HS; *Jalcom.*, 2006, 426*,* 286-289.

[5] Dar, AM; Ahsanulhaq, Q; Kim, SY; Sohn, MJ; Kim, BW; HS. Shin, SH; *Appl. Surf. Sci.* , 2009, 255*,* 6279-6284.

[6] NK. Reddy, KN; Q. Ahsanulhaq, Q; Y. B. Hahn, YB; *Appl. Phys. Lett*. 2008, 93*,* 083124-083126.

[7] Navale, CSC; Gosavi, WS; Mulla, SI; *Talanta*, 2008, 75*,* 1315-1319.

[8] Kumar, M; Singh, V; Singh, F; Lakshmi, VK; Mehta, RB; Singh, PJ; *Appl. Phys. Lett.,* 2008, 92*,* 171907-171909.

[9] Q. Ahsanulhaq, Q; Kim, HJ; Reddy, KN; Hahn, BY. *J. Ind. Eng. Chem*., 2008, 14*,* 578–583.

[10] Ahsanulhaq, Q; Kim, HS; Kim, HJ; Hahn, BY. *Mater. Res. Bull.* 2008, 43*,* 3483-3489.

[11] Yousefi, R; Kamaluddin, B; Ghoranneviss, M; Hajakbari, F. *Appl. Surf. Sci.,* 2009, 255*,* 6985-6988.

[12] Dar, AM; Kim, SY; Kim, BW; Sohn, MJ; Shin, SH; *Appl. Surf. Sci.,* 2008, 254*,* 7477-7481.

[13] Setter, N; Eur, J. *Ceram. Soc.*, 2001, 21*,* 1279-1293.

[14] Wang, LZ. *Mater. Today,* 2007, 10, 20-27.

[15] Cava, JR. *J. Am. Ceram. Soc.,* 2000, 83*,* 5-28.

[16] Haghiri-Gosnet MA; Renard, PJ. *J. Phys. D: Appl. Phys.,* 2003, 36*,* R127-R150.

[17] Mao, Y; Park, JT; Wong, SS; *Chem. Commun.,* 2005, 17*,* 5721-5735.

[18] Rao, RNC; Deepak, LF; Gundiah, G; Govindaraj, A. *Prog. Solid State Chem.,* 2003, 31, 5-134.

[19] Reddy KN; Ahsanulhaq, Q; Kim, HJ; Devika, M; Hahn, BY; *Nanotechnology,* 2007, 18*,* 445710.

[20] Reddy, KN; Ahsanulhaq, Q; Kim, HJ; Hahn, BY; *Appl. Phys. Lett.,* 2008, 92*,* 043127-043129.

[21] Reddy, KN; Ahsanulhaq, Q; Kim, HJ; Hahn, BY; *Europhys. Lett.,* 2008, 81*,* 38001.
[22] Ahsanulhaq, Q; Kim, HS; Hahn, BY. *J. Alloy Comp.* 2009, 484*,* 17-20.
[23] Qurashi, A; Tabet, N; Faiz, M; Yamazaki, T." *Nanoscale Res Lett.,* 2009, 4*,* 948-954.
[24] Huang, HM; Wu, YY; Feick, H; Tran, N; Weber, E; Russo, R; Yang, DP. *Science,* 2001, 292*,* 1897-1899,
[25] Ahsanulhaq, Q; Kim, HJ; Hahn, BY; *Nanotechnology*, 2007, 18*,* 485307.
[26] Ahsanulhaq, Q; Umar, A; Hahn, BY. *Nanotechnology,* 2007, 18*,* 115603.
[27] Kong, CY; Yu, PD; Zhang, B; Fang, W; Feng, QS. *Appl. Phys. Lett.,* 2001, 78*,* 407-409.
[28] Liang, HC; Meng, WG; Lei, Y; Phillipp, F; Zhang, DL; *Adv. Mater.,* 2001, 13, 1330-1333.
[29] Zhu, QY; Hsu, KW; Terrones, M; Grobert, N; Terrones, H; Hare, PJ; Kroto, WH; Walton, MRD. *J. Mater. Chem.,* 1998, 8*,* 1859-1860.
[30] Wu, CX; Song, HW; Wang, YK; Hu, T; Zhao, B; Sun, PY; Du, JJ. *Chem. Phys. Lett.,* 2001, 336*,* 53-56.
[31] Wang, LZ; Gao, PG; Gole, LJ; Stout, DJ; *Adv. Mater*., 2000, 12*,* 1938-1940.
[32] Wu, CX; Song, HW; Huang, DW; Pu, HM; Zhao, B; Sun, PY; Du, JJ; *Chem. Phys. Lett.,* 2000, 328*,* 5-9.
[33] Zhang, ZH; Kong, CY; Wang, ZY; Du, X; Bai, GZ; Wang, JJ; Yu, PD; Ding, Y; Hang, LQ; Feng, QS. *Solid State Commun*., 1999, 109, 677-682.
[34] Liang, HC; Meng, WG; Wang, ZG; Wang, WY; Zhang, DL; Zhang, YS; *Appl. Phys. Lett.,* 2001, 78*,* 3202-3204.
[35] Bai, GZ; Yu, PD; Zhang, ZH; Ding, Y; Wang, PY; Gai, ZX; QL. Hang, LQ; Xiong, CGSQ; Feng, QS. *Chem. Phys. Lett.,* 1999, 303*,* 311-314.
[36] Pan, WZ; Dai, RZ; Wang, LZ; *Science,* 2001, 291*,* 1947-1949.
[37] Dai, RZ; Pan, WZ; Wang, LZ. *Solid State Commun.,* 2001, 118*,* 351.
[38] Pan, WZ; Dai, RZ; Wang, LZ. *Appl. Phys. Lett.,* 2002, 80, 309-311.
[39] Dai, RZ; Gole, LJ; Stout, DJ; Wang, LZ. *J. Phys. Chem., B* 2002, 106, 1274-1279.
[40] Yang, DY; Lieber, MC. *Science,* 1996, 273*,* 1836-1840.
[41] Yang, DP; Yan, QH; Mao, S; Russo, R; Johnson, J; Saykally, RJ; Morris, N; Pham, J; He, RR; Cho, JH. *Adv. Funct. Mater.*, 2002, 12*,* 323-331.
[42] Pan, WZ; Dai RZ; Wang, ZL. *Science,* 2001, 291*,* 1947-1949.
[43] Wang, LY; Jiang CX; Xia, Y. *J. Am. Chem. Soc*., 2003, 125*,* 16176-16177.
[44] Li, C; Zhang, D; Han, S; Liu, X; Tang TC; Zhou, C. *Adv. Mater.,* 2003, 15*,* 143-151.

[45] Kobayashi, Y; Hata, H; Salama, M; Mallouk, ET; *Nano Lett.*, 2007, 7, 2142-2145.
[46] Fish, WP; *Physics Education*, 1971, 6, 7.
[47] Qurashi, A; El-Maghraby, ME; Yamazakia, T; Kikuta, T. *J. Alloy Compd*., 2009 480, L9-L12.
[48] Hossain , FM; Takahashi, T; Biswas, S. *Electrochemi. Communi*. 2009, 11, 1756-1759.
[49] Manfred, VAAV. *Zeitschrift fur Physik,* 1938, 108, 553.
[50] Manfred. AV. *Z.Techn. Phys.,* 1938, 108, 407.
[51] Xu, S; Wei, YG; Kirkham, M; Liu, J; Mai, WJ; Snyder, RL; Wang, ZL. *J. Am. Chem. Soc.,* 2008, 130, 14958-15959.
[52] Ahsanulhaq, Q; Kim, HS; Hahn, BY. *J. Alloy and Comp.,* 2009, 484, 17-20.
[53] Qurashi, A; Yamazaki, T; Maghraby, ME; Kikuta, T. *Appl. Phys. Lett.,* 2009, 95, 153109-153111.
[54] Tak, Y; Yong, K. *J. Phys. Chem., B* 2005, 109, 19263-19269.
[55] Ruska, E; Ruska, E. Nobel Prize autobiography, 1986.
[56] Shah, AM; Qurashi, A. *J. Alloy Comp.,* 2009, 482, 548-551.
[57] Qurashi, A; Maghraby, ME; Yamazaki, T; Shen, Y; Kikuta, T. *J. Alloy Comp.,* 2009, 481, L35-L39.
[58] Sarid, D. *Scanning Force Microscopy, Oxford Series in Optical and Imaging Sciences,* Oxford University Press, New York (1991).
[59] Li, Q; Kumar, V; Li, Y; Zhang, H; Marks, JT; Chang, RPC. *Chem. Mater.,* 2005, 17, 1001-1006.
[60] Ahsanulhaq Q; "PhD thesis" Chonbuk National University 2008 Korea.
[61] Moulder, FJ; Stickle, FW; Sobol, EP; Bomben, DK. *Handbook of X-ray Photoelectron Spectroscopy published by Perkin-Elmer Corp., Eden Prairie, MN, USA*. 1992.
[62] Wagner, DC; Riggs, MW; Davis, EL; Moulder, FJ; Mullenberg, EG. *Handbook of X-ray Photoelectron Spectroscopy, published by Perkin-Elmer Corp*., Eden Prairie, MN, USA, 1979.
[63] Dar, AM; Ahsanulhaq, Q; Kim, SY; Sohn, M.; Kim, BW; Shin, SH. *Appl. Surf. Sci.,* 2009, 255, 6279-6284.

In: Structural Analysis
Editor: M.L. Camilleri, pp. 73-91
ISBN: 978-1-61668-987-2

Chapter 4

A METHOD FOR SUPPORTING EFFORTS TO IMPROVE EMPLOYEE MOTIVATION USING A COVARIANCE STRUCTURE

Yumiko Taguchi [1], ***Daisuke Yatsuzuka*** [2] ***and Tsutomu Tabe*** [2]

[1]Department of Business Administration and Communication, Shohoku College, 428 Nurumizu, Atsugi, Kanagawa 243-8501 Japan
[2]Department of Industrial and Systems Engineering, College of Science and Engineering, Aoyama Gakuin University, 5-10-1 Fuchinobe, Sagamihara, Kanagawa 229-8558 Japan

Abstract

This study elucidates a method for showing the priority of factors used to generate motivation in companies, in order to support efforts to improve employee motivation. We verify the effectiveness of the method by a questionnaire survey. This study proceeds towards the above-described objectives in the following three steps. Step 1: Discussing the factors which constitute employee motivation in the literature. Step 2: Contriving a method to set the priority of improvement-forming factors by using covariance structure analysis and graphical modeling. Step 3: Verifying the method proposed in this study based on results obtained. We had the employees at a restaurant fill out a questionnaire by the method proposed in this study. We confirmed that the improvement priority was effective as a support for improvement.

1. Introduction

According to the Ministry of Economy, Trade and Industry, there have been recent increases in both the numbers of Japanese companies launching overseas operations and the numbers of foreign companies moving into Japan [1] [2]. With the globalization of business, Japanese companies are more likely to diversify overseas and overseas companies are more likely to expand into Japan. Within this environment, the competition between Japanese companies and overseas counterparts is expected to increase. Numerous social trends in Japan pose challenges to the competitiveness of Japanese companies, including workforce reductions due to the low birthrate [3], job hopping by younger workers [4], loss of personnel as baby-boomers reach the age of mandatory retirement [5], and general declines in the work ethic and levels of energy at the workplace [4]. Within this social context, companies must improve their levels of performance with limited workforce. If they are to succeed, their employees must be motivated. The effects of motivation on productivity are tremendous. Low motivation reduces employee performance to only 20-30% of the actual capacity of the employees, whereas high motivation boosts performance to 80-90% [6]. To optimize the work efficiency of employees, a management team should raise employee motivation and maintain it at high levels.

Theories in conventional studies on motivation include the two-factor theory of emotion[7], the ERG theory [8], and the Need-Hierarchy Theory [9]. All three theories focus strictly on the mechanism or structure of motivation. As such, none of them help us concretely identify the specific measures required to improve motivation in an individual company. They do little to improve employee motivation or equip companies with strategies for responding adeptly to the requests of their employees on a fulltime basis.

In this study we elucidate a method for identifying the priority of improvements used to enhance employee motivation. After introducing the method itself, we report the results of a questionnaire survey used to verify the effectiveness of the method.

2. Problem-Solving Approach

This study proceeds towards the above-described objectives in the following three steps. Step 1: Discussing the factors which constitute employee motivation in the literature. 2) Contriving a method to set the priority of improvement-forming factors. Step 3) Verifying the method proposed in this study based on results obtained.

2.1. Discussing the Factors which form Motivation

To identify motivation-forming factors for this study, we first need to consider the motivations of employees working for companies. Herzberg proposed a motivation-hygiene theory based on interview surveys with employees, hypothesizing a framework of factors which contribute to job satisfaction (motivator factors) combined with factors which contribute to job dissatisfaction (hygiene factors). Both motivator factors and hygiene factors have an important bearing on motivation. Next, Herzberg went on to describe another eight factors deeply related to motivations in this theory: evaluation, human relationships, shop, working conditions, achievement, pay, the work itself, and growth. Here, we treat these eight factors as the eight major motivation-forming factors in the present study. We also establish specific items related to the eight factors to allow us to easily specify improvements of the factors. In doing so, we assume that the status of the motivation-forming factors contributes to employee satisfaction. Through our discussion on this approach, we derive the motivation formation factors shown in Figure 1 below (cause-and-effect diagram).

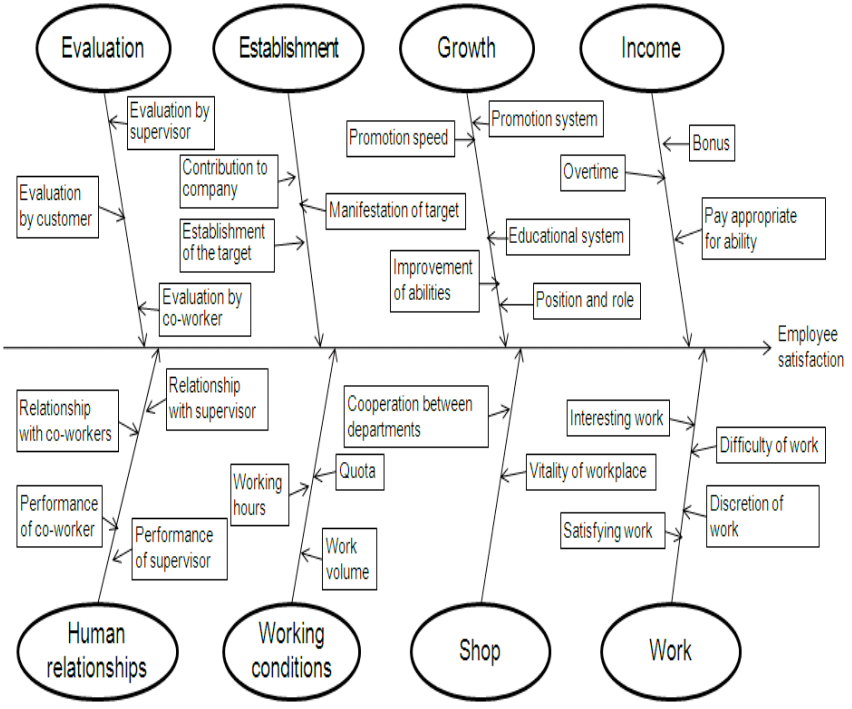

Figure 1. motivation-forming factors in this study.

There are eight major motivation-forming factors (hereinafter referred to as "motivation factors"), i.e., income, growth, establishment, evaluation, work, shop, working conditions, and human relationships. Each motivation factor consists of minor factors (i.e., sub-factors). "Income" consists of three sub-factors: pay appropriate for ability, bonus, and overtime pay. "Growth" consists of five sub-factors: promotion system, educational system, position and role, promotion speed, and improvement of job abilities. "Establishment" consists of three sub-factors: manifestation of target, establishment of the target, and contribution to company. "Evaluation" consists of three sub-factors: evaluation by supervisor, evaluation by co-worker, and evaluation by customer.

"Work" consists of four sub-factors: difficulty of work, discretion of work, interesting work, and satisfying work. "Shop" consists of two sub-factors: vitality of the workplace and cooperation between departments. "Working conditions" consist of three sub-factors: work volume, quota, and working hours. "Human relationships" consist of four sub-factors: relationship with supervisor, performance of supervisor, relationship with co-workers, and performance of co-workers.

2.2. Contriving a Method to Induce Improvement Priority

In this study, we assume that the factors with stronger influence on employee satisfaction will need to be improved in order to improve their priority against the motivation-forming factors set in 2.1 above. In measuring this influence, we need to consider the following three points as the characteristics of the motivation-forming factors.

I. In a preliminary survey, we surveyed the level of employee satisfaction associated with each of the motivation factors covered in the employee questionnaire. The employees surveyed indicated that it was difficult to imagine motivation factors and answer questions about them. Thus, it was difficult to observe the state of the eight motivation factors quantitatively.
II. It is necessary to set model freely because companies, departments and workplaces have different factors to form motivation.
III. The motivation factors extracted from the motivation-formation factors are intricately interrelated. Satisfaction with human relationships, for example, affects the level of satisfaction with work. Additionally, satisfaction with the state of the work affects the levels of satisfaction

with both growth and establishment. These relationships can be set by empirically. The settings, however, may vary between setters. The setting does not necessarily reflect the situation of motivation of employees.

To realize items I and II above, we apply a covariance structure analysis [10] that analyzes the relationships between factors quantitatively. The total effect of each factor is calculated from the path coefficient between factors obtained from the analysis results. This is used as the level of influence on satisfaction degree of employees for each factor.

Additionally, we use a graphical modeling [11] capable of elucidating and organizing the relationship between motivation factors in an objective and exploratory manner in order to construct a model for covariance structure analysis, in consideration of item III shown above. Data on the state of factors are collected directly from the opinions of employees and the results of the questionnaire survey on the employee's level of satisfaction with work.

Graphical model shown above will be explained in the next section. The specific method to prioritize the improvement items is described in chapter 3.

2.3. Use of Graphical Modeling

Graphical modeling is a method to arrange relationships between variables by obtaining partial correlation coefficients, as shown in Figure 2.

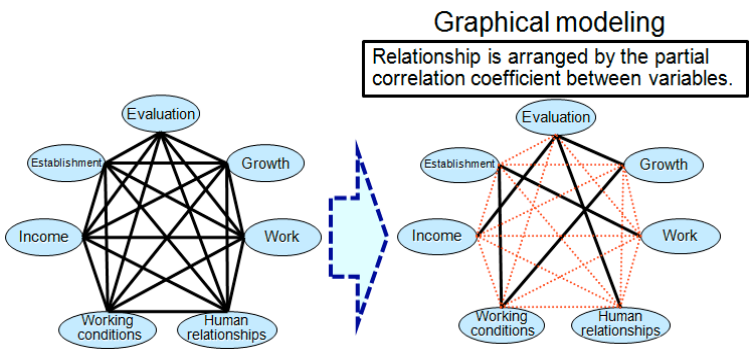

Figure 2. Graphical modeling.

The relationships are derived from data, not from models constructed as hypotheses. In this study, we use graphical modeling to arrange relationships among eight motivation factors.

A partial correlation coefficient is obtained from a simple correlation coefficient among variations. Specifically, we obtain a partial correlation coefficient from equation (1) by expressing the correlation matrix as $R = (r_{ij})$, and the inverse matrix as $R^{-1} = (r^{ij})$. If a partial correlation coefficient is 0, there is no relationship between the variables.

$$r_{ij \cdot rest} = \frac{-r^{ij}}{\sqrt{r^{ii}} \cdot \sqrt{r^{jj}}} \tag{1}$$

3. Method to Derive the Priority of Motivation Improvements

Based on 2.2 shown above, we calculate the priority of motivation improvements in this study in six steps, as shown in Figure 3.

Specifically, 1) Setting variables for the analytic procedure, 2) carrying out the questionnaire survey on the level of employee satisfaction with work, 3) understanding a simple correlation coefficient between motivation factors by confirmatory factor analytic procedure, 4) arranging the relationships between motivation factors by graphical modeling, 5) constructing a model and performing a covariance structure analysis, 6) calculating the influence of each sub-factor on total employee satisfaction, and calculating the improvement priority.

3.1. Handling the Variables in this Study

Three variables are used for the confirmatory factor analysis and covariance structure analysis in this study: a latent variable, an observed variable, and an error variable.

Eight hardly observable motivation factors are set as latent variables.

An observed variable uses the following two satisfaction levels as quantitatively obtained data. The first is the level of satisfaction with 27 sub-factors out of the motivation-formation factors. The second is the level of employee satisfaction with work as a whole.

There is assumed to be a causality between the latent variable and observed variable, as shown in Figure 4.

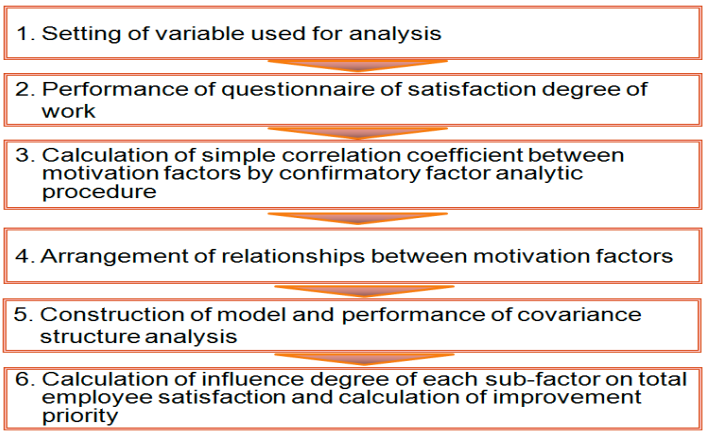

Figure 3. Method to derive the priority of improvements.

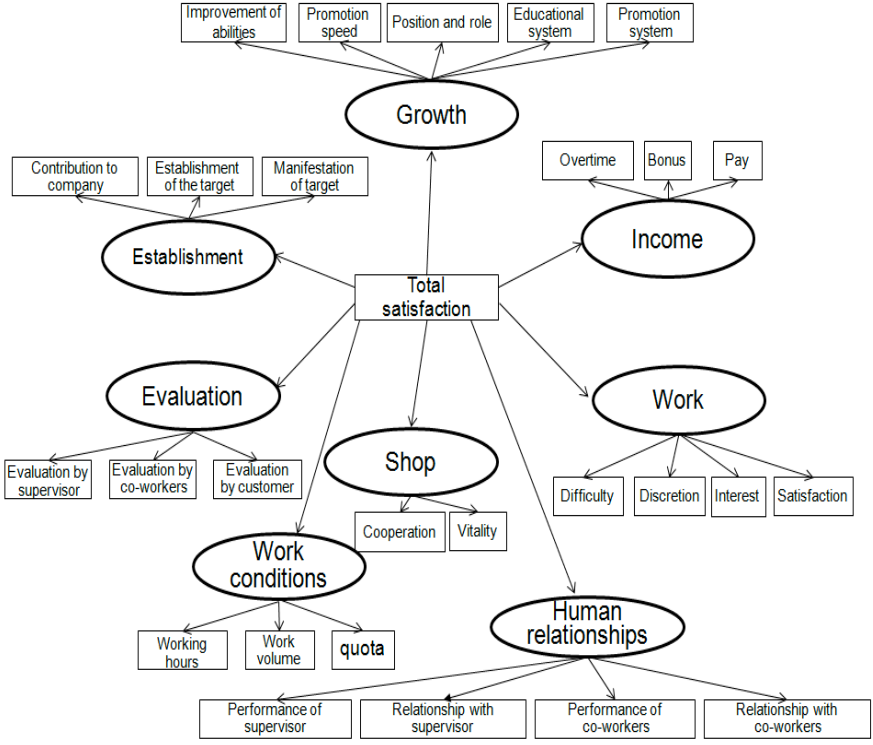

Figure 4. Variables used in this study, and the relationships among them.

The error variable is a constructive concept that assembles effects of any factor not expressed by the model. In this study, error variables are established for both the observed variables and latent variables.

If the error variable has a considerable impact on the observed variable and latent variable, there are likely to be other influences that the model cannot express. In this case, the model cannot explain the relationship.

3.2. Questionnaire on Satisfaction with Work

The questionnaire is roughly divided into surveys on two items: 1) the level of satisfaction with work as a whole and 2) the level of satisfaction with the sub-factors.

2) above are data for observed variables.

The satisfaction level was evaluated on a 6-point scale. Options 1-3 denote dissatisfaction. Options 4-6 denote satisfaction.

As an example, Figure 5 shows the questionnaire format for the sub-factor "Evaluation."

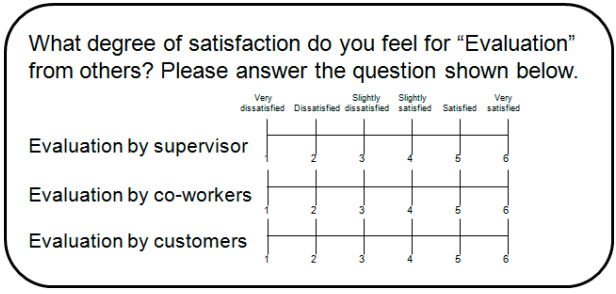

Figure 5. Questionnaire format for "Evaluation".

3.3. Understanding a Simple Correlation Coefficient between Motivation Factors by Confirmatory Factor Analysis

A confirmatory factor analysis, can freely construct and verify the relationships among conceivable factors (latent variable) and observed variables, and factors. In this study, we perform a confirmatory factor analysis to confirm whether or not there is correlation between the eight motivation factors.

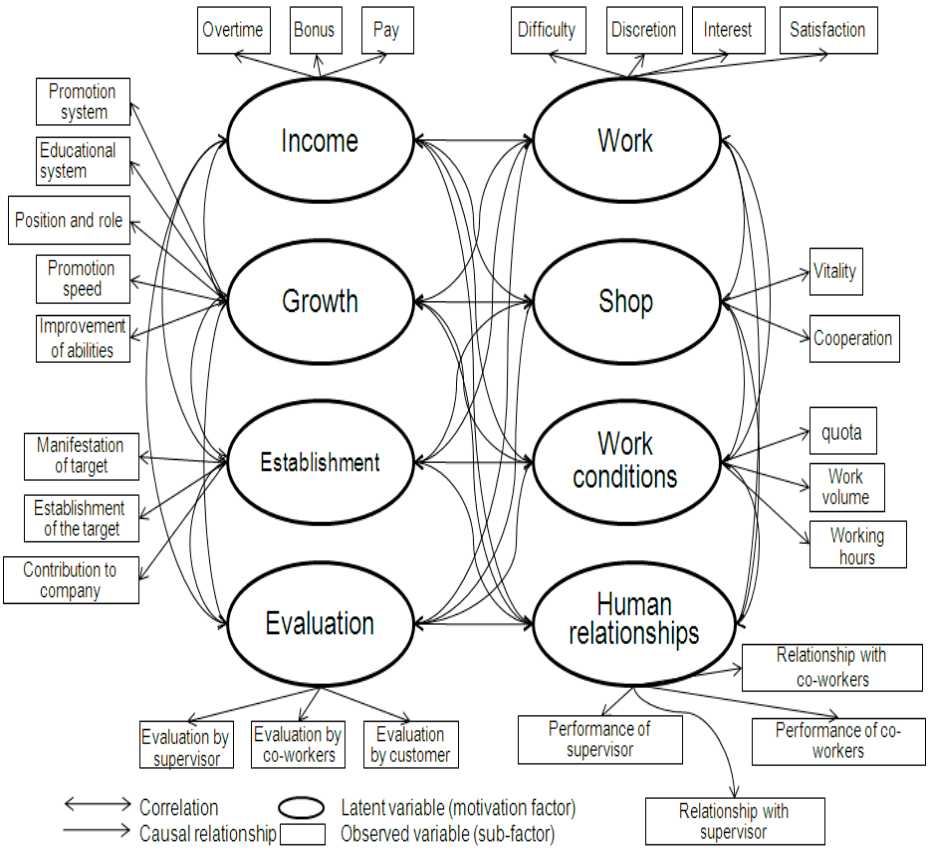

Figure 6. A model used in confirmatory factor analysis.

We perform the analysis by setting up the model shown in Figure 6. The model assumes that there is co-variation between all latent variables and a causal relationship between latent variables and observed variables. The analysis is conducted with Amos software for multivariate analysis. The simple correlation coefficients between motivation factors are obtained. If we find, when focusing on a characteristic factor, that a simple correlation coefficient value with another characteristic is significantly low, we conclude that the characteristic factor of focus has no relationship with the other motivation factors. In other words, it is determined to be a non-correlated factor and removed from the target factors for graphical modeling.

3.4. Arranging the Relationships Between Motivation Factors by Graphical Modeling

Based on the simple correlation coefficient between motivation factors obtained by the confirmatory factor analysis in the previous section, we obtain partial correlation coefficients between motivation factors using the graphical modeling described above. Motivation factors with partial correlation coefficients of zero are assumed to be unrelated.

3.5. Constructing a Model and Performing a Covariance Structure Analysis

At first, we use construct a model expressing the structure of motivation-formation factors in consideration of the relationships between motivation factors obtained by the graphical modeling described above. Arrows are used to illustrate the causal relationships (time relationships) between the motivation factors which are determined to have relationships. Next, the Amos software for multivariate analysis is used to conduct a covariance structure analysis based on the model.

3.6. Calculating the Influence of Each Sub-Factor on the total Level of Satisfaction, and Calculating the Improvement Priority

The influence of each motivation formation factor on the total level of satisfaction is obtained by the following three steps.

Step 1). Based on the path coefficient obtained from the covariance structure analysis for each observed variable, obtain the product of the path coefficients of the observed variable from the total satisfaction level.

Step 2). Compute the total sum (hereinafter referred to as the "total effect") of the products of the path coefficients to determine the improvement priority, including the direct effect and indirect effect. Figure 7 is an example of a calculation of the total effect of sub-factors, the "establishment of a target," and "cooperation." The sub-factor "cooperation" shows indirect effect from the total satisfaction level via motivation factors "establishment."

Step 3). As a result of step 2 above, factors with total sums have higher improvement priority.

4. Discussion of Effectiveness

The effectiveness of the methodology proposed in this study is verified in the following three steps.

Step 1. Issue a questionnaire to employees of an existing company.
Step 2. Apply the method proposed in this study to the questionnaire data shown above to generate improvement priority for motivation-formation factors.
Step 3. Compare the generated improvement priority to a model in which relationships between motivation factors are not considered from the viewpoint of the goodness of fit of the model.

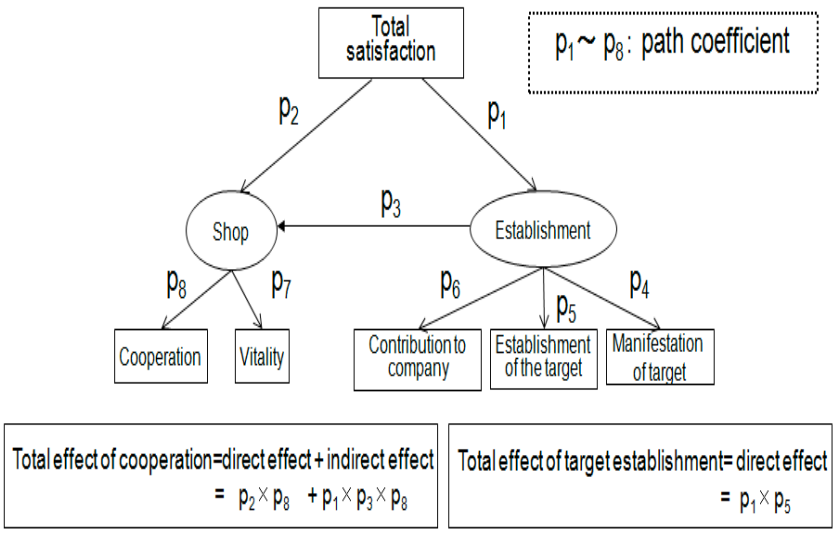

Figure 7. An example of calculating the influence of each sub-factor on the total satisfaction.

4.1. Questionnaire Survey

Questionnaires were issued to a restaurant. The hours of business were 17:00 to 24:00, 365 days a year.

The subjects were 31 employees of the restaurant. The questionnaire was conducted from November 21 to December 5, 2008. The contents of the questionnaire are shown in 3.2.

4.2. Generating the Improvement Priority for Motivation-Formation Factors

Based on the questionnaire response data, we obtained the improvement priority by the method described in chapter 3. The results are shown below.

4.2.1. Results of Confirmatory Factor Analysis and Graphical Modeling

Table 1 shows correlations of the latent variables (i.e., eight motivation factors) determined via the conformity factor analysis. As shown in Table 1, the simple correlation coefficient between shop and other motivation factors (factors other than income) is very small. There seems to be little relationship. Thus, we sought to determine partial correlation coefficients by graphically modeling the relationships of the seven motivation factors other than "shop." The table2 shows the partial correlation coefficients.

Table 1. Simple correlation coefficients between latent variables

	Evaluation	Establishment	Income	Working conditions	Human Relationships	Work	Growth	Shop
Evaluation	1	0.47	0.86	0.51	0.53	0.63	0.73	0.03
Establishment	0.47	1	0.85	0.73	0.51	0.68	0.85	0.09
Income	0.86	0.85	1	0.47	0.12	0.06	0.88	0.73
Working conditions	0.51	0.73	0.47	1	0.34	0.41	0.64	0.25
Human Relationships	0.53	0.51	0.12	0.34	1	0.86	0.60	0.03
Work	0.63	0.68	0.06	0.41	0.86	1	0.77	0.16
Growth	0.73	0.85	0.88	0.64	0.60	0.77	1	0.12
Shop	0.03	0.09	0.73	0.25	0.03	0.16	0.12	1

Table 2. Partial correlation coefficients between latent variables.

	Evaluation	Establishment	Income	Working conditions	Human Relationships	Work	Growth
Evaluation	–	0.46	0	0	0	0	0
Establishment	0.46	–	0	0	0	0	0.83
Income	0	0	–	0.35	0	0	0
Working conditions	0	0	0.35	–	0	0.76	0
Human Relationships	0	0	0	0	–	0.65	0
Work	0	0	0	0.76	0.65	–	0.71
Growth	0	0.83	0	0	0	0.71	–

As shown in Figure 8, six relationships between latent variables are observed as a result of the partial correlation coefficients: income and working conditions, work and human relationships, work and work condition, work and growth, establishment and evaluation, and establishment and growth.

Figure 9 is a model of motivation formation in this study considering six relationships. Motivation factors with confirmed relationships in the graphical modeling are shown in boldface.

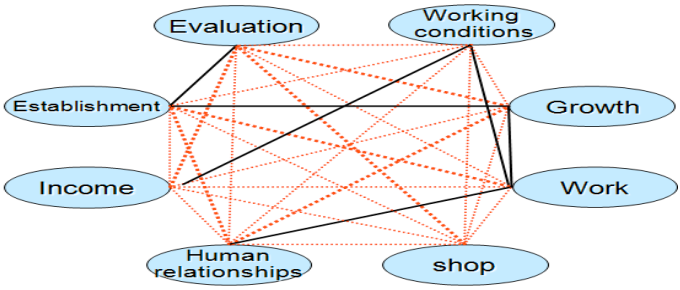

Figure 8. Organized relationship among latent variables.

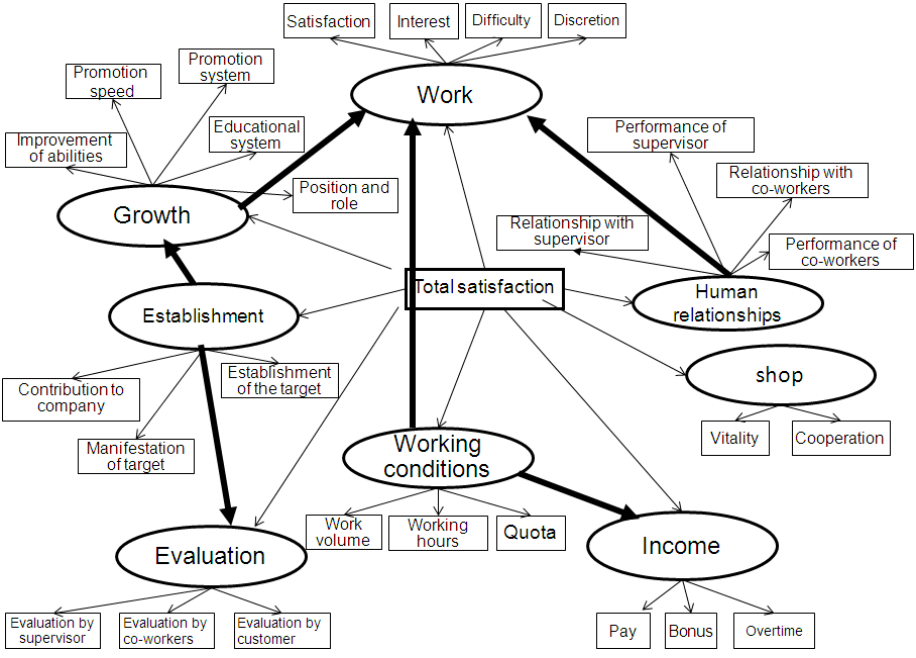

Figure 9. Model of this study.

4.2.2. Conducting a Covariance Structure Analysis and Calculating the Improvement Priority

The model set up in the previous section 4.2.1 was expressed on AMOS and analyzed. Figure 10 shows the results. The numbers are path coefficients between variables.

Based on the result shown above, table 3 shows the total effect and improvement priority by sub-factor.

The three major factors are work volume, establishment of the target, and working hours.

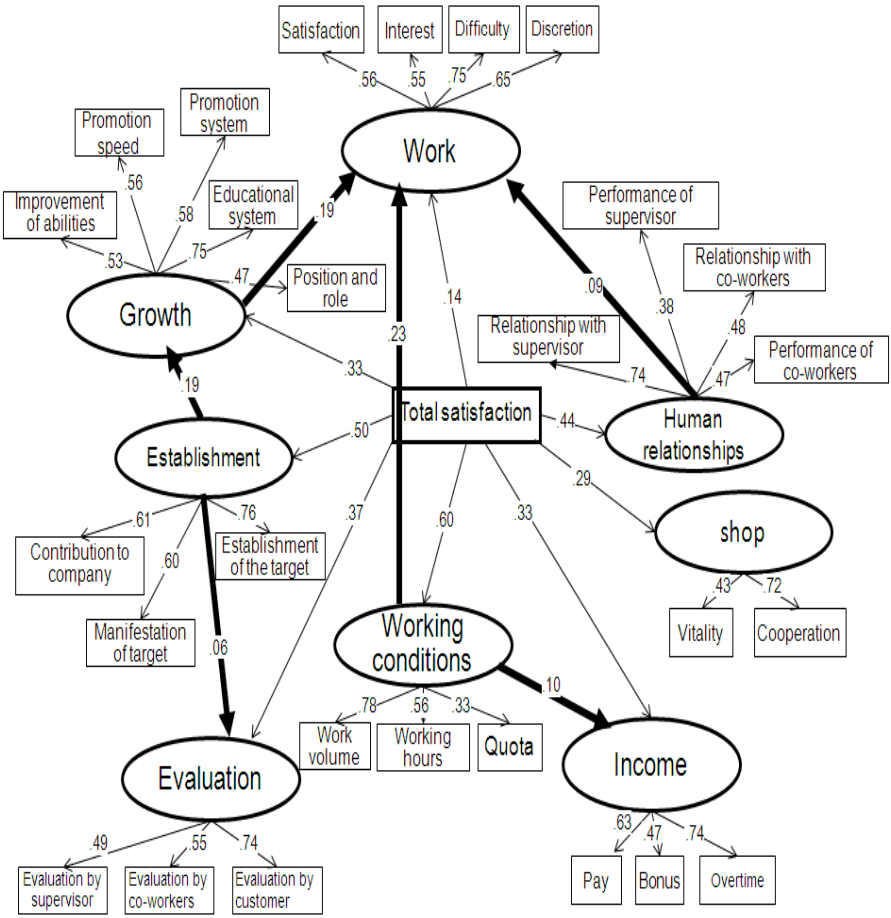

Figure 10. Result of covariance structure analysis in this study.

Table 3. Result of calculation of improvement priority

Variable name	Direct effect	Indirect effect 1	Indirect effect 2	Indirect effect 3	Indirect effect 4	Total effect	Improvement priority
Evaluation by customer	0.274	0.022	-	-	-	0.296	9
Evaluation by co-worker	0.204	0.017	-	-	-	0.221	17
Evaluation by supervisor	0.181	0.015	-	-	-	0.196	24
Contribution to company	0.305	-	-	-	-	0.305	6
Manifestation of target	0.300	-	-	-	-	0.300	7
Establishment of the target	0.380	-	-	-	-	0.380	2
Improvement of abilities	0.175	0.050	-	-	-	0.225	15
Promotion speed	0.185	0.053	-	-	-	0.238	14
Promotion system	0.191	0.055	-	-	-	0.246	12
Educational system	0.248	0.071	-	-	-	0.319	5
Position and role	0.155	0.047	-	-	-	0.202	22
Pay	0.208	0.038	-	-	-	0.246	12
Bonus	0.155	0.028	-	-	-	0.183	25
Overtime	0.244	0.044	-	-	-	0.288	10
Relationship with supervisor	0.326	-	-	-	-	0.326	4
Performance of supervisor	0.167	-	-	-	-	0.167	26
Relationship with co-workers	0.211	-	-	-	-	0.211	19
Performance of co-workers	0.207	-	-	-	-	0.207	21
Work volume	0.468	-	-	-	-	0.468	1
Working hours	0.336	-	-	-	-	0.336	3
Quota	0.198	-	-	-	-	0.198	23
Vitality	0.125	-	-	-	-	0.125	27
Cooperation	0.209	-	-	-	-	0.209	20
Satisfaction	0.078	0.022	0.035	0.077	0.010	0.222	16
Interest	0.077	0.022	0.034	0.076	0.010	0.219	18
Difficulty	0.105	0.030	0.047	0.104	0.014	0.300	7
Discretion	0.091	0.026	0.041	0.090	0.012	0.260	11

4.3. Comparison with a Model that Disregards Relationships among Motivation Factors

Next, we conducted a covariance structure analysis that disregards the relationships between motivation factors. Figure 11 shows the results. Table 4 shows the improvement priority calculated based on the results.

We compared the model constructed by the method proposed by this study (i.e., a model considering the relationships between motivation factors) to a model that disregards the relationships between motivation factors. Figure 12 shows the results. Compared items consist of GFI and AGFI showing the goodness of fit of the model and the improvement priority.

GFI and AGFI are rather high in the model of this study, as no relationships between motivation factors are modeled. Therefore, the model of this study has validity.

In comparing the improvement priorities between the two models, we find that the improvement with the highest priority differed. The top priority improvement in the model disregarding the relationships between motivation factors was "satisfaction of work." We asked for the opinions of the employee of the company where the questionnaire was conducted.

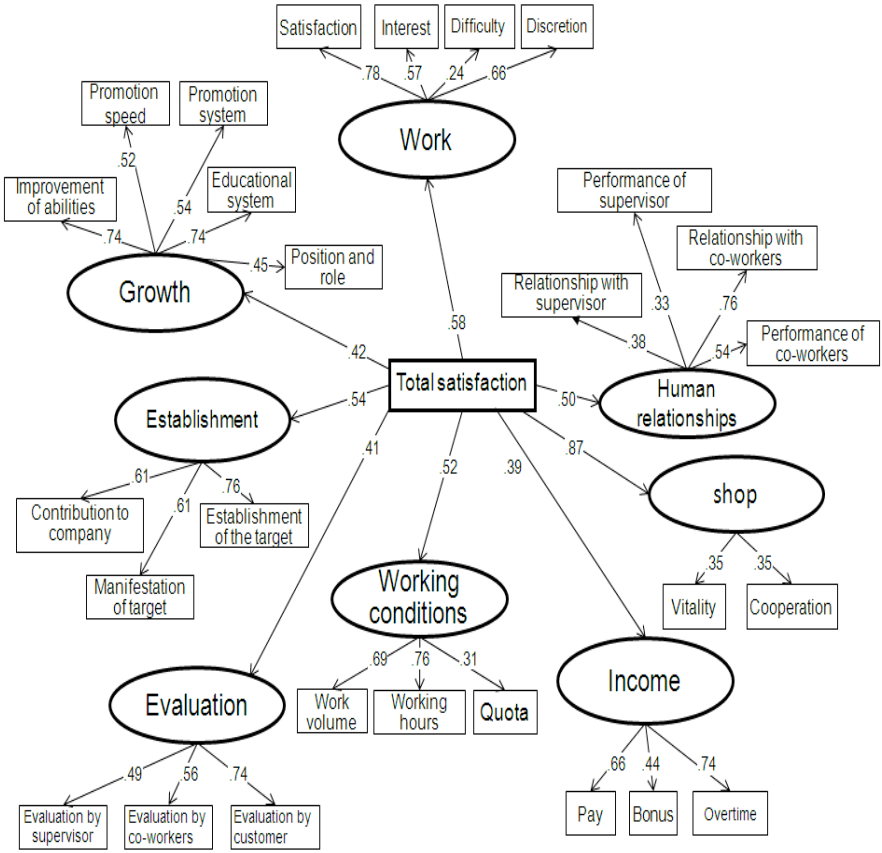

Figure 11. Result of covariance structure analysis disregarding the relationships between motivation factors.

Some respondents commented as follows: "There is a problem with the work volume. There is little problem, however, in the level of 'satisfaction of work.' The improvement priority in consideration of the relationships between motivation factors reflects the current situation better." Therefore, the improvement priority in consideration of the relationships between motivation factors mentioned in this study is more reliable.

Table 4. Improvement priority disregarding the relationships between motivation factors

Variable name	Direct effect	Total effect	Improvement priority
Evaluation by customer	0.303	0.303	15
Evaluation by co-worker	0.310	0.310	12
Evaluation by supervisor	0.201	0.201	21
Contribution to company	0.329	0.329	8
Manifestation of target	0.329	0.329	8
Establishment of the target	0.410	0.410	2
Improvement of abilities	0.311	0.311	10
Promotion speed	0.218	0.218	20
Promotion system	0.227	0.227	19
Educational system	0.311	0.311	10
Position and role	0.189	0.189	23
Pay	0.257	0.257	18
Bonus	0.296	0.296	16
Overtime	0.121	0.121	27
Relationship with supervisor	0.190	0.190	22
Performance of supervisor	0.165	0.165	24
Relationship with co-workers	0.380	0.380	5
Performance of co-workers	0.270	0.270	17
Work volume	0.359	0.359	6
Working hours	0.395	0.395	3
Quota	0.161	0.161	25
Vitality	0.305	0.305	13
Cooperation	0.305	0.305	13
Satisfaction	0.452	0.452	1
Interest	0.331	0.331	7
Difficulty	0.139	0.139	26
Discretion	0.383	0.383	4

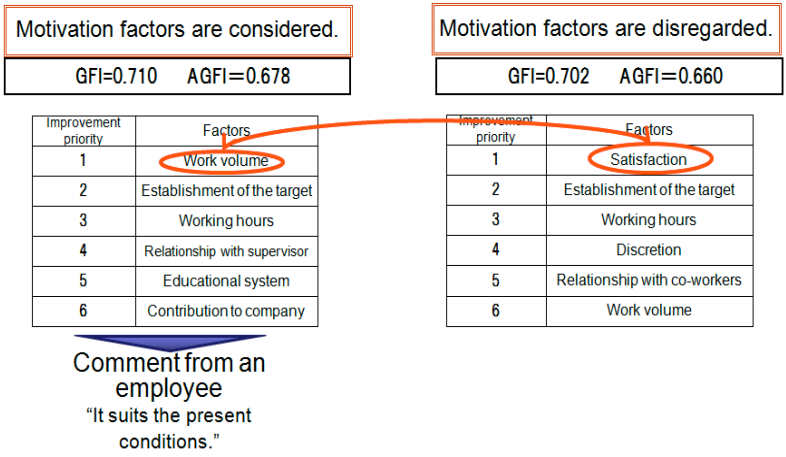

Figure 12. Comparison between the model disregarding motivation factors and this study.

5. Result

We had the employees at a restaurant fill out a questionnaire by the method proposed in this study. We confirmed that the improvement priority was effective as a support for improvement.

As shown above, we elucidated a method to propose improvement priority in order to support the efforts of managers in a company to improve the motivation of their employees.

In the future, we will need to collect data from categories of business other than the restaurant business and discuss whether the improvement priority is effective in those categories.

References

[1] Ministry of Economy, Trade and Industry. (2009). *Survey of Overseas Business Activities.* Retrieved May 25, 2010, from http://www.meti.go.jp/english/statistics/tyo/kaigaizi/index.html.

[2] Ministry of Economy, Trade and Industry. (2009*). Survey of Trends in Business Activities of Foreign Affiliates.* Retrieved May 25, 2010, from http://www.meti.go.jp/english/statistics/tyo/gaisikei/index.html.

[3] Health, Labour, & Welfare Ministry. (2005). *White paper on the Labour Economy 2005 Summary.* Retrieved May 25, 2010, from http://www.mhlw.go.jp/english/wp/l-economy/index.html.

[4] Nomura Research Institute, Ltd. (2005). *Regeneration of motivation for work is important for management strategy in 2010 (in Japanese).* Retrieved May 25, 2010, from http://www.nri.co.jp/news/2005/051205.html.

[5] Taro Saito. (2005). Effect of retirement of baby boomers on the labor market (in Japanese). *NLI Research Institute report*, 98, 8-13.

[6] Paul Hersey, Kenneth, H. & Blanchard, Dewey, E. Johnson. (1996). *Management of Organizational Behavior: Utilizing Human Resources (Seventh Edition)*. New Jersey: Prentice-Hall, Inc., 10-11.

[7] Frederick Herzberg, Bernard Mausner, Barbara Bloch Snyderman. (1993). *The Motivation to Work*. New Jersey: Transaction Publishers.

[8] Paul Hersey, Kenneth, H. & Blanchard, Dewey, E. Johnson. (1996). *Management of Organizational Behavior: Utilizing Human Resources (Seventh Edition)*. New Jersey: Prentice-Hall, Inc., 40-45.

[9] Paul Hersey, Kenneth, H. & Blanchard, Dewey, E. Johnson. (1996).

Management of Organizational Behavior: Utilizing Human Resources (Seventh Edition). New Jersey: Prentice-Hall, Inc., 45.

[10] Jöreskog, K. G. (1978). Structural analysis of covariance and correlation matrices. *Psychometrika*, 43(4), 43-477.

[11] Dempster, A. P. (1972). Covariance selection. *Biometrics*, 28, 157-175.

In: Structural Analysis
Editor: M.L. Camilleri, pp. 93-99
ISBN: 978-1-61668-987-2

Chapter 5

A BLOCK MULTIFRONTAL SUBSTRUCTURE METHOD FOR SOLVING LINEAR ALGEBRAIC EQUATION SETS IN FE ANALYSIS SOFTWARE

Sergiy Fialko*
Institute of Informatics, Tadeusz Kosciuszko Cracow University of Technology, Warszawska str. 24, 31-155 Cracow, Poland

Abstract

A block substructure multifrontal method for solution of large symmetrical sparse equation sets that appear in finite element problems of structural and solid mechanics is proposed for desktop multicore computers. The analysis of a structure's topology reduces the fill-ins and allows the coupling of equations into blocks. A symmetrical storage scheme for dense matrices and performance optimizations provide a combination of an efficient usage of random-access memory and a high rate of factorization.

Introduction

The proposed method for solving large sparse symmetrical equation sets which appear in applications of the finite element method to problems of structural mechanics is based on an analysis of the design model topology rather

* E-mail address: sfialko@poczta.onet.pl

than on that of the sparse matrix structure itself as it is done for the classical multifrontal method [1, 9]. The adjacency graph for nodes of the finite element model together with lists of nodes for each finite element make up the basis for such an analysis. The natural coupling of equations into groups made possible by the existence of several equations per node produces dense matrix blocks in the global sparse stiffness matrix and simplifies its decomposition into dense sub-matrices. This entails an increased performance of computation when the BLAS 3 level matrix multiplication is used [2].

The Block Substructure Multifrontal Method

The given structure (Figure 1.a, 1.b) is divided into separate finite elements and then is assembled step-by-step according to a chosen reordering algorithm. The substructures and separate finite elements that contain a node to be eliminated at a given assembling-elimination step (a fully assembled node) are then coupled (Figure 2). The formed substructure produces a matrix considered as a dense one and consisting of fully assembled equations associated with the given node and an incomplete part [3–6]. The fully assembled equations are eliminated immediately. Table 1 presents the assembling-eliminating process for the example shown in Figure 1.a. Running through Table 1 from bottom to top makes up a substructure (frontal) tree (Figure 3) which presents the sequence of creation of the substructures.

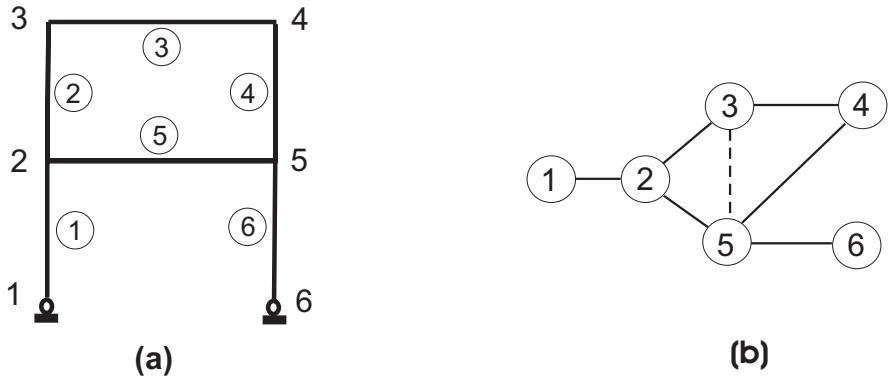

Figure 1. An example of a structure (a plane frame (a)) and its corresponding nodal adjacency graph (b). The finite element numbers are shown by figures in circles. The minimum degree algorithm [7] produces the node elimination ordering 1,6,4,3,5,2. The fill-in 3-5 is shown as a dash line.

Table 1. The assembling-eliminating process.

Substructure	Number of eliminated node	List of nodes	List of previous substructures	List of finite elements
Sstr 1	1	2,1	–	1
Sstr 2	6	5,6	–	6
Sstr 3	4	5,3,4	–	3,4
Sstr 4	3	2,5,3	3	2
Sstr 5	5	2,5	4,2	5
Sstr 6	2	2	1,5	–

The new substructure numbering (Figure 3) allows one to reduce the storage of incomplete parts of the frontal matrices. The partial factorization procedure is:

$$\begin{pmatrix} \mathbf{C} & \mathbf{W} \\ \mathbf{W}^T & \mathbf{D} \end{pmatrix} = \begin{pmatrix} \tilde{\mathbf{C}} & \tilde{\mathbf{W}} \\ 0 & \mathbf{L} \end{pmatrix} \begin{pmatrix} \mathbf{I} & 0 \\ 0 & \mathbf{I}_S \end{pmatrix} \begin{pmatrix} \mathbf{I} & 0 \\ \tilde{\mathbf{W}}^T & \mathbf{L}^T \end{pmatrix}, \tag{1}$$

where $\mathbf{C}$ is an incomplete part and block row $\mathbf{W}^T$, $\mathbf{D}$ consists of fully assembled equations. The sign diagonal $\mathbf{I}_s$ allows us to consider an indefinite matrix too.

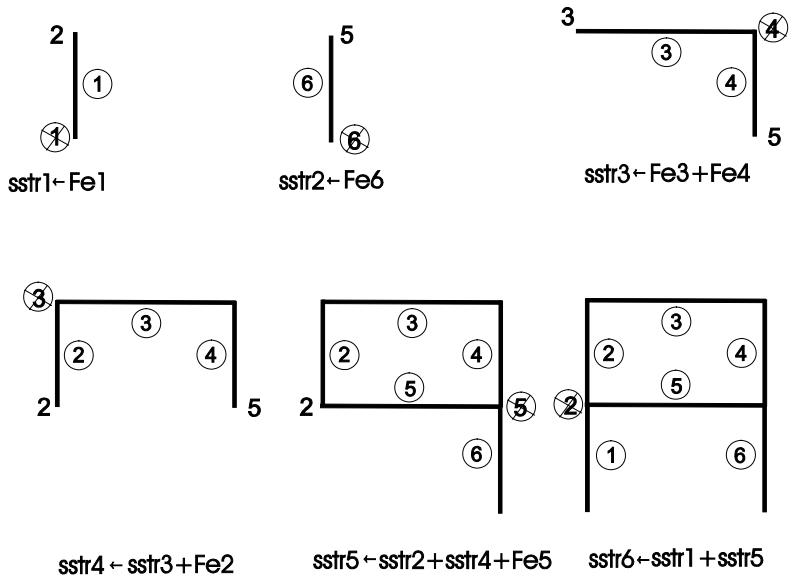

Figure 2. The assembling-eliminating process. Each substructure sstr is assembled from substructures created at previous steps and separate finite elements Fe. Fully assembled nodes are eliminated and are marked by crossed digits in circles.

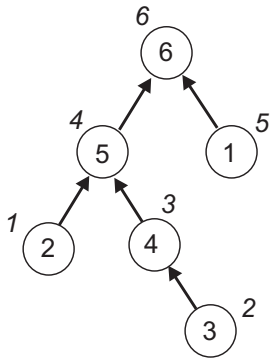

Figure 3. The substructure tree. New substructure numbers are shown in italic.

For large-scaled problems, multiple fully assembled nodes occur at some assembling steps. They produce sequential branches in the frontal tree. The coupling of corresponding fully assembled equations into large blocks is a very important factor in increasing the performance.

The partial factoring occurs in three stages

$$\begin{aligned} &1.\quad \mathbf{D} = \mathbf{L}\cdot\mathbf{I}_S\cdot\mathbf{L}^T \;\rightarrow\; \mathbf{L},\mathbf{I}_S \\ &2.\quad \mathbf{W}^T = \mathbf{L}\cdot\mathbf{I}_S\cdot\widetilde{\mathbf{W}}^T \rightarrow\; \widetilde{\mathbf{W}} \\ &3.\quad \mathbf{C} = \widetilde{\mathbf{C}} + \widetilde{\mathbf{W}}\cdot\mathbf{I}_S\cdot\widetilde{\mathbf{W}}^T \rightarrow \widetilde{\mathbf{C}} = \mathbf{C} - \widetilde{\mathbf{W}}\cdot\mathbf{I}_S\cdot\widetilde{\mathbf{W}}^T \end{aligned} \tag{2}$$

Stage 1 consists of factoring the diagonal block **D**. Stage 2 presents the solution of an equation set with low triangle matrix L and multiple right-hand parts. And Stage 3 is the calculation of the Schur complement.

The parallelization on the basis of OpenMP is applied at both Stage 2 and Stage 3. The existing Blas 3 level DGEMM, DSYRK procedures from the Intel MKL library and other high performance libraries require the N^2 entries to store matrix **C** even if **C** is symmetrical.

A special microkernel based on [8] has been developed to perform the fast computation of $\widetilde{\mathbf{C}} = \mathbf{C} - \widetilde{\mathbf{W}}\cdot\mathbf{I}_S\cdot\widetilde{\mathbf{W}}^T$ using a vectorization of operations, XMM register blocking, cache blocking and packing of data to reduce the reading misses. This approach maintains a symmetrical storage scheme and requires approximately $N^2/2$ entries to store **C** [6]. It is very important for desktop computers which have a very restricted RAM storage.

Numerical Results

A desktop computer Intel® Core™2 Quad CPU Q6600 @2.40 GHz, RAM DDR2 800 MHz 8 GB has been used. A square plate with the mesh 800x800 is under consideration (3 849 594 equations). The proposed method (BSMFM) is compared with the sparse direct solver of the ANSYS 11.0 software and demonstrates an efficient usage of random-access memory (Table 2).

The second test (a cube consisting of brick volumetric finite elements with the mesh 50x50x50, Table 3) illustrates a good performance of the BSMFM solver.

Table 2. Duration of numerical factoring, s for plate 800x800.

Method	Platform	Number of processors		
		1	2	4
BSMFM	ia32	978	768	670
ANSYS 11.0	ia32	Insufficient random-access memory		

Table 3. Duration of numerical factoring, s for cube 50x50x50.

Method	Platform	Number of processors		
		1	2	4
BSMFM	ia32	827	504	365
ANSYS 11.0	ia32	1 610	882	544

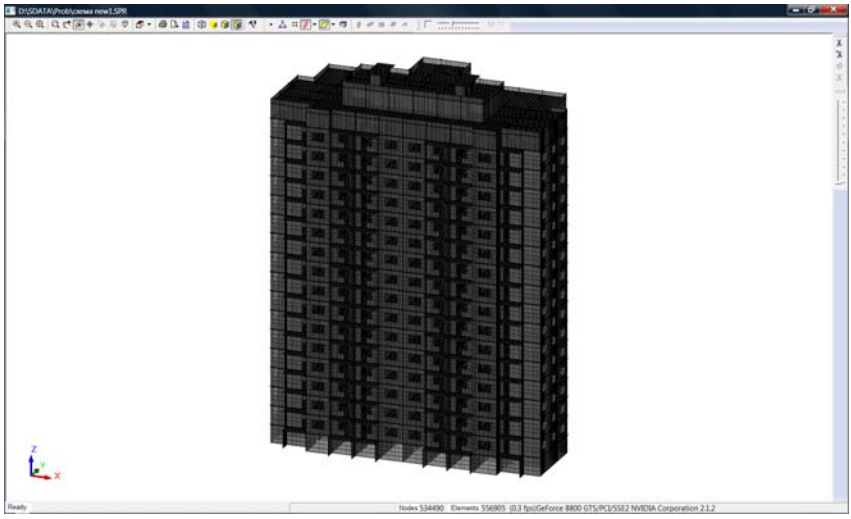

Figure 4. Finite element model of a multistory building (3 198 609 equations).

The last numerical example (3 198 609 equations, Figure 4) is taken from the computational practice of SCAD Soft (www.scadsoft.com). The numerical factoring time is 1 332 s on four processors. The Intel 64 platform has been used.

Conclusion

The proposed method demonstrates at the same time a good performance and an efficient usage of the random-access memory. It is based on mechanical concepts which allow one to produce the efficient coupling of equations into groups. This improves the rate of numerical factoring. The developed microkernel for calculation of the Schur complement makes it possible to maintain a symmetrical storage scheme and implement various schemes of high performance. The disk storage is involved when the dimension of a problem is too large to be allocated in RAM.

References

[1] Amestoy, PR; Duff, IS; L'Excellent, JY. Multifrontal parallel distributed symmetric and unsymmetric solvers. *Comput Meth Appl Mech Eng*. 2000, 184, 501-520.

[2] Demmel, JW. Applied Numerical Linear Algebra; SIAM, *Philadelphia*, 1997, 421.

[3] Fialko, S. Yu. Stress-Strain Analysis of Thin-Walled Shells with Massive Ribs. *Int App Mech*., 2004, 40, 4, 432-439.

[4] Fialko, S. Yu., A block sparse direct multifrontal solver in SCAD software, Proceedings of the CMM-2005–Computer Methods in Mechanics. *Czestochowa, Poland*, 73-74, 2005.

[5] Fialko, S. A Sparse Shared-Memory Multifrontal Solver in SCAD Software. Proceedings of the International Multiconference on Computer Science and Information Technology. October 20-22, 2007, Wisła, Poland, 3 (2008), ISSN 1896-7094, ISBN 978-83-60810-14-9, IEEE Catalog Number CFP0864E-CDR277-283, 2008. (http://www.proceedings2008.imcsit.org/pliks/47.pdf).

[6] Fialko, S. The direct methods for solution of the linear equation sets in modern FEM software; SCAD SOFT, Moscow, 2009, 160. (in Russian).

[7] George, A; Liu, JWH. Computer Solution of Large Sparse Positive Definite Systems, Prentice-Hall, Inc., *Englewood Cliffs*, NJ, 1981, 256.

[8] Goto, K; Van De Geijn, R. A. Anatomy of High-Performance Matrix Multiplication. *ACM Transactions on Mathematical Software*., 2008, 34, 3, 1-25.

[9] Gould, NIM; Hu, Y; Scott, JA. A numerical evaluation of sparse direct solvers for the solution of large sparse, symmetric linear systems of equations. Technical report RAL-TR-2005-005, *Rutherford Appleton Laboratory*, 2005, 31.

In: Structural Analysis
Editor: M.L. Camilleri, pp. 101-128
ISBN 978-1-61668-987-2

Chapter 6

NON LINEAR STRUCTURAL ANALYSIS. APPLICATION FOR EVALUATING SEISMIC SAFETY

Juan Carlos Vielma [a],*, ***Alex Barbat*** [b] ***and Sergio Oller*** [b]
[a] Lisandro Alvarado University
[b] Technical University of Catalonia

Keywords: Non-linear analysis, ductility, overstrength, seismic safety.

1. Introduction

Performance-Based Design is currently accepted commonly as the most advanced design and evaluation approach. However, successful application of this procedure depends largely on the ability to accurately estimate the parameters of structural response.

Determination of these parameters requires application of analysis procedures where the main non-linear behavior features (constitutive and geometrical) of structures are included. This chapter presents and discusses these features of non-linear behavior and how they are incorporated in the process of static or dynamic structural analyses. Non-linear analysis leads to determination of significant structural response parameters whenever estimating seismic responses such as ductility, overstrength, response reduction factor and damage

*E-mail address: jcvielma@ucla.edu.ve

thresholds; being these the main response parameters for evaluating the seismic safety of structures. In order to illustrate application of the non-linear procedure being described, a set of concrete-reinforced moment-resisting framed buildings with various numbers of levels was selected. These buildings were designed according to ACI-318 [1] for high and very high level of seismic hazard.

Seismic safety of regular concrete-reinforced framed buildings is studied using both the static and dynamic non-linear analyses. Static analysis consists in using the pushover procedure and dynamic analysis is done by using the incremental dynamic analysis (IDA). Analysis was performed using the PLCd computer code [2] which allows incorporation of the main characteristics of reinforcement and confinement provided to the cross sections of structural elements (beams and columns). A set of 16 concrete-reinforced framed buildings with plane and elevation regularity was designed according to ACI-318 [1] and for loads prescribed by the ASCE7-05 [3]. Results obtained from static and dynamic non-linear analyses allowed calculation of global ductility, overstrength and behavior factors. Behavior factors are compared with design values prescribed by the ASCE7-05, in order to verify validity of design values.

Seismic safety of buildings has been evaluated using an objective damage-index obtained from the capacity curve, computed for normalized roof displacements corresponding to performance point. Additionally, five damage thresholds are defined using the values of inter-story drifts associated with several Limit States. Damage thresholds lead to obtain fragility curves and damage probability matrices, used in order to evaluate the seismic safety of the code-designed buildings under study.

2. Seismic Design of Buildings

The main objective of the seismic design is to obtain structures capable of sustaining a stable response under strong ground motions. Some aspects of the current seismic analysis procedures allow for adapting non-linear features into an equivalent elastic analysis and, obviously, formulation of these procedures is essential for assuring a satisfactory earthquake-resistant design.

In earthquake-resistant engineering, stable behavior is achieved through compliance with conceptual design, thus implying regularity of the structure both in plane and elevation as well as continuity of resistant elements to lateral loads. It is also essential that the structure elements are able to dissipate energy, reaching damage levels which do not threaten the stability of the structure as a

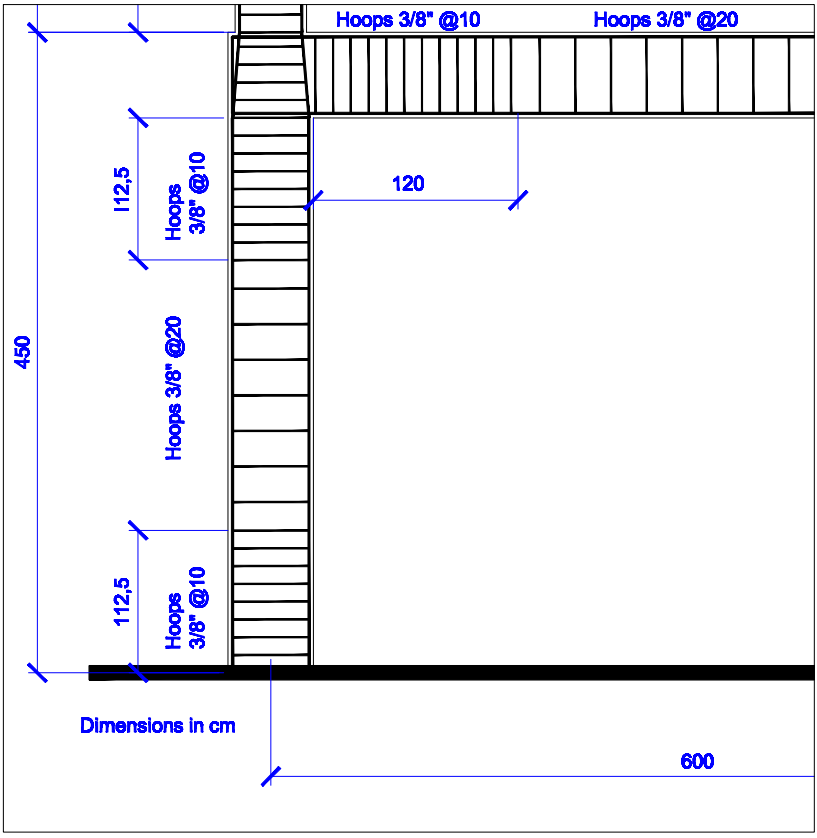

Figure 1. Typical reinforcement in beam-column special zones.

whole. In order to achieve this global behavior in concrete-reinforced buildings it is necessary to supply proportional confinement in special zones of beams and columns, finding these zones near to beam-column joints, see Figure 1.

It is especially interesting to know the seismic behavior of code-designed buildings. In order to study the behavior of low and medium vibration periods, a set of regular concrete-reinforced moment-resisting framed buildings (MRFB) designed according to ACI-318 were analyzed. Low and medium period responses were obtained by considering variable number of stories (3, 6, 9 and 12). Structural redundancy was included varying spam number (3, 4, 5 and 6). For each building structure, inner and outer frames were defined to the corre-

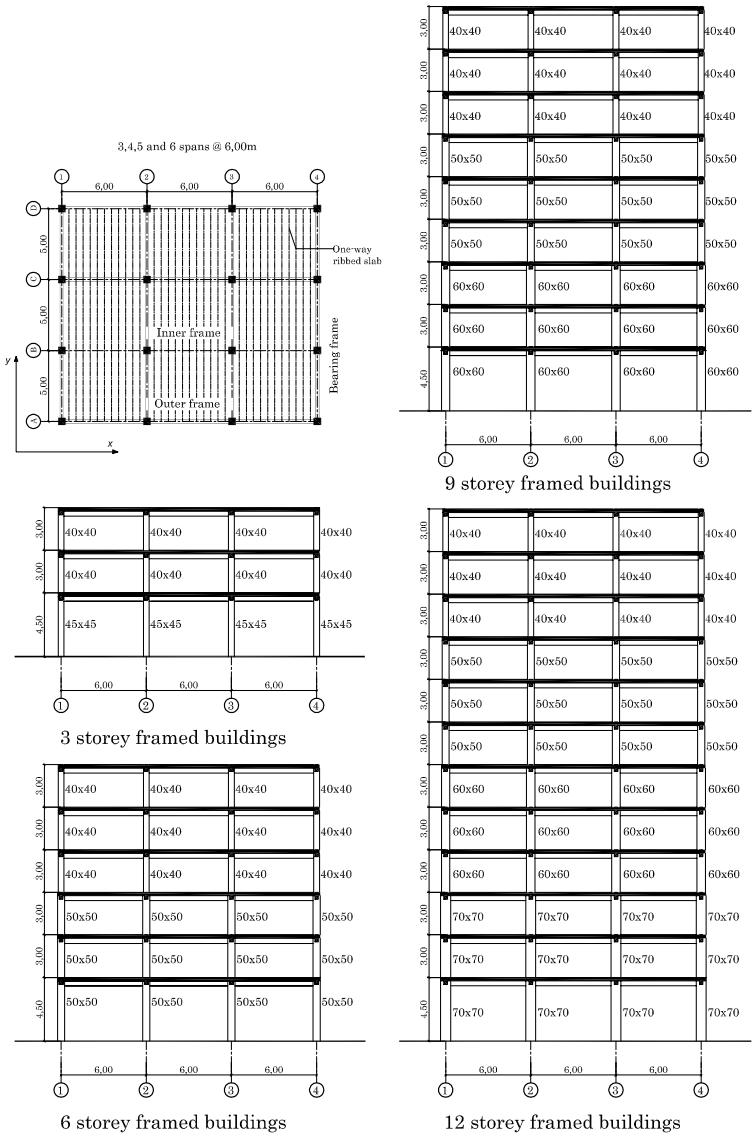

Figure 2. Plan and elevation views of designed buildings.

sponding load ratio (seismic load/gravity load). Frame members were analyzed, designed and detailed following the code prescriptions for special moment- resisting frames (high ductility level). Seismic demand is defined for type B soil (stiff soil) and for a peak ground acceleration of 0.3g and 0.4g. Geometric characteristics of typical frames are shown in Figure 2.

Non-linear analysis procedures have been used in previous studies to assess the seismic design of buildings designed according to specific design codes [4–6]. Static incremental non-linear analysis (Pushover Analysis) is an analysis procedure commonly adopted by the scientific community and practicing engineers in order to evaluate the seismic capacity of new or existing buildings. This analysis can be performed by using a predefined lateral load distribution; lateral load distribution is usually applied following a specific pattern, which corresponds to the shape of lateral displacements obtained from the modal analysis.

Dynamic analysis can be applied using an adequate set of records obtained from strong motion databases or from spectrum-compatible design synthesized accelerograms.

2.1. Seismic Response Parameters

The seismic response parameters considered most relevant in recent works are: global ductility, overstrength and behavior factor which can be calculated by applying deterministic procedures based on non-linear response of structures subject to static or dynamic loads. Although it is difficult to find a method to determine global yield and ultimate displacements [7], a simplified procedure is applied in this work.

The procedure is based on non-linear static response obtained via finite element techniques, which allows generating idealized bilinear capacity curve shape shown in Figure 3, with a secant segment from the origin to a point that corresponds to 75% of maximum base shear [8, 9]. The second segment, representing the branch of plastic behavior was obtained by finding the intersection of the aforementioned segment with another horizontal segment, corresponding to maximum base shear. Using this compensation procedure guarantees that energies dissipated by the ideal system and by the modeling one, are equal (see Figure 3).

For a simplified non-linear static analysis, there are two variables that typify the quality of seismic response of buildings. The first is global ductility μ, defined as

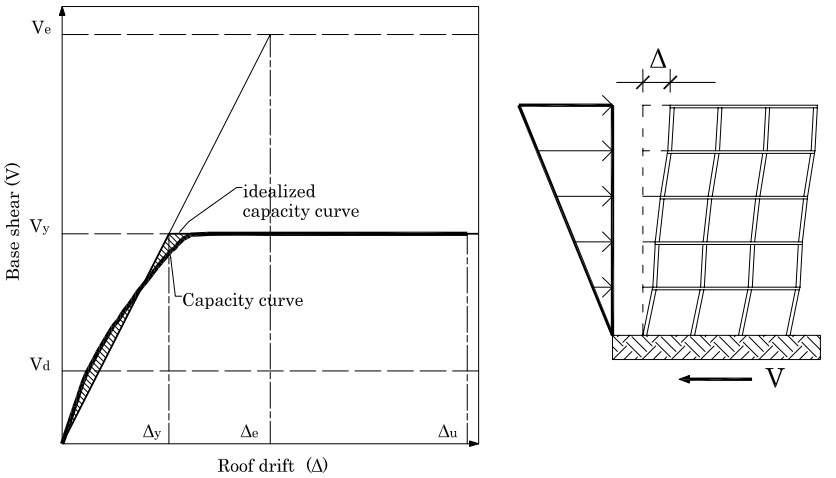

Figure 3. Scheme for determining displacement ductility and overstrength.

$$\mu = \frac{\Delta_u}{\Delta_y} \tag{1}$$

calculated based on values of yield drift, Δ_y, and ultimate drift, Δ_u, represented in the idealized capacity curve shown in Figure 3.

Second variable is the overstrength of the building R_R, defined as ratio of yielding base shear, Vy to design base shear, Vd (see Figure 3).

$$R_R = \frac{V_y}{V_d} \tag{2}$$

3. Structural Modeling

In order to obtain non-linear responses of buildings, it is necessary to model the structures taking into account their geometrical and mechanical specifications. Plane frames are used for static and dynamic analyses. This requires defining the different types of frames, mainly depending on the relationship between seismic and gravity loads carried on by the frames. Therefore, three types of frames are defined: outer and inner load frames, and bracing frames, see Figure 4.

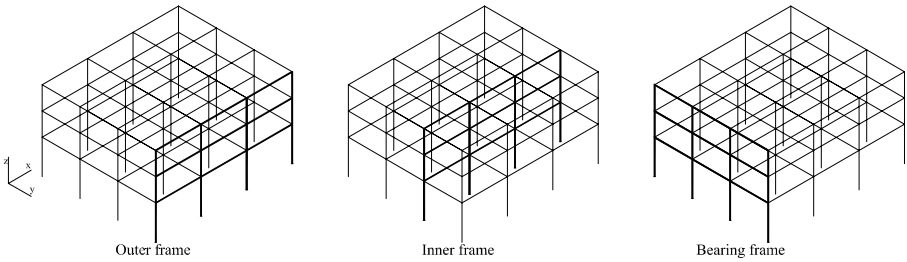

Figure 4. Definition of different building frames.

Thus frames are driscretized by taking into consideration the existence of special zones in beams and columns. This requires definition of the elements covering the length of special confined zones. Figure 5 shows a typical discretization obtained for a three stories frame.

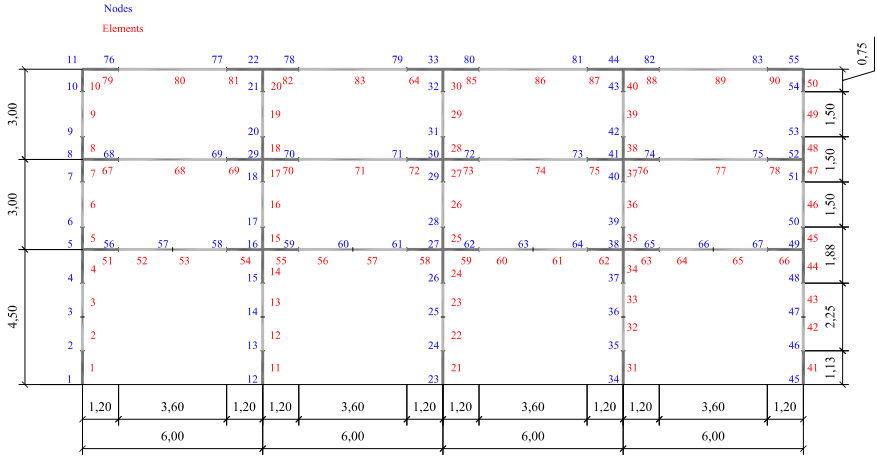

Figure 5. Frame discretization.

4. Non Linear Analysis

Advances made in the field of non-linear structural analysis and development of improved computational tools have enabled the application of more

realistic analysis procedures for new and existent buildings, taking into account the main features of their seismic non-linear behavior, such as constitutive non-linearity (plasticity and damage) and geometrical non-linearity (large deformations and displacements).

Non-linear incremental static and dynamic analyses are performed using the PLCd finite element code [2, 10, 11]. PLCd is a finite element code which works with two and three-dimensional solid geometries as well as with prismatic, reduced to one-dimensional members. By combining both numerical precision and reasonable computational costs [12, 13] it provides a solution and it can deal with kinematics and material non-linearity. To control their evolution, it uses various 3-D constitutive laws to predict material behavior (elastic, visco-elastic, damage, damage-plasticity, etc. [14]) with different yielding surfaces (Von-Mises, Mohr-Coulomb, improved Mohr-Coulomb, Drucker-Prager, etc. [15]). Newmark's method [16] is used to perform dynamic analysis. A more detailed description of the code can be found in Mata *et al.* [12, 13]. TFor dealing with composite materials, the main numerical features included in the code are: 1) Classical and serial/parallel mixing theory is used to describe the behavior of composite components [17]. 2) 2) Anisotropy Mapped Space Theory enables the code to consider materials with a high level of anisotropy, without associated numerical problems [18]. 3) Debonding Fiber-matrix, which reduces the composite strength due to failure of reinforced-matrix interface, is also considered [19].

Experimental evidence has shown that inelasticity in beam elements can be formulated in terms of cross-sectional quantities [20] and, therefore, beam's behavior can be described by using concentrated models, sometimes called plastic hinge models, which confine all inelastic behavior at beam ends using ad-hoc force-displacement or moment-curvature relationships [21]. But in the formulation used in this computer program, the procedure consists of obtaining the constitutive relationship at cross-sectional level by integrating a selected number of points corresponding to fibers directed along the beam's axis [22]. Thus, the general nonlinear constitutive behavior is included in the geometrically exact nonlinear kinematics formulation for beams proposed by Simo [23], considering an intermediate curved-reference configuration between the straight-reference beam and the current configuration. To solve the resulting non-linear problem, displacement based method is used. Plane cross-sections remain plane after deformation of the structure; therefore, no cross sectional warping is considered, avoiding inclusion of additional warping variables in the formulation or iterative

procedures to obtain corrected cross-sectional strain fields. Thermodynamically consistent constitutive laws are used to describe the material behavior of these beam elements, thus allowing obtaining a more rational estimation of the energy dissipated by structures. The simple mixing rule for material composition is also considered when modeling materials for these elements, composed by several simple components. Special attention is paid to obtain the structural damage-index capable of describing the structure load-carrying capacity.

According to the Mixing Theory, N different components coexist in a structural element, all of them undergoing the same strain; therefore, strain compatibility is forced among material components. Free energy density and dissipation of composite are obtained as the weighted sum of free energy densities and dissipation of components, respectively. Weighting factors K_q are the participation volumetric fraction of each compounding substance, $K_q = \frac{V_q}{V}$, obtained as the quotient between the $q-th$ component volume, V_q, and total volume, V [10–13].

Discretization of frames was performed using finite elements whose lengths vary depending on column and beam zones with special confinement requirements. These zones are located near the nodes where maximum seismic demand is expected, and are designed according to general dimensions of structural elements, diameters of longitudinal steel, span length and storey heights. Frame elements are separated into equal thickness layers with different composite materials, characterized by their longitudinal and transversal reinforcement ratio (see Figure 6). Transverse reinforcement benefits are included by using the procedure proposed by Mander *et al.* [24]. This procedure consists of improving the concrete compressive strength depending on quantity and quality of the longitudinal and transversal reinforcement.

4.1. Non Linear Static Analysis

In order to evaluate inelastic response of structures, pushover analysis was performed applying a set of lateral forces corresponding to seismic actions of the first vibration mode. Lateral forces were gradually increased starting from zero; passing through the value inducing transition from elastic to plastic behavior and finally reaching the value corresponding to ultimate drift (i.e. point at which the structure can no longer sustain any additional load and collapses). Before the structure is subject to lateral loads simulating a seismic action, it is first subject to the action of gravity loads, lumped in the nodes defined by the beam-columns joints, in concurrence with combinations applied in the elastic analysis. The

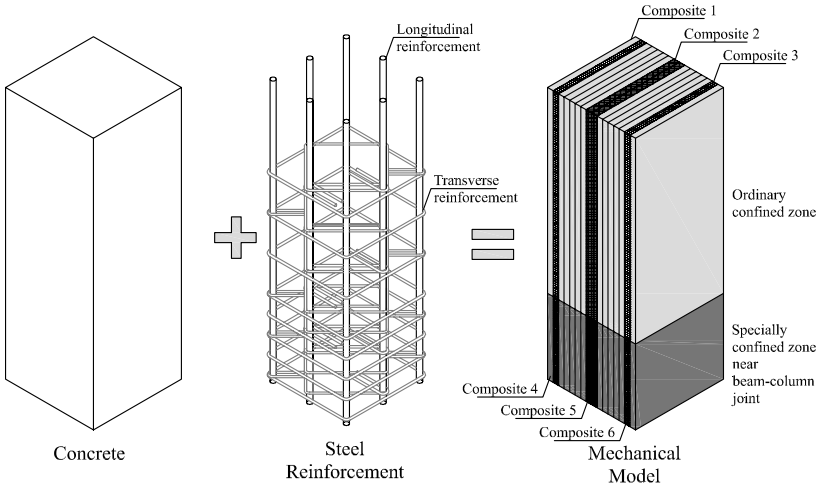

Figure 6. Discretization of RC frame elements.

method applied does not allow for evaluation of torsion effects, being the model used a 2D one. Capacity curves obtained in the analysis are shown in Figure 7.

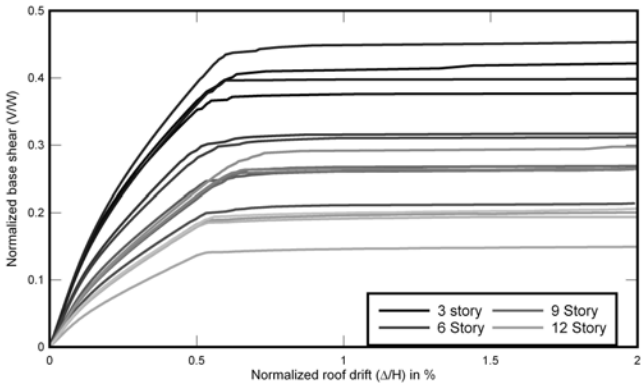

Figure 7. Capacity curves of the studied buildings.

Non-linear static analysis calculates cumulative damage in structural elements by using the procedures described in Section 4.3..Results of local damage-index at collapse displacement calculated for two of the buildings under study are shown in Figure 8. In this figure, each rectangle represents the magni-

tude of damage reached by the element. It is important to observe that for low rise buildings (N=3) the maximum values of damage correspond to the elements located at both ends of the first storey columns; this damage concentration corresponds to a soft-storey mechanism. Instead, high rise buildings (N=6, 9 and 12) show their maximum damage values at low level beam ends, according to the desired objective of conceptual design which is to produce structures with weak beams and strong columns.

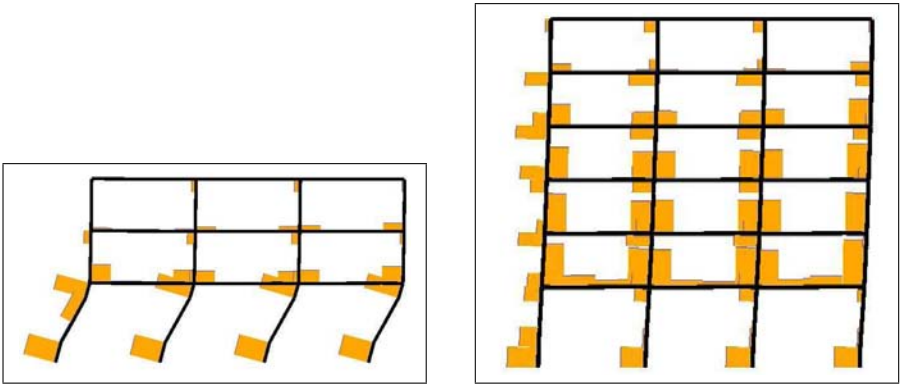

(a) 3 stories building (b) 9 stories building

Figure 8. Distribution of local damage-index at collapse displacement.

Figure 9 shows overstrength computed values for outer frames of the buildings under study, plotted in function of number of stories. Results clearly demonstrate that the influence of number of spans, equivalent to considering different numbers of resistant lines, is very low. In all cases, overstrength computed values are closer to each other. It can also be seen that these values of combined overstrength factors and redundancy are slightly lower than the value prescribed by ASCE-7 for design of ductile-framed buildings.

4.2. Non Linear Dynamic Analysis

In order to evaluate the dynamic response of buildings, the IDA (Incremental Dynamic Analysis) procedure was applied. This procedure consists in performing time-history analysis for registered ground motions or for artificially synthesized accelerograms scaled in such a way of inducing increasing levels of inelasticity in each new analysis [25]. A set of six artificial accelerograms, com-

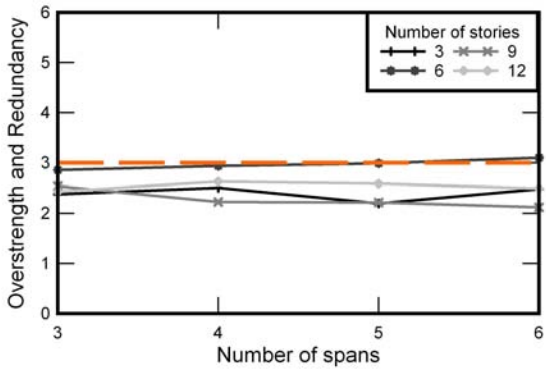

Figure 9. Overstrength and redundancy vs. number of stories.

patible with B type soil of the ASCE-7 elastic design spectrum, was generated, see Figure 10.

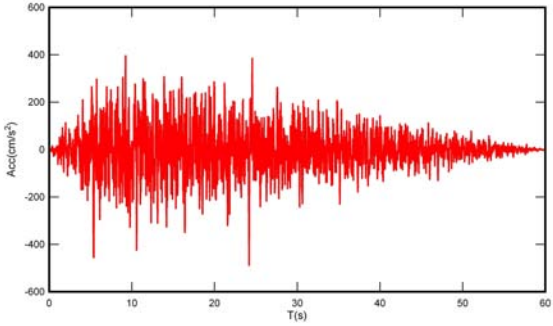

Figure 10. Synthesized accelerograms compatible with the ASCE-7 elastic design spectrum.

Figure 11 shows the elastic design spectrum and the 5% damping response spectra computed from the set of artificial accelerograms for the two levels of seismic hazard (0.3g and 0.4g) used in elastic design of buildings.

Peak acceleration equal to basic design acceleration is assumed in the analysis. Record is scaled from this value until a plastic response is reached by the structure; this procedure continues on and on until achieving collapse displacement. A maximum value of structural response is calculated for each value of scaled acceleration. IDA curves are obtained by plotting the earthquake peak

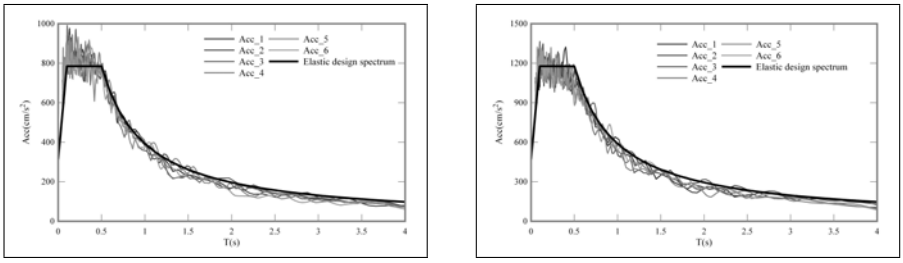

(a) 30%g (b) 40%g

Figure 11. Elastic design spectrum and response spectra.

acceleration in function of maximum value of the computed structural response. Collapse is reached when the capacity of the structure drops [9, 26, 27]. A usual criterion is to consider that collapse occurs whenever the slope of the curve is less than 20% of the elastic slope [25, 28]. Figure 12 shows IDA curves computed for the 3-span outer frame of the 3 storey building. Note that the collapse points of frames are closer to the values of the capacity curves.

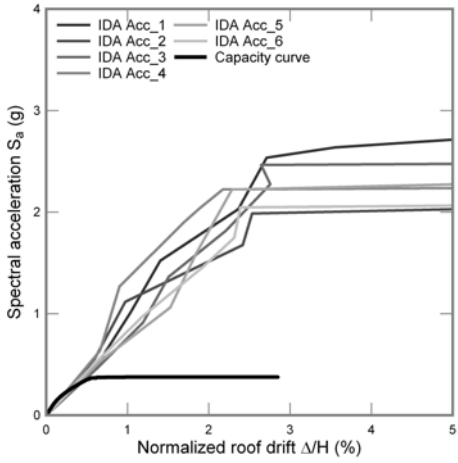

Figure 12. Set of IDA curves and capacity curve.

The dynamic analysis is useful to assess behavior factors q of the buildings. For this purpose the following equation has been proposed [4]:

Table 1. Computed behavior factors of outer frames (0.3g)

Number of storeys	$q_{equation}$	q_{code}	$\frac{q_{equation}}{q_{code}}$
3	19.70	8.00	2.46
6	16.45	8.00	2.05
9	15.46	8.00	1.93
12	16.09	8.00	2.01

$$q = \frac{a_{g(Collapse)}}{a_{g(Design_yield)}} \tag{3}$$

where $a_{g(Collapse)}$ and $a_{g(Design_yield)}$ are collapse and yielding design peak ground acceleration, respectively. The former is obtained from IDA curves and the latter is calculated from elastic analysis of the building. Average values of the q computed behavior factor of the buildings under study are shown in Table 1; these values correspond to the dynamic response obtained for the set of ten synthesized accelerograms, and are compared to behavior factors prescribed by the design codes.

Computed behavior factors show that, regardless of building height, seismic design performed by using the ACI318 leads to structures with satisfactory lateral capacity whenever subjected to strong motions.

4.3. Objective Damage Index

Some indexes measure the global seismic damage of a structure from its local damage, i.e. the contribution in a given instant of cumulative damage in structural elements to the structure being subject to seismic demand. Among the indexes which have served as baseline for many researches, it can be mentioned the one proposed by Park and Ang [29] which can determine damage in an element, based on non-linear dynamic response by the following expression:

$$DI_e = \frac{\delta_m}{\delta_u} + \frac{\beta}{\delta_u P_y} \int dE_h \tag{4}$$

where δ_m is the maximum displacement, δ_u is the ultimate displacement, β is a parameter adjusted depending on materials and structural type, P_y is the yield

strength and $\int dE_h$ is dissipated hysteretic energy. This damage-index is valid for an element at a local level; however, it is possible to apply this index for calculating the values for a specific structural level, or for the whole structure.

Another damage-index based on stiffness degradation is proposed by Gupta *et al.* [30]. They have formulated an expression based on the relationship between ultimate and yielding displacements, equivalent to ultimate and yielding stiffness. This formulation also includes a design ductility value according to:

$$DI = \frac{\frac{x_{maz}}{z_{00}} - 1}{\mu - 1} \tag{5}$$

A local damage-index is calculated using the PLCd finite element program with a constitutive damage and plasticity model enabling the correlation of damage with lateral displacements [16, 31]

$$D = 1 - \frac{\|P^{in}\|}{\|P_0^{in}\|} \tag{6}$$

where $\|P^{in}\|$ and $\|P_0^{in}\|$ are the norm of current and elastic values of the internal forces vectors, respectively. Initially, the material remains elastic and $D = 0$, but when all the energy of the material has been dissipated $\|P^{in}\| \to 0$ and $D = 1$.

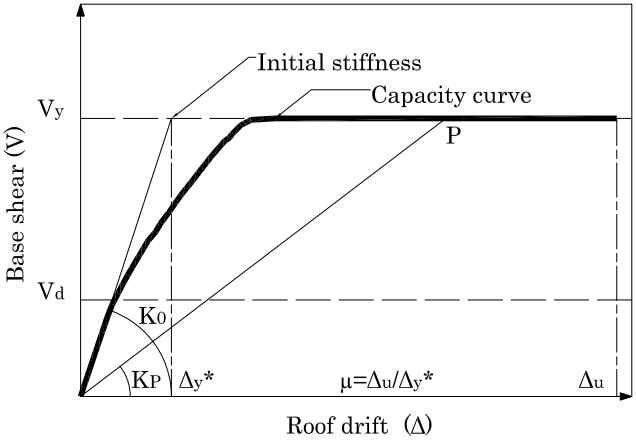

Figure 13. Parameters for determination of damage-index.

It is important to know the level of damage reached by a structure subject to certain demand. This is possible if the damage-index is normalized with respect

to the maximum damage which can occur in the structure [32]. This objective damage-index $0 \leq D \leq 1$ achieved by a structure at any P is defined as

$$D_{obj}^{P} = \frac{D_P}{D_C} = D_P \frac{\mu}{1-\mu} = \frac{(1-\frac{K_P}{K_0})\mu}{1-\mu} \tag{7}$$

For example, for P point, which might be the performance point resulting from the intersection between inelastic demand spectrum and capacity curve (obtained from pushover analysis), it corresponds a stiffness K_P. Other parameters are initial stiffness K_0 and ductility μ, calculated by using yielding displacement Δ_y^* corresponding to the intersection of initial stiffness with maximum shear value (see Figure 13).

Objective damage-index is computed using Eq. 7, from the non-linear static analysis. Figure 14 shows evolution of objective damage-index respecting the normalized roof drift, computed for all frames of the 3 stories building. Curves are similar to those obtained for frames of the same number of stories.

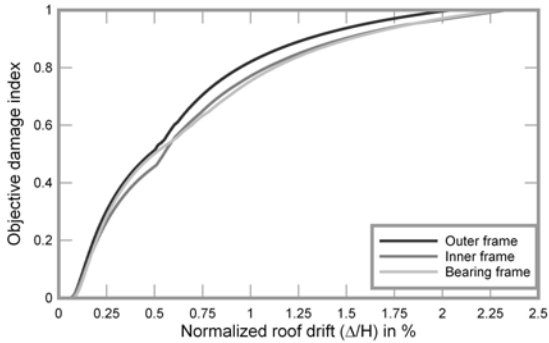

Figure 14. Evolution of damage-index of the 3 stories building.

5. Seismic Safety

Nowadays, it is widely accepted among the scientific community that the Performance-Based Design is the most rational procedure. This requires definition of a set of Limit States in order to evaluate the damage that may be caused by earthquakes. These Limit States are frequently defined by engineering demand parameters, among which the most used are inter-story drift, global drift

and global structural damage. These demand parameters define damage thresholds associated with Limit States, which allows calculating fragility curves and damage probability matrices used in seismic safety assessment of buildings.

Consequently, it is necessary to select the evaluation criterion which represents the moment when the structure reaches a specific limit state. According to the above, interstory drift is a dimensionless value which quantifies properly the damage under lateral loads. Among published values, a set of inter-story drifts were selected from which specific damage reaches a threshold corresponding to a Limit State.

Damage thresholds are determined using the VISION 2000 procedure [33], in which they are expressed in function of interstory drifts. In this chapter, five damage state thresholds are defined both from interstory drift curve and from capacity curve. For the slight damage state, roof drift corresponding to an interstory drift of 0.5% is considered. Service damage state corresponds to the roof drift for which an interstory drift of 1% is reached in almost all the structure stories. Repairable damage state is defined by an inter-story drift of 1.5%. A severe damage state is identified by a roof drift producing a 2.0% of interstory drift at each level of the structure. Finally, a total damage state (collapse) corresponds to ultimate roof displacement obtained from the capacity curve. Mean values and standard deviation were computed from the non-linear response of buildings with the same geometric and structural type, with a variation of the number of spans from 3 to 6 [34, 35].

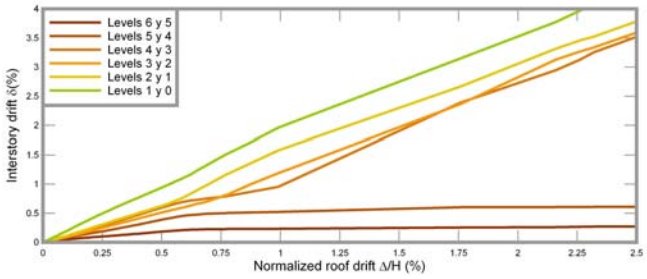

Figure 15. Determination of the damage thresholds.

To determine damage thresholds it is necessary to plot the evolution of interstory drifts with respect to global drift (roof displacement normalized with total building height). With this plot it is possible to obtain the global drift limit corresponding to a state i, characterized by interstory drift, see Figure 15. In

the case of a building with n levels, n evolution curves are obtained; global drift of a Limit State corresponding to the intersection of the first curve with the inter-story drift characterizing the Limit State.

Figure 16 Figure 16 shows the results obtained from outer frames of the 6 storey buildings designed for an acceleration of 0.3g. This figure shows that there is a clear dispersion of results for displacement at collapse, but these are kept within a range between 2.25% and 2.5%, compared to the values reported by Kircher *et al.* [36] and Dymiotis *et al.* [37], which are between 2% and 4%.

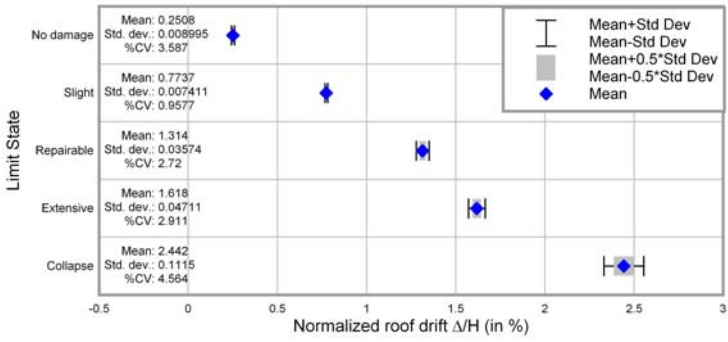

Figure 16. Mean and standard deviation for damage thresholds.

Figure 17 shows a comparison of results obtained by the above procedure with experimental results reported by Dymiotis *et al.* [37]. It can be seen that values obtained from non-linear analysis fit quite well with experimental values, regardless of the number of spans being considered.

Given this difference in results, Vielma *et al.* [34] have proposed the following expressions to determine interstory drifts δ (expressed in%) from normalized roof drifts of the buildings (Δ/H expressed in%)):

$$\begin{aligned}
\delta &= 0.1299 + 0.4358\left(\frac{\Delta}{H}\right) && for N = 3 \\
\delta &= 0.1503 + 0.5256\left(\frac{\Delta}{H}\right) && for N = 6 \\
\delta &= 0.06518 + 0.6280\left(\frac{\Delta}{H}\right) && for N = 9 \\
\delta &= 0.01184 + 0.6312\left(\frac{\Delta}{H}\right) && for N = 12
\end{aligned} \tag{8}$$

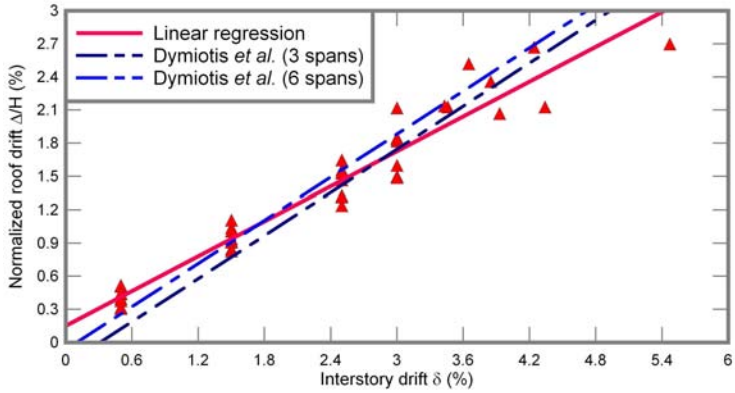

Figure 17. Comparison of numerical and experimental results.

Figure 18 shows damage thresholds values applied to the capacity curve of the outer frame of the 3 level building, designed for acceleration of 0.3g. By using Equation 7, objective damage-indexes are calculated with thresholds associated to Limit States.

The combined use of thresholds and damage-indexes allows a quick characterization of the seismic response of a building and provides sufficient criteria for evaluating the behavior of a particular configuration or pre-design subject to specific demand buildings, e.g. the spectrum prescribed by the design code.

5.1. Performance Point

In order to evaluate seismic safety of the buildings, the performance point represents an adequate measure. It is obtained by maximum drift of an equivalent single degree of freedom induced by the seismic demand. The points of all cases being studied have been determined by using the N2 procedure [38] which requires transformation of the capacity curve into a capacity spectrum, expressed in terms of spectral displacement, S_d and spectral acceleration, S_a. The former is obtained by means of equation

$$S_d = \frac{\delta_c}{MPF} \tag{9}$$

where δ_c is the roof displacement. The term MPF term is the modal participation factor calculated from the response in the first mode of vibration.

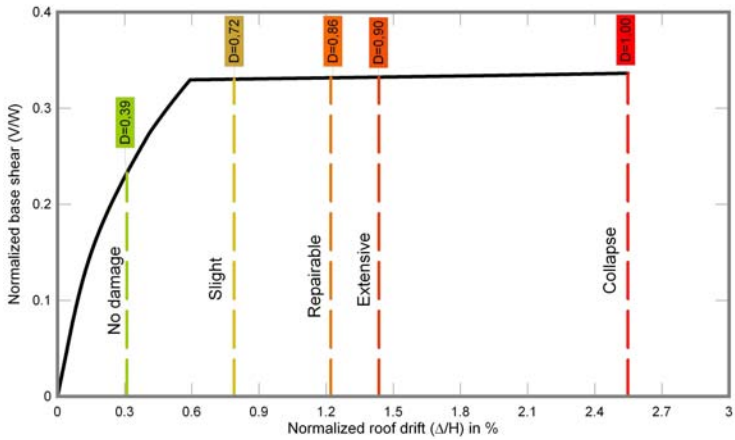

Figure 18. Damage thresholds with associated damage-index values.

$$MPF = \frac{\sum_{i=1}^{n} m_i \phi_{1,i}}{\sum_{i=1}^{n} m_i \phi_{1,i}^2} \tag{10}$$

Spectral acceleration S_a is calculated by means of:

$$S_a = \frac{\frac{V}{W}}{\alpha} \tag{11}$$

where V is the base shear, W is the seismic weight and α is a coefficient obtained as

$$\alpha = \frac{(\sum_{i=1}^{n} m_i \phi_{1,i})^2}{\sum_{i=1}^{n} m_i \phi_{1,i}^2} \tag{12}$$

Figure 19 shows a typical capacity spectra crossed with the corresponding elastic demand spectrum. Idealized bilinear shape of the capacity spectra is also shown.

Spectral displacement values corresponding to performance point are shown in Table 2. An important feature influencing the non-linear response of buildings is the ratio between performance point displacement and collapse displacement. This ratio indicates whether the behavior of a structure is ductile or fragile. Lower values correspond to the 12-storey buildings, which have a weak-beam strong-column failure mechanism.

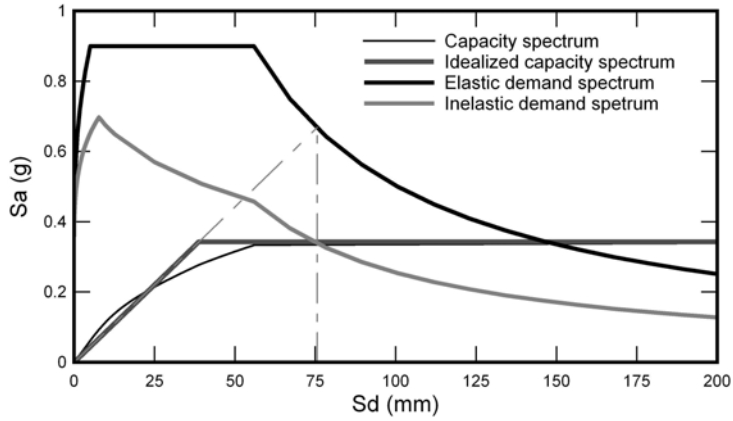

Figure 19. Determination of performance point.

Table 2. Roof drift of performance points for the studied buildings

Number of stories	Performance point (%)	Normalized roof drift		Ratio	
		Static analysis	Dynamic analysis (average)	Static analysis	Dynamic analysis (average)
3	0.71	2.93	2.52	0.24	0.28
6	0.47	2.41	2.65	0.20	0.18
9	0.44	2.58	2.67	0.17	0.17
12	0.28	2.49	2.70	0.11	0.10

5.2. Fragility Curves

Fragility curves are particularly useful for evaluating seismic safety of buildings. They are obtained by using spectral displacements determined for damage thresholds and considering a lognormal probability density function for spectral displacements which define damage states [39–42].

$$F(S_d) = \frac{1}{\beta_{ds} S_d \sqrt[n]{2\pi}} \exp[-\frac{1}{2}(\frac{1}{\beta_{ds}} \ln \frac{S_d}{\bar{S}_{d,ds}})^2] \tag{13}$$

where $\bar{S}_{d,ds}$ is the mean value of spectral displacement for which the building reaches damage state threshold d_s and β_{ds} is the standard deviation of the natural logarithm of spectral displacement for damage state d_s. The conditional probability $P(S_d)$ of reaching or exceeding a particular damage state d_s, given the spectral displacement S_d, is defined as

$$P(S_d) = \int_0^S F(S_d) dS_d \tag{14}$$

With fragility curves it is possible to calculate the values of probability of exceeding a particular limit state. Probabilities are calculated for a specific displacement or acceleration, usually obtained from a level of demand. Demand generally corresponds to the point of performance described in the previous subsection. Figure 20 shows fragility curves calculated for inner frames of the 3 and 12 storey buildings.

For more complete results the reader is referred to [27, 34, 35]

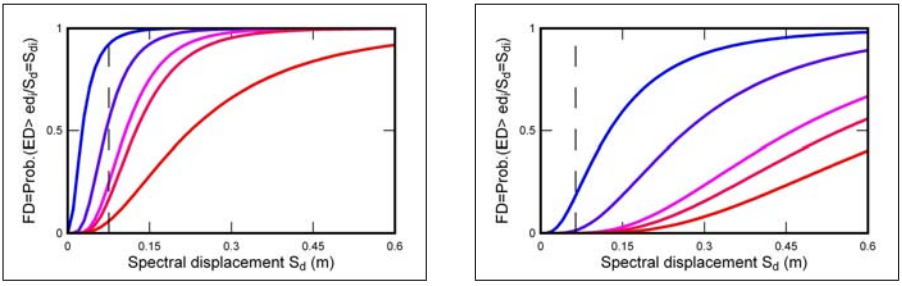

(a) Inner frame of the 3 stories building (b) Inner frame of the 12 stories building

Figure 20. Fragility curves with performance point displacement.

Figure 21 shows damage probability matrices calculated for performance points achieved for inner frames of the 3 and 12 storey buildings. It is important to note that for frames of the same building, probabilities vary according to load ratio (seismic load/gravity load). Another important feature is the increasing values of probabilities that low rise buildings reach higher damage states; as discussed in previous sections, collapse of these buildings is associated with the soft-storey mechanism. For example, in the case of inner frames of the 3-level building, probability to reach collapse is four times higher than in the case of the outer frame of the same building. In contrast, 6, 9 and 12 storey buildings show very low probabilities to reach higher damage states, regardless of load ratio and

span number. For these buildings, predominant damage states are non-damage and slight damage.

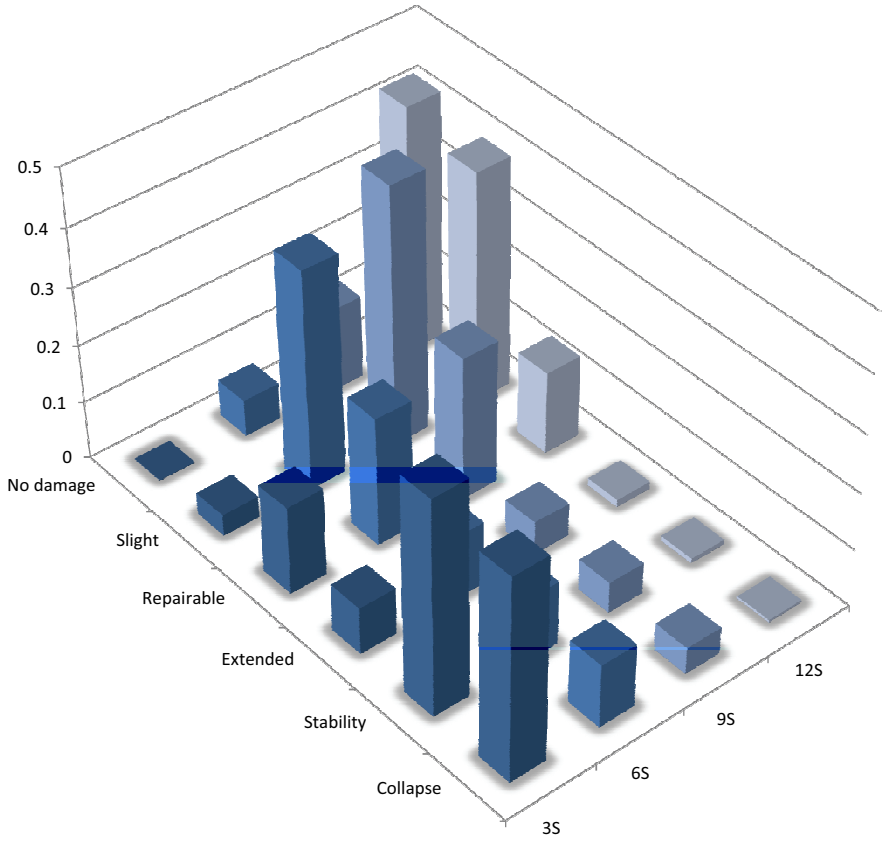

Figure 21. Damage probability matrices of outer frames.

Damage probability matrices contain the cumulative probability of reaching a specific limit state. This allows a qualitative assess of structural response during a specific seismic action. In Figure 21 it is possible to appreciate the probability matrices of internal frames, highlighting that frames of buildings with 3 levels have a probability of reaching more advanced stages of damage compared to frames of buildings of 6, 9 and 12 levels. This feature is repeated regardless of number of spans and location of frame. The difference in the response of low buildings is due to the fact that the failure mechanism of these

buildings is the soft story mechanism, in which damage is concentrated at the ends of columns in ground level, resulting in loss of global stability.

5.3. Concluding Remarks

Steps in this chapter show the importance of non-linear analysis in the evaluation of seismic safety of buildings. By incorporating the characteristics of the constitutive non-linearity of materials (plasticity and damage) and geometric (large deformations and displacements) of the structure, it is possible to estimate adequately the design parameters prescribed in codes.

These parameters are applied based on the experience of scientists and engineers; therefore, their validation helps to improve understanding the behavior of structures subject to earthquakes.

In order to apply the non-linear analysis in the evaluation of buildings designed according to current earthquake-resistant codes (ACI-318, ASCE-7), a group of concrete-reinforced buildings have been selected. These buildings have been studied by applying static and dynamic procedures which have allowed calculating ductility and overstrength values and response-reduction factors. Overall, assessment has enabled the awareness that design parameters are adjusted appropriately to safety requirements.

In the study, all parameters except overstrength values are higher than those prescribed by the design code. Computed values are slightly lower than those prescribed in the ASCE-7. Overstrength values are often interpreted as safety factors by some designers.

Among the assessment procedures explained, one is the verification of the appropriateness of applying the objective damage-index as a tool to quickly evaluate overall performance of structures when they are subject to a specific seismic demand.

Analyses applied demonstrated that although buildings are designed to apply the same special requirements to ensure adequate seismic performance, the safety exhibited by these buildings is not the same. This can be verified by observing the fragility curves obtained for buildings of 3 and 12 levels, where the first are more likely to reach advanced stages of damage. This feature is due to the failure mode characteristic of low buildings that corresponds to a soft-story mechanism.

References

[1] ACI, *Building code requirements for structural concrete,* (ACI318-05). Detroit: American concrete institute, 1st ed., 2005.

[2] PLCd, *Non-linear thermo mechanic finite element oriented to PhD student education*. Barcelona: CIMNE, 1st ed., 2008.

[3] ASCE, *Minimum Design Loads for Buildings and Other Structures*. Reston: American Society of Civil Engineers, 1st ed., 2005.

[4] A. M. Mwafi and A. Elnashai, "Calibration of force reduction factors of RC buildings," *J Earthq Eng*, vol. 6(2), pp. 239–273, 2002.

[5] A. M. Mwafi and A. Elnashai, "Overstrength and force reduction factors of multistory reinforced-concrete buildings," *Struct des tall buil*, vol. 11, pp. 329–351, 2002.

[6] L. Sanchez and A. Plumier, "Parametric study of ductile moment-resisting steel frames: a first step towards Eurocode 8 calibration," *Earthq Eng Struct D*, vol. 37, pp. 1135–1155, 2008.

[7] M. J. N. Priestley, G. M. Calvi, and M. J. Kowalski, *Displacement-based seismic design of structures*. Pavia Italy: IUSS Press, 1st ed., 2007.

[8] R. Park, "State-of-the-art report: ductility evaluation from laboratory and analytical testing," in *Proceedings of the 9th WCEE*, (Tokyo-Kyoto, Japan), pp. 605–616, IAEE, 1988.

[9] J. C. Vielma, A. H. Barbat, and S. Oller, "Seismic performance of waffle slabs buildings," *P I Civil Eng-Str B*, vol. 162, pp. 169–182, 2009.

[10] S. Oller and A. H. Barbat, "Moment-curvature damage model for bridges subjected to seismic loads," *Comput Methods Appl Mech Engrg*, vol. 195, pp. 4490–4511, 2006.

[11] E. Car, S. Oller, and E. Oñate, "A large strain plasticity for anisotropic materials: Composite material application," *Int J Plasticity*, vol. 17(11), pp. 1437–1463, 2001.

[12] P. Mata, S. Oller, and A. H.Barbat, "Static analysis of beam structures under nonlinear geometric and constitutive behaviour," *Comput Methods Appl Mech Engrg*, vol. 196, pp. 4458–4478, 2007.

[13] P. Mata, S. Oller, and A. H.Barbat, "Dynamic analysis of beam structures under nonlinear geometric and constitutive behaviour," *Comput Methods Appl Mech Engrg*, vol. 197, pp. 857–878, 2008.

[14] S. Oller, E. Oñate, J. Oliver, and J. Lubliner, "Finite element non-linear analysis of concrete structures using a plastic-damage model," *Eng Fract Mech*, vol. 35(1-3), pp. 219–231, 1990.

[15] J. Lubliner, J. Oliver, S. Oller, and E. Oñate, "A plastic-damage model for concrete," *Int J Solids Struct*, vol. 51, pp. 501–524, 1989.

[16] A. H. Barbat, S. Oller, E. Oñate, and A. Hanganu, "Viscous damage model for Timoshenko beam structures," *Int J Solids Struct*, vol. 34, pp. 3953–3976, 1997.

[17] J. Faleiro, S. Oller, and A. H. Barbat, "Plastic-damage seismic model for reinforced concrete frames," *Comput Struct*, vol. 86, pp. 581–597, 2008.

[18] S. Oller, E. Car, and J. Lubliner, "Definition of a general implicit orthotropic yield criterion," *Comput Meth Appl Mech Eng*, vol. 192(7-8), pp. 895–912, 2003.

[19] X. Martinez, F. Rastellini, S. Oller, and A. H.Barbat, "A numerical procedure simulating rc structures reinforced with FRP using the serial/parallel mixing theory," *Comput Struct*, vol. 86, pp. 1604–1618, 2008.

[20] O. Bayrak and S. Sheik, "Plastic hinge analysis," *J Struct Eng (ASCE)*, vol. 127, pp. 1092–1100, 2001.

[21] E. Spacone and S. El-Tawil, "Nonlinear analysis of steel-concrete composite structures: State of the art," *J Struct Eng (ASCE)*, vol. 126, pp. 159–168, 2000.

[22] Y. Shao, S. Aval, and A. Mirmiran, "Fiber-element model for cyclic analysis of concrete-filled fiber reinforced polymer tubes," *J Struct Eng (ASCE)*, vol. 131, pp. 292–303, 2005.

[23] J. C. Simo, "A finite strain beam formulation. The three-dimensional dynamic problem part I," *Comput Methods Appl Mech Engrg*, vol. 49, pp. 55–70, 1985.

[24] J. B. Mander, M. J. N. Priestley, and R. Park, "Observed stress-strain behaviour of confined concrete," *J Struct Eng (ASCE)*, vol. 114, pp. 1827–1849, 1988.

[25] D. Vamvatsikos and C. A. Cornell, "Incremental dynamic analysis," *Earthq Eng Struct D*, vol. 31(3), pp. 491–514, 2002.

[26] S. Kunnath, *Earthquake engineering for structural design*. Boca Raton: CRC Press, 1st ed., 2005.

[27] J. C. Vielma, A. H. Barbat, and S. Oller, "Seismic safety of low ductility buildings used in Spain," *Bull Earthquake Eng*, vol. 8, pp. 135–155, 2010.

[28] S. W. Han and A. Chopra, "Approximate incremental dynamic analysis using the modal pushover analysis procedure," *Earthq Eng Struct D*, vol. 35(3), pp. 1853–1873, 2006.

[29] Y. J. Park and A. H.-S. Ang, "Mechanistic seismic damage model for reinforced concrete," *J Struct Eng (ASCE)*, vol. 111, pp. 722–739, 1985.

[30] P. S. Gupta, S. R. Nielsen, and P. H. Kierkegaard, "A preliminary prediction of seismic damage-based degradation in RC structures," *Earthq Eng Struct D*, vol. 30, pp. 981–933, 2001.

[31] E. Car, S. Oller, and E. Oñate, "An anisotropic elastoplastic constitutive model for large strain analysis of fiber reinforced composite materials," *Comput Meth Appl Mech Eng*, vol. 185(2-4), pp. 245–277, 2000.

[32] J. C. Vielma, A. H. Barbat, and S. Oller, "An objective seismic damage index for the evaluation of the performance of RC buildings," in *Proceedings of the 14th WCEE*, (Beijing, China), IAEE, 2009.

[33] SEAOC, *Vision 2000 Report on Performance Based Seismic Engineering of Buildings*. Sacramento, California, USA: Structural Engineers Association of California, 1st ed., 1995.

[34] J. C. Vielma, A. H. Barbat, and S. Oller, "Umbrales de daño para estados límite de edificios porticados de concreto armado diseñados conforme al ACI-318/IBC-2006," *Revista Internacional de Desastres Naturales*, vol. 8, pp. 119–134, 2009.

[35] J. C. Vielma, *Caracterización de la respuesta sísmica de edificios de hormigón armado mediante la respuesta no lineal*. PhD thesis, Technical University of Catalonia, 2008.

[36] C. Kircher, A. Nassar, O.Kustu, and W. Holmes, "Development of building damage functions for earthquake loss estimation," *Earthq Spectra*, vol. 13(4), pp. 663–682, 1997.

[37] C. Dymiotis, A. Kappos, and M. Chrissanthopoulos, "Seismic reliability of RC frames with uncertain drift and member capacity," *J Struct Eng (ASCE)*, vol. 125(9), pp. 1038 – 1047, 1999.

[38] P. A. Fajfar, "Nonlinear analysis method for performance based seismic design," *Earthq Spectra*, vol. 16(3), pp. 573–591, 2000.

[39] P. E. Pinto, R. Giannini, and P. Franchin, *Seismic reliability analysis of structures*. Pavia Italy: IUSS Press, 1st ed., 2006.

[40] A. H. Barbat, L. G. Pujades, and N. Lantada, "Seismic damage evaluation in urban areas using the capacity spectrum method: application to Barcelona," *Soil Dyn Earthq Eng*, vol. 28, pp. 851–865, 2008.

[41] A. H. Barbat, L. G. Pujades, and N. Lantada, "Performance of buildings under earthquakes in Barcelona, Spain," *Comput.-Aided Civ. Infrastruct*, vol. 21, pp. 573–593, 2006.

[42] N. Lantada, L. G. Pujades, and A. H. Barbat, "Vulnerability index and capacity spectrum based methods for urban seismic risk evaluation. a comparison," *Nat Hazards*, vol. 25(3), pp. 299–326, 1989.

INDEX

D

E

F

G

H

I

J

K

L

M

N

O

P

R

S

T

U

V

W

X

Z